WAVE HEIGHT AND SPECTRAL TRANSFORMATION IN THE SHALLOW WATERS OF KERALA COAST AND THEIR PREDICTION

THESIS SUBMITTED TO THE

COCHIN UNIVERSITY OF SCIENCE AND TECHNOLOGY

FOR THE DEGREE OF

DOCTOR OF PHILOSOPHY

IN

PHYSICAL OCEANOGRAPHY

UNDER THE FACULTY OF MARINE SCIENCES

by

N. P. KURIAN

CENTRE FOR EARTH SCIENCE STUDIES

COCHIN - 682 018

JULY 1987

to my beloved parents

DECLARATION

I do hereby declare that this Thesis contains results of research carried out by me under the guidance of Dr. M. Baba, Scientist-in-charge, Centre for Earth Science Studies, Regional Centre, Cochin and has not previously formed the basis of the award of any degree, diploma, associateship, fellowship or other similar title of recognition.

Ernakulam

2.7.1987

N. P. KURIAN
Regional Centre
Centre for Earth Science Studies
Cochin - 682 018

CERTIFICATE

This is to certify that this Thesis is an authentic record of research work carried out by Mr. N. P.Kurian under my supervision and guidance in the Centre for Earth Science Studies for Ph.D. Degree of the Cochin University of Science and Technology and no part of it has previously formed the basis for the award of any other degree in any University.

Dr. M. BABA
(Research Guide)
Scientist-in-charge
Regional Centre
Centre for Earth Science Studies
Cochin - 682 018

Ernakulam,
2.7.1987.

ACKNOWLEDGEMENTS

I am immensely grateful to Dr. M. Baba, Scientist-in-charge, Centre for Earth Science Studies, Regional Centre, for the valuable guidance, constant encouragement and critical scruitiny of the manuscript. But for his rich knowledge and vast experience, this work would have been far from complete.

I express my deep sense of gratitude to Dr. Harsh K. Gupta, Director, Centre for Earth Science Studies, for the constant encouragement and the facilities extended.

I owe much to Shri. T.S. Shahul Hameed for helping me in the various computations and for some useful and timely discussions. Thanks are due to my colleagues, S/Shri. K. V. Thomas, Joseph Mathew, S. Mohanan, K.P. Bhaskaran, D.Raju, Reji Skariah, Smt.Sreekumari Kesavan, and N.Santha, who have been of much help to me during various stages of this work. Thanks are also due to Dr.K. Premchand and Shri. C.M. Harish for some useful discussions.

The Vikram Sarabhai Space Centre (VSSC), Trivandrum provided the computer facilities for part of the work. I am greatly indebted to Dr.C.G. Sukumaran Nair, Scientist, V.S.S.C. for sparing his valuable time for helping me in the computations there.

S/Shri K.K. Varghese, A. Varkey Babu, M. Ramesh Kumar, P.P. Simon and Asokan Andy have contributed much in making the field programmes a success. S/Shri P.P. Ouseph and M.N. Muralidharan Nair helped me in the laboratory analysis. Thanks are due to the staff of the Regional Centre, Centre for Earth Science Studies, who have helped me in one way or other during this investigation.

Finally, I must thank my wife, Molly, who made it possible for me to concentrate on this research without being saddled by the household affairs.

CONTENTS

PREFACE

There has been a significant increase in the coastal developmental activities all along the Indian coastline during the last two or three decades owing to shore protection works, offshore oil explorations, industrial development, effluent and sewage disposal, harbour development, etc. The Kerala coast had assumed particular importance due to the recurring problem of intensive beach erosion coupled with the high density of population and the consequent developmental activities.

Coastal engineering projects including shore protection measures along our coast are badly in need of reliable wave data, among other parameters, for design and planning of operations. Unlike the deep water wave climate, the shallow water wave climate exhibits much spatial variation owing to the complex transformation processes. As measurement of waves at each and every location is expensive in terms of manpower and facilities, the thrust of late, has been on the use of prediction models.

There are basically two methods for prediction of shallow water waves, viz. the graphical method and the numerical method. The numerical methods are being widely used, now-a-days, because they are fast, accurate and are

especially useful when the prediction over a large spatial frame is required. Practically little has been done on the development of numerical models for the prediction of height and spectral transformation of waves as applicable to our coasts.

Synchronized deep and shallow water wave measurements which are essential for study of wave transformation are very much lacking for our coasts. Under these circumstances, a comprehensive study of the wave transformation in the shallow waters of our coast was felt very important and is undertaken in the present investigation.

For the first time in our country synchronized deep and shallow water wave data sets have been obtained, that too from two widely differing and fully exposed coastal environments, and a critical evaluation of all the wave characteristics including spectral, have been carried out.

Another unique achievement is the field evaluations oftwo different models, one a wave height transformation and another a wave spectral transformation, utilising the above data sets. The role of frictional attenuation of waves in the above has been studied critically. These models with their similar evaluation (though limited) elsewhere, have proved their universal applicability and will be a useful

tool for coastal engineers and oceanographers in the fast and accurate prediction of shallow water wave characteristics.

A categorisation of the Kerala coast, according to the wave intensity, emanated from the present study will be useful in the design of coastal and harbour structures appropriate to the particular coast, in locating ports, harbours and other landing facilities, in establishing wave power generation projects and for many other applications where waves play an important role.

The thesis comprises of seven chapters. In the first introductory chapter, the status of the problem, the aim, objective and applications of the investigation are projected. In the second chapter, a review of wave transformation processes, the relevant literature on numerical models and the status of wave transformation studies along our coast is presented. The third chapter confines to the field programmes and method of data analysis undertaken. A critical discussion on the measured deep water and nearshore wave characteristics and their transformation is presented in the fourth chapter. The chapter 5 deals with the numerical model based on the wave ray approach, its modifications and verification with measured data. A random wave transformation model using the spectral approach is discussed and tested in chapter 6. The last chapter 7 gives

the summary, conclusions and recommendations based on the present investigation. The computer programmes used are given in Appendix I and II.

Based on the present investigations, three papers have been published:

1. Kurian, N.P., Baba, M., and Hameed, T.S.S., 1985. Prediction of nearshore wave heights using a refraction programme. Coastal Engineering, 9: 347-356.
2. Kurian, N.P., and Baba, M., 1986. A comparative study of the performance of waverider and pressure recorder. Proc. 3rd Indian Conference on Ocean Engng., Bombay, 2: K 21 - 28.
3. Kurian, N.P., and Baba, M., 1987. Attenuation of wave energy due to bottom friction. J. Coastal Res. (in press).

A list of other papers, related to this field, published by the author is given in Appendix III.

LIST OF SYMBOLS

A	Phillips constant
C	Wave phase velocity
C_f	Friction factor
C_g	Wave group velocity
d	Depth
D	Median sediment size
$e_1, e_2, \ldots e_6$	Coefficients
E	Wave energy density
f	Wave frequency
f_m	Spectral peak frequency
g	Acceleration due to gravity
H	Wave height
H_s	Significant wave height
$\bar{H}$	Average wave height
k	Wave number
K_f	Friction coefficient
K_r	Refraction coefficient
K_s	Shoaling coefficient
L	Wave length
m	Bottom slope
$m_o, m_1 \ldots$	Spectral moment
s	Distance measured along wave ray
T	Wave period
T_z	Zero crossing period
T_p	Spectral peak period

α	Polar angle
β	Wave ray separation factor
γ_s	Curvature of wave ray
Δx	Grid element size in x direction
Δy	Grid element size in y direction
ϵ	Spectoral width parameter
θ	Angle of wave approach
ν	Kinematic viscosity of sea water
ρ	Density of sea water
ϕ	Dissipation function

ABBREVIATIONS

Ch.	:	chapter
Fig.	:	figure
h	:	hour
Hz	:	hertz
IDWR	:	Indian Daily Weather Report
km	:	kilometre
kmph	:	kilometre per hour
m	:	metre
mm	:	millimetre
s	:	second
μ	:	micron
%	:	percentage
o	:	subscript to indicate deep water

CHAPTER I

INTRODUCTION

Information on wave climate is of paramount importance for the planning and execution of ocean engineering projects and for the proper management of the coastal zone. The morphodynamics of the littoral zone is controlled by the wave climate, as waves are the principal source of input energy into this zone (Komar, 1976). To design various structures and plan their construction a clear picture of the maximum wave forcing and wave climate should be available. There is a fairly sharp optimum cost of design for coastal structures (Fig. 1.1). Without a fairly good estimate of wave conditions, it would be nearly impossible to come close to this optimum and the cost would unnecessarily increase (Ploeg, 1968). Since most of the coastal or marine structures are designed for a long life time, long-term wave data is essential to account for the variability of waves during their life time. Of late, the wave data requirements have gone up further as ocean waves have been accepted as a potential alternate renewable source of electrical energy.

Three different methods are being followed at present for obtaining information on waves:

(i) The ship-based visual observations have been a major source of wave information till recently. This method

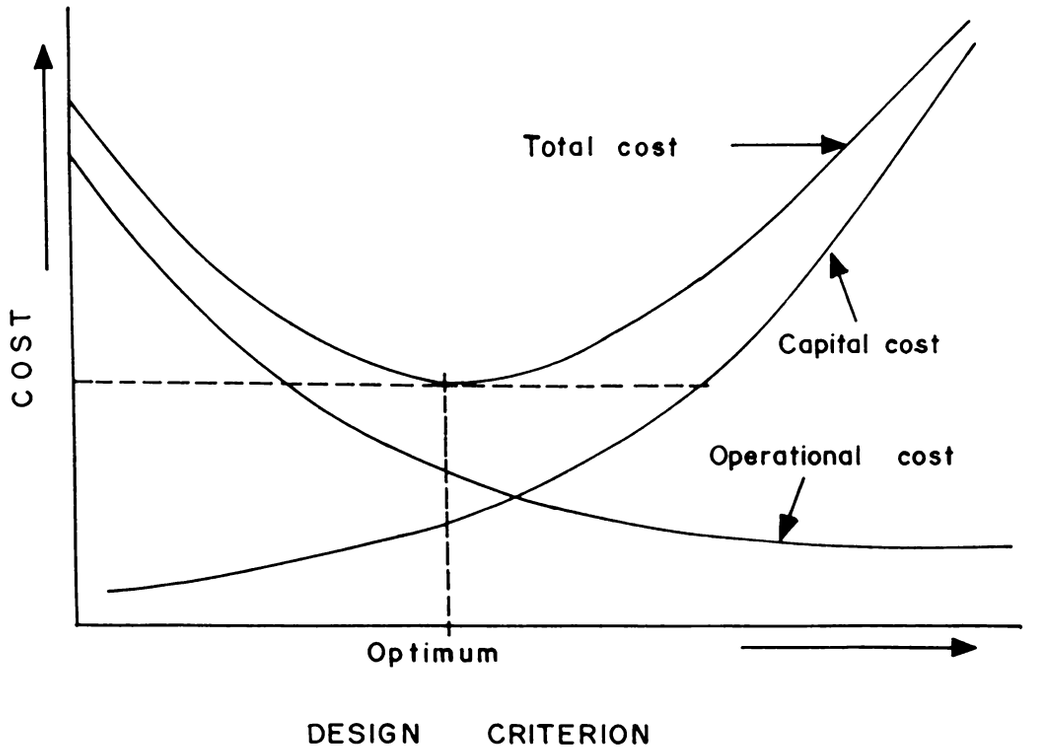

Fig. 1.1 Schematic relationship between Cost and Design Criteria of marine structures (after Ploeg, 1968)

has the limitations owing to the inaccuracies inherent in visual observations and uncertainties in the schedule of observations. As ships generally avoid storms, the wave climate derived through this method will not represent rough sea conditions.

(ii) Another source of wave data is wave hindcasting, which is done by making use of pressure/wind data obtained from weather stations and ship observations. The accuracy of such a hindcast/forecast depends on the density of data points and the models employed.

(iii) The third source of wave information is recorded wave data, which is the most reliable one. For the measurement of waves different types of surface, subsurface and above surface wave recording systems are used.

The recorded wave data, though most reliable, has the main constraint of being very expensive. Generally, the wave recording is made in deep water to represent a given coast. However, for coastal engineering applications shallow water data is required. Unlike the deep water wave climate, the shallow water wave climate exhibits much spatial variations (Baba et al.,1987). For coastal engineering applications the deep water data is reduced to shallow water conditions using some presently available computational methods, which are sometimes felt to be insufficient for obtaining reliable

design wave parameters. Hence, the wave recordings are to be made at different coastal points to obtain a reliable picture. The recording of waves at each and every coastal point will be exhorbitantly expensive in view of the man power and facilities required.

The above problem can be solved in a cost-effective manner by improving the computational methods so that they can reliably predict the shallow water waves from a knowledge of the deep water wave data. This deep water wave data input may be instrumentally recorded data or ship observations or hindcast data, depending on the level of accuracy desired. This method of approach is particularly advisable, when coastal wave data over an extensive area for a long duration is required.

Thus the problem is essentially one of understanding the wave transformation processes at the coastal area of interest and formulation of suitable numerical models for the prediction of wave transformation. There has been a thrust on the development of wave transformation models which can compute the shallow water wave parameters with reasonable accuracy and many models are available in literature (Dobson, 1967; Coleman and Wright, 1971; Treloar, 1986 etc.). An essential pre-condition in the applicability of such models is their evaluation in the field and their

further modifications based on it. The number of such field verifications is comparatively few when compared to the number of models available.

Evaluation of the available models in the coastal waters of Kerala or other parts of Indian coasts is very much lacking. Similarly, studies on wave transformation based on synchronised wave measurements in deep and shallow waters are not reported. Such studies are essential in arriving at wave transformation models suitable for our coasts.

This thesis embodies results of investigation carried out with the following objectives:

(i) A study of the wave transformation along the Kerala coast by making synchronised measurements of deep and shallow water waves.

(ii) A study of the applicability of a few numerical models for prediction of shallow water wave heights and wave spectra off the Kerala Coast and incorporation of necessary modifications wherever required.

(iii) Suggestion of suitable shallow water wave prediction models based on the evaluation with measured wave data.

Since the accuracy of predicted wave directions by different models have been validated in real world

situations (Bryant, 1979), the present investigation concentrates on the transformation of wave height and spectra only.

CHAPTER 2

WAVE TRANSFORMATION IN SHALLOW WATERS- A REVIEW

The various wave transformation processes are discussed in this chapter. The present knowledge on the methods of wave refraction and wave transformation studies are reviewed. Literature on the graphical method of wave refraction study, which has been the only method used for the Indian coasts, are also cited. The advances made in the development of numerical models are presented.

2.1. Wave Transformation Processes

When waves enter the shallow water from deep water, they are influenced by the bottom causing their transformation. The different processes causing wave transformation are refraction, shoaling, diffraction, reflection, dissipation of energy due to bottom friction, percolation, etc. and breaking. While some of these processes can be easily accounted theoretically, others are not amenable to easy mathematical analysis.

2.1.1. Refraction

According to the elementary progressive (Airy) wave theory, the phase velocity C is given by the equation

$$C = \sqrt{\frac{gL}{2\pi} \tanh 2\pi\frac{d}{L}} \qquad (2.1)$$

This equation shows that wave celerity depends on the depth of water in which the wave propogates. If the wave celerity decreases with depth, wave length must decrease proportionately. Variations in wave celerity occurs along the crest of the wave moving at an angle to the underwater contours because that part of the wave in deep water is moving faster than that in shallow water. This variation causes the wave crest to bend to align with the bottom contours (Fig. 2.1). This bending effect is called refraction and it depends on the relation of water depth to wave length (d/L). Different bathymetric features will lead to different patterns of bending of wave crests. Examples of such refraction patterns for different bottom topographic features are shown in Fig. 2.2.

The refraction of water waves is analogous to refraction of other types of waves such as light and sound. Using this analogy, O'Brien (1942) suggested the use of Snell's law of geometrical optics for solving refraction due to bathymetry. The change of direction of an orthogonal as it passes over a slope (Fig. 2.1) may be approximated by Snell's law as

$$\mathrm{Sin}\alpha_2 = \left(\frac{C_2}{C_1}\right)\mathrm{Sin}\,\alpha_1 \qquad (2.2)$$

where α_1 is the angle a wave crest makes with the bottom contours over which the wave is passing, α_2 is the angle as

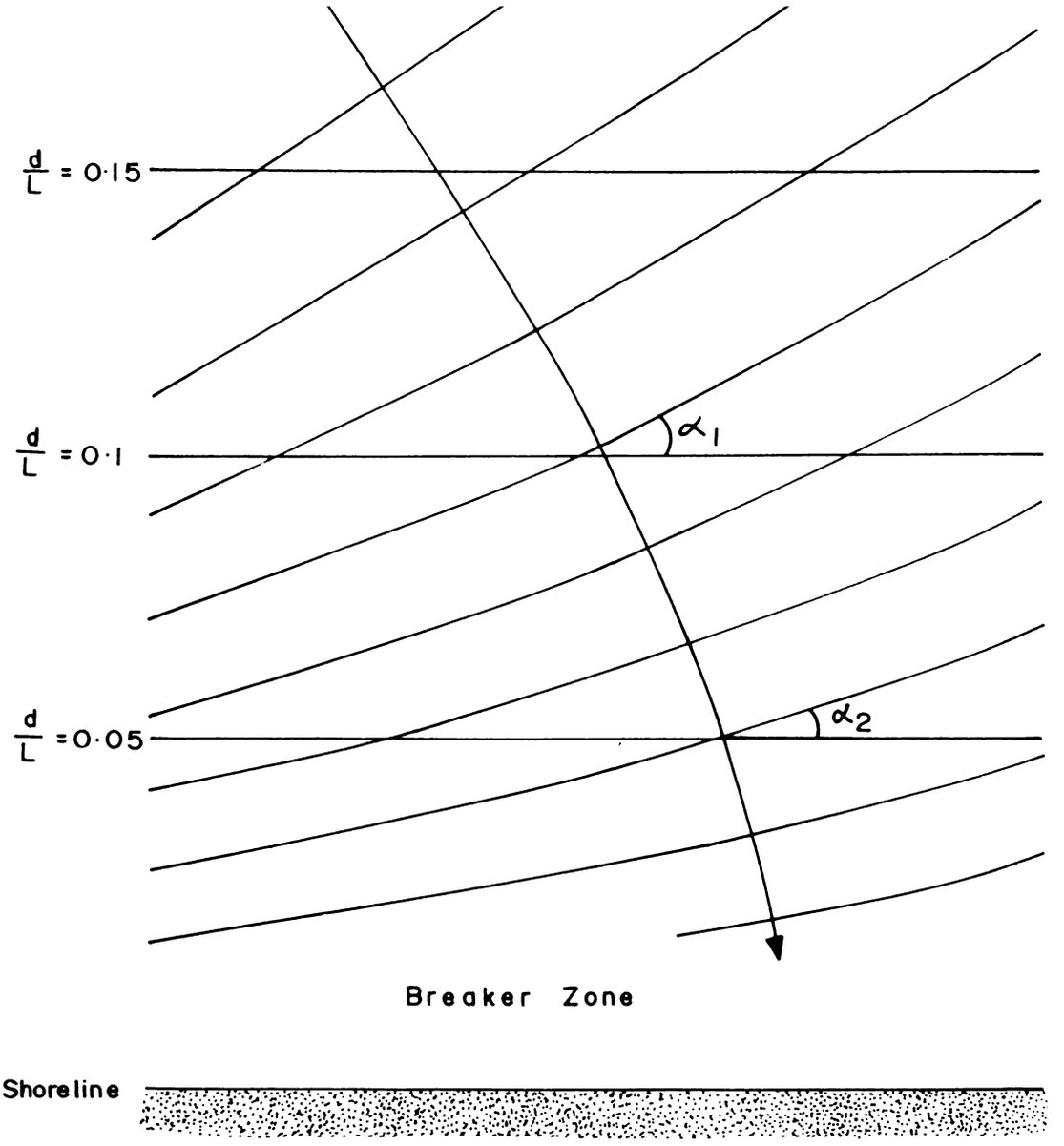

Fig.2.1 Definition Sketch of Refraction by Bathymetry.

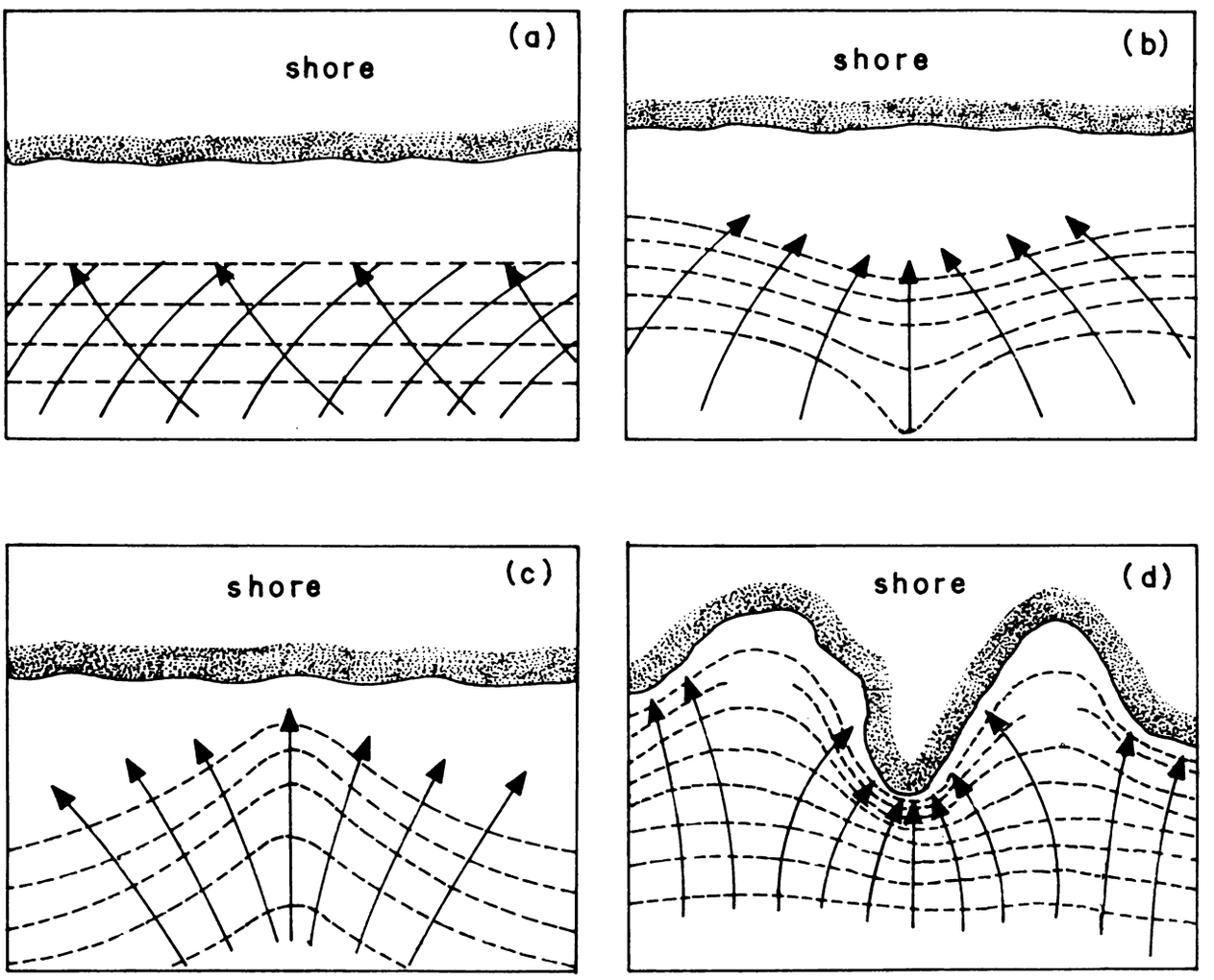

Fig·2.2 Examples of Typical Wave Refraction Patterns (a) Straight and Parallel Bottom Contours (b) Submarine Ridge (c) Submarine Canyon (d) Headland. (——wave crests, ⟶ wave ray, ----bottom contour)

the wave crest passes over the next bottom contour and C_1 and C_2 are the phase velocities at the depth of the first contour and second contour respectively.

The extent of refraction is expressed in terms of the refraction coefficient (K_r) which is defined by

$$K_r = \left(\frac{b_o}{b}\right)^{1/2} \tag{2.3}$$

where b_o and b are the distances between the selected orthogonals in deep water and shallow water respectively. Refraction coefficient, (K_r) is independent of wave height.

In addition to refraction caused by variations in bathymetry, waves may be refracted by currents or any other phenomenon which causes one part of a wave to travel slower or faster than the other part. Refraction by a current occurs when waves intersect the current at an angle. In regions of tidal current or major ocean currents the effects of refraction by currents can be important.

2.1.2. Shoaling

As waves move into shallow water, the group velocity slightly increases and then decreases with decreasing water depth. Where the group velocity increases wave crests move further apart and wave heights decrease corresponding to a decrease in wave energy. Decreasing group velocity occurs

for most of the nearshore region so that wave crests move closer together and wave heights increase corresponding to an increase in wave energy. This process is called wave shoaling.

The variations in the height of the shoaling waves can be obtained from a consideration of the energy flux, i.e. the energy transmitted forward across a plane between two adjacent orthogonals. If the loss of energy due to bottom drag, reflection, etc. is negligible, then the energy flux is constant, such that the shallow water energy flux

$$E\,Cg = E_o\,Cg_o \tag{2.4}$$

In the above, it is assumed that the effect of refraction as discussed in Section 2.1.1. is not there which is the case when waves approach normal to the coastline with parallel bottom contours. Applying the linear wave theory

$$Cg = nC \tag{2.5}$$

$$n = \frac{1}{2}\left[1 + \frac{2kd}{\mathrm{Sinh}2kd}\right] \tag{2.6}$$

$$\frac{H}{H_o} = \sqrt{\frac{E}{E_o}} \tag{2.7}$$

It can be finally derived that

$$\frac{H}{H_o} = \left[\frac{1}{2n}\,\frac{C_o}{C}\right]^{1/2} = K_s \tag{2.8}$$

K_s is called the shoaling coefficient. The changes in wave height with depth is given by equation (2.8). This equation predicts a small decrease in the wave height in the intermediate water depths ($\frac{1}{25} \leq \frac{d}{L} \leq \frac{1}{2}$) to a value below the deep water height. This decrease is followed by a rapid increase in H with further decrease in depths. The temporary height reduction in intermediate water depths is brought about by n increasing faster than C decreases. This decrease in H, followed by a rapid increase has been observed by Iverson (1951) in laboratory wave studies. The actual observed increase in wave height is found to be more rapid and lead to higher waves than predicted by equation (2.8). This is partly due to the failure of Airy wave theory at very shallow depths and large wave heights. A consideration of finite wave height theories yields a better prediction of the final increase in wave height prior to breaking (Munk, 1949). The shoaling coefficient is independent of wave height.

2.1.3. Diffraction

Diffraction of water waves is a phenomenon in which energy is transferred laterally along a wave crest. It is most noticeable where an otherwise regular train of waves is interrupted by a barrier such as a breakwater or an islet. This process is similar to that for light or sound waves. The diffraction process causes wave energy to pass into the

shadow zone. Wave height distribution in a harbour or sheltered bay is determined to some degree by the diffraction characteristics of both the natural and manmade structures affording protection from incident waves. Diffracted waves are very important for coastal zones sheltered by offshore islands.

2.1.4. Reflection

Water waves may be either partially or totally reflected by coastal structures, beaches, etc. Impermeable vertical walls will reflect almost all incident wave energy and the height of a reflected wave will be equal to the height of the incident wave. Multiple reflections and absence of sufficient energy dissipation within a harbour complex can result in a build-up of energy which appears as wave agitation and surging in the harbour. The amount of wave energy reflected from a beach depends on the roughness, permeability and slope of the beach in addition to the steepness and angle of approach of incident waves. Reflected waves are observed to move away from steep beaches. In all cases of reflection, the reflected waves will encounter incoming waves producing complicated interference patterns.

2.1.5. Friction and Percolation

The common method of dealing with the transformation of waves as they propogate from deep water into shallow water is in terms of shoaling and refraction and it is assumed that there is no loss of energy at the bottom and that the energy is conserved between the wave orthogonals.

Keulegan (1948) and Putnam and Johnson (1949) have shown that dissipation of energy due to friction at the sea bed and percolation within the bed can bring about significant loss of energy, with a possible reduction in wave height. This is seen particularly for high waves of long period which are propogated into a shallow region of very gently sloping bottom. The rapid attenuation of energy for waves of long period can be explained qualitatively as due to the fact that the long waves effectively feel bottom over a greater distance than short waves.

Putnam and Johnson (1949) have shown for sinusoidal waves of small steepness (assuming that the Airy theory is valid in the presence of a frictional boundary layer at the bottom), that the amount of energy, D_f , dissipated per unit area at the bottom per unit time (averaged over a wave length) is

$$D_f = \frac{4}{3}\pi^2 \frac{\rho C_f H^3}{T^3 \left(\operatorname{Sinh} \frac{2\pi d}{L}\right)^3} \qquad (2.9)$$

Here C_f is called the friction factor which depends on the bottom sediment characteristics and wave parameters. The amount of energy loss due to percolation of water through a permeable sea bed assuming Airy wave theory is given by Putnam (1949) as

$$D_p = \frac{\pi q^2}{\nu} \frac{\rho p H^2}{L(\text{Cosh } \frac{2\pi d}{L})^2} \qquad (2.10)$$

for a bed having a depth greater than 0.3L. Here D_p is the dissipated energy per unit area of the bottom per unit time (averaged over a wave length) and p is the permeability factor.

In the presence of energy loss the transformed wave height is expressed as (Bretschneider and Reid,1954)

$$H = K K_r K_s H_o \qquad (2.11)$$

K represents the wave height reduction factor arising from energy dissipation which may be due to bottom friction, percolation, or both. Wave height reduction due to each of them can be expressed in terms of the friction coefficient, K_f ,and percolation coefficient ,K_p.

In the case of sandy bottoms, the effect of percolation can be significant, particularly in coarse sands. However,

for a muddy or clayey bottom, percolation presumably plays a very minor role and frictional effects will be dominant. For both percolation and friction, the bottom slope plays a major role since it decides the duration over which the waves will feel the bottom and expend energy by these dissipational processes. This slope factor makes the effect of bottom friction more severe for waves propagating over muddy bottom since they are comparatively gentle in slope.

2.1.6. Wave Breaking

When waves oversteepen, they become unstable and break. This can happen in deep water as well as in shoaling waters. The latter only is of interest here and hence it is discussed.

As the waves propagate in shoaling waters, the wave steepness H/L progressively increases due to increasing H and decreasing L. The wave crests also become narrower and peaked, the trough becoming wide and flat. Eventually the waves oversteepen, become unstable, and break. Depending on their steepness and the slope of the beach, four types of breakers are seen, viz. spilling, plunging, collapsing and surging.

Munk (1949) derived several relationships from a modified solitary wave theory relating the breaker height H_b, the breaking depth d_b ,the deep water height H_o and deep

water wave length L_o. His expressions are given by

$$\frac{H_b}{H_o} = \frac{1}{3.3(H_o/L_o)^{1/3}} \tag{2.12}$$

and

$$\frac{H_b}{d_b} = 0.78 \tag{2.13}$$

Subsequent observations and investigations by several authors have established that H_b/H_o and H_b/d_b depend on beach slope and on incident wave steepness (US Army, 1977). According to Komar (1983), the ratio of the breaker height H_b to depth d_b varies in the range 0.75 - 1.2, the exact value depending mainly on the beach slope. The Shore Protection Manual (US Army, 1977) suggests a formulation

$$\frac{H_b}{d_b} = b - a\, H_b/gT^2 \tag{2.14}$$

Where $a = 43.75\ (1 - e^{-19\,m})$ (2.15)

$$b = \frac{1.56}{1+e^{-19.5\,m}} \tag{2.16}$$

The value of H_b/d_b if known for a beach can be used for estimating the position of the breaker zone.

2.2. Wave Transformation and its Prediction

2.2.1. Transformation of Monochromatic Waves

Early works on wave transformation were concerned only with the transformation of monochromatic waves. It was based on the assumption that the ocean waves can be represented by a single period, direction and height. Studies with this approach were, till fifties, concentrated only on the aspects of shoaling and refraction and made use of the graphical method.

2.2.1.1. Graphical methods:

The graphical methods of wave refraction analysis are fundamentally based on the following assumptions (US Army, 1977):

(i) Wave energy between wave rays or orthogonals remains constant;

(ii) Direction of wave advance is perpendicular to the wave crest;

(iii) Speed of a wave of given period at a particular location depends only on the depth at that location.

(iv) Changes in bottom topography are gradual;

(v) Waves have long crests, constant period, small amplitide and are monochromatic ; and

(vi) Effects of currents, winds and reflection from beaches and underwater topographic variations are

negligible.

The graphical method of wave refraction analysis by Arthur et al. (1952) was being widely used till recently for computation of wave refraction. As these methods did not require any sophisticated equipment and the use of refraction templates did not require much of technical expertise, these methods became very popular. Studies using graphical methods are many for the Kerala coast as well as other parts of the coastlines of our country (Das et al. 1966; Reddy, 1970; Reddy and Varadachari, 1972; Varadarajulu, 1972; Antony, 1976; Gouveia et al. 1976; Reddy et al. 1979; John and Nayak, 1981; Prasad et al, 1981; Veerayya et al. 1981; Dhanalakshmi, 1982; Reddy et al. 1982; Shenoi and Prasannakumar, 1982; Prasannakumar et al, 1983; etc.).

2.2.1.2. Numerical methods

Of late, the numerical methods are being widely used because they are fast and accurate and are most useful when the study over an extensive area is required. Since sixties, a number of works are reported on the subject of numerical calculation and automatic plotting of refraction diagrams (Griswold, 1963; Harrison and Wilson, 1963; Wilson, 1966; Dobson, 1967; Mahadevan and Renukaradhya, 1983; etc.).

The above numerical methods are also based on the wave energy conservation assumption and accommodate only wave

refraction and shoaling. The fact that these models suffer from the assumptions made has been confirmed by the works of Johnson (1947), Longuet-Higgins and Stewart (1960), Chu (1975), Liu and Dalrymple (1984), etc. The other wave transformation processes also had to be accommodated in these methods to make them represent the natural conditions. Attempts were made by various researchers (Bretschneider and Reid, 1954; Bryant, 1979; Hendersen and Webber, 1980; etc.) to include these processes also in the wave transformation models and test their applicability in the field conditions.

Pioneering study on wave energy losses by bottom friction and percolation are presented by Putnam and Johnson (1949) and Putnam (1949). Beach Erosion Board (1953) discusses the results of laboratory studies conducted to test the theories of Putnam and Johnson. Friction tests for natural ripples indicated that loss of energy was dependent upon the stage of ripple formation and that the energy loss reached maximum during the formation of the ripples. For natural ripples, they found that the maximum rate of frictional loss agreed reasonably with the rate computed by the theoretical method of Putnam and Johnson. Percolation tests indicated that the energy loss by percolation were far less than the theoretical values. The test resulted in the general conclusion that energy loss by percolation were insignificant for sands of low permeability. The tests also

showed that in model tests where sands larger than 0.5mm are used as beach material, percolation losses can be very large, especially with sand sizes larger than 2 mm.

Bretschneider and Reid (1954) have carried out a theoretical investigation on the transformation of waves in shallow water by bottom friction, percolation, refraction and shoaling. Using the dissipation functions introduced by Putnam and Johnson (1949) and Putnam (1949) a general solution of the steady state wave height transformation equation is presented by them. Their computations show the relative insignificance of percolation over bottom friction. A semi-empirical expression for wave energy dissipation and wave attenuation by bottom friction have been developed by Kamphuis (1978).

Grosskopf (1980) evaluates the Bretschneider and Reid (1954) method for calculating the effect of bottom friction and shoaling using data gathered from 18 m and 10 m depths. He found that this method gave a close correlation with observed data, especially in cases where the wave spectrum is narrow and single-peaked. Most of the large underpredictions occurred, when no change or an actual increase in wave height was observed from offshore to inshore, possibly due to strong wind-wave generation.

Hallermeir (1983) provides a calculation procedure for nearshore wave height changes considering the energy dissipated by rough turbulent flow over a strongly agitated bed of quartz sand. From the computations he found that the general effect of energy dissipation was that the nearshore wave height remained more nearly constant than that predicted by linear wave theory.

Considering the importance of bottom friction as a significant energy dissipation factor, numerical models have been developed or the existing ones modified incorporating this factor (Coleman and Wright, 1971; Wright and Coleman, 1972, 1973; Skovgaard and Bertelsen, 1974, Skovgaard et al. 1975). Wright (1976) used the computer programme by Wright and Coleman (1972, 1973) to study the energy-regime of the Sydney-Jervis Coastal region and compared it with few coastal regions in the other parts of the world. Based on his studies in Broken Bay, Australia, Bryant (1979) concludes that the computer programme by Dobson (1967) with its subsequent modifications by Coleman and Wright (1971) can be used for calculation of breaker wave heights from deep water wave data.

Wherever coastal structures or offshore islands are there, diffraction and reflection also come into picture in addition to the refraction, shoaling and dissipation. Some insight into the problem of refraction-diffraction has been

provided by Battjes (1968). Houston (1981) presents a two dimensional finite element numerical model that calculates combined refraction and diffraction of short waves. Tsay and Liu (1982) presents a numerical study of wave refraction and diffraction problem based on the parabolic approximation. Since diffraction and reflection are not dealt with in the present investigation, no detailed discussion of the literature is being carried out here.

2.2.1.3. Friction factor

There is no consensus in literature regarding the friction factor to be used in the models. Bretschneider and Reid (1954) used a constant value of C_f = 0.01 in estimating frictional dissipation over the smooth fine grained bottom. Hasselmann and Collins (1968) obtained a value of 0.015 for the offshore waters of Panama City. More recently, the friction coefficient has been shown to vary significantly above and below these values. The friction factors obtained by some of the authors for different coastal waters are listed in Table 2.1.

Kamphuis (1975) presents the friction factor diagram after experimentation on shear stresses below waves and determination of bottom roughness. His work defines the wave friction factor in the laminar, smooth and rough turbulent regimes. Hsiao and Shemdin (1978) proposes a

Table 2.1. Friction Factors computed or used by different authors

Author	Location	Friction Factor
Bretschneider and Reid (1954)	Gulf of Mexico	0.01
Hasselmann and Collins(1968)	Panama City, Florida	0.015
Hsiao and Shemdin (1978)	Panama City, Florida	0.035 - 0.05
Hsiao and Shemdin (1978)	Marineland, Florida	0.008
Iwagaki and Kakimura (1967)	Japanese Coastal Waters	0.03 - 0.09
Grosskopf (1980)	Field Research Facility, CERC.	0.004 - 0.07
Van Ieperen (1975)	South Africa	0.06 - 0.10
Bryant (1979)	New South Wales	0.02
Wright (1976)	New South Wales	0.02

method for determination of friction factor for flat bottom as well as rippled sandy bottom by using this friction factor diagram. Nielsen (1983,1985) recommends determination of the friction factor for rough turbulent flow over natural sand beds by the following formulae suggested by Jonsson (1980):

$$C_f = \exp\left[5.213\left(\frac{r}{a}\right)^{0.194} - 5.977\right] \qquad (2.17)$$

$$\text{for } \frac{r}{a} < 0.63$$

$$C_f = 0.30 \quad \text{for } \frac{r}{a} \geq 0.63$$

where r is the Nikuradse bed roughness decided by the ripple geometry and the skin friction Shields parameter (Nielsen, 1983) and a is the water particle semiexcursion.

A somewhat simpler formula of Kajiura ~~(1968)~~ reported in Nielsen (1985) is

$$C_f = 0.37\left(\frac{r}{a}\right)^{2/3} \text{ for } \frac{r}{a} > 0.02 \qquad (2.18)$$

Values of C_f greater than 1 are also reported in literature (Nielsen, 1983, 1985).

Different authors have used different friction factors for field evaluation of numerical models. While Grosskopf

(1978) got good results for C_f between 0.004 and 0.07, Bryant (1979) used a value of C_f = 0.02. Wright (1976) used a C_f value of 0.02.

2.2.1.4. Effect of currents

An introduction to the problem of refraction by currents is given by Johnson (1947). When waves propogate obliquely into a zone containing a current, the wave gets refracted. The extent to which the current will refract the incident wave depends on the initial angle between the wave crests and the direction of current flow, the characteristics of the incident waves and strength of the current. Transformation takes place also when a current is aligned with an orthogonal. Currents flowing in the opposite direction to the wave propogation will cause a decrease in wave length and an increase in wave height. Wave steepness may be increased sufficiently to cause wave breaking (Earle and Bishop, 1984). On the other hand a following current will tend to increase the wave length and decrease the height. Using second order Stokes theory, Jonsson et al (1970) have derived H/H_o and L/L_o in various depths for a dimensionless current parameter.

Battjes (1982) presents the effects of tidal currents on the wave height in the tidal delta region of Oosterschelde estuary in the Netherlands. Observations of

the variations of wave height with tidal elevation during a tidal cycle show a hysteresis. This is confirmed from computations using a theoretical model, which includes depth and current refraction. Christoffersen and Jonsson (1985) defines a wave friction factor and a current friction factor for a combined current and wave motion. Two 2-layer eddy viscosity models are presented in order to describe the velocity field and associated shear stress.

2.2.2. Transformation of Random Waves

The ocean waves are always random in nature. However, for simplicity in the computation of wave transformation, the wave field is usually represented by a monochromatic wave. This may not give a completepicture of wave conditions along the shorelines. Hence it is more appropriate to represent the sea in its natural condition (random) in the transformation models.

One of the established methods of representing the random sea is through the wave spectrum, which gives the distribution of energy density in the frequency domain. Hence studies on spectral transformation is essential in understanding and predicting the random wave characteristics in shallow water.

2.2.2.1. Deep and shallow water spectra

There have been quite a good number of studies on spectra of deep and shallow waters. The spectral forms are usually studied and compared in terms of the slope of the high frequency side, spectral width and the spectral peakedness.

For deep water wind generated gravity waves Phillips (1958) proposed that the maximum energy density may be expressed as

$$S_m(f) = \alpha g^2 (2\pi)^{-4} f^{-5} \qquad (2.19)$$

where α is a universal constant. This has been the basis for the later models (Pierson-Moskowitz, JONSWAP, etc.). The other forms used for deep water conditions are after Bretschneider (1963), Scott (1965), Neuman (1953), etc., among which Scott has been widely recommended for the west coast of India (Dattatri, 1977; Deo and Narasimhan, 1979; Narasimhan and Deo, 1979; etc.).

For the Phillips model the shape of the high frequency tail is inversely proportional to the fifth power of frequency(f^{-5}). But in the deep water conditions many authors (Hasselmann et al, 1973; Dattatri et al., 1977; Narasimhan and Deo, 1979 etc.) obtained higher values. Further studies (Toba, 1973; Forristall, 1981; Kahma, 1981;

Kitaigorodskii, 1983) have shown that the power is close to four.

For shallow waters, Goda (1974) found that the slope of the spectra in the high frequency range is milder than f^{-5}. Kitaigorodskii et al. (1975) proposed a spectral form for shallow waters with a slope of f^{-3}. Many recent researchers (Ou, 1977; Vincent, et al, 1982; Baba and Harish, 1986) have obtained in general lower values (even 1.5) for shallow waters.

According to Lee and Black (1978), deep water spectrum which has low energy in the low and high frequency bands increases as the waves enter the shallow water and the energy shift from the peak. This shift results in the production of multiple crests. Similar observations are made by Harris (1972). According to Thompson (1980), multi-peakedness is a typical characteristic of shallow water spectra. Vincent (1982) opines that the frictional mechanism, the nonlinear transfer mechanism and the white-capping/breaking all have roles in the modification of wave spectra in shallow water and the shape is decided by the balance among the three. Le Mehaute (1982) compared shallow water and deep water spectra from wave measurements at 18m and 212 m depth respectively. According to his results, a complex deep water wave field (evidenced by a broad band

spectrum with multiple peaks) is converted by the bathymetry to a simple, almost monochromatic, wave train of much lower amplitude and longer period. Thompson (1974) also had observed very narrow spectra in the coastal zone.

Provis and Steedman (1986) established seven wave measuring stations along a line perpendicular to the coast in the Great Australian Bight extending upto a depth of 1150 m offshore. From the spectral comparisons they found that there was no significant change in the nondimensional spectrum. They observed significant energy loss. A reduction in energy to about one quarter as the waves travel from the offshore to the inshore station of depth 26m was observed.

2.2.2.2. Numerical models

Compared to the monochromatic approach, there are relatively less number of studies in the development of theoretical concepts and numerical techniques concerning spectral transformation. Pierson et al. (1955) was the first to suggest a method to estimate the effect of wave refraction on a wave spectrum. His method essentially consists of constructing monochromatic wave refraction diagrams for many different wave frequencies and directions and then combining the various wave components at the shallow water point of interest to get the spectrum.

Karlsson (1969) developed a finite differnce technique to compute the spectral transformation over parallel bottom contours. Collins (1972) extended this work to include the effects of bottom friction. He formulated two numerical models for shallow water wave prediction and tried to correlate them with observed data. According to him nonlinear interactions within the wave spectrum is of importance in deciding energy content in the low frequency part in shoaling waters.

Shiau and Wang (1977) and Hubertz (1980) reported numerical techniques to compute the transformation of wave spectrum over irregular bottom topographies and prevailing currents. Both of these models have the same numerical procedure. The model by Shiau and Wang (1977) was field tested by Wang and Yang (1976) at the Island of Sylt, West Germany. They made wave measurements at 7 selected stations in shallow water constituting one transect perpendicular to the shoreline and another parallel to the shoreline. They found that the numerical prediction yielded quite acceptable results in the energy-containing wave components and long-wave components and the numerical results were unsatisfactory in high frequency components where local

effects of energy dissipation, generation or transfer are deemed to be more important.

The method of Shiau and Wang (1977) were further improved by Wang and Yang (1981) to include the effects of bottom friction. The field data at the Island of Sylt supported the validity of the numerical model. The results suggest that prior to wave breaking, the transformation of wave components is mainly influenced by shoaling and refraction. They observed that the bottom frictional effect could also be important in the energy containing range. This is in deviation to the observations of Wang and Yang (1976). Hubertz (1981) discusses results of field testing of his spectral model and another wave ray model in an area near the CERC's Field Research Facility at Duck, North Carolina. A comparison of the results from both the models and measurements indicates that landward of the pier end (depth about 8m) greater reduction of wave height is found in the measured than in the model tests. This attenuation is assumed to be due to frictional and diffractive effects, which are not simulated by these models.

Le Mehaute and Wang (1982) present methods for computation of spectral transformation that are applicable when shoaling and refraction effects dominate dissipative effects, which occur near shorelines. It is found from

verification with field data that the main peak of the spectrum is well accounted by the theory. Further it is recommended that any improvement of existing theories should take nonlinear effects into account.

Chen and Wang (1983) has developed a model for computing non-stationary wave transformation from deep water to shallow water incorporating shoaling, refraction, current effects, other nonlinear dissipative processes and local wind wave generation processes. The model evaluation was tried using only one set of wave data collected in the North Sea.

Forristall and Reece (1985) observed during the Sea Wave Attenuation Measurement Experiment (SWAMP) that theoretically calculated refraction and shoaling account for the changes observed in the spectra when the wave height is low. As the wave height increases, a nonlinear attenuation mechanism becomes more and more important. According to them, the rate of attenuation can be described as a strong function of deep water H_s and a weak function of wave frequency, to first order.

Treloar (1986) presents a method by which offshore frequency-direction wave spectra may be used to determine inshore wave coefficients in a current-depth refractive area.

2.3. Summary

The different shallow water wave transformation processes are refraction, shoaling, reflection, diffraction, dissipation of energy due to bottom friction, percolation etc. and wave breaking. Refraction and shoaling have been studied extensively and the early methods for shallow water wave prediction accounted for only these two processes. The necessity for introduction of nonlinear dissipation processes and other transformation processes in the models have been confirmed from the recent works of different authors. Effects of currents assume significance in zones of strong coastal currents or near tidal inlets. Diffraction and reflection need to be accounted only in cases where coastal structures or offshore islands are present. Different formulations are avilable in literature regarding shallow water wave breaking and they can be used in models for determination of breaker positions and breaker heights.

There are two different approaches for modelling of shallow water wave transformation. One is the wave ray approach which is based on monochromatic assumption. The graphical method of wave refraction based on this approach was being used till recently. Of late, the numerical methods are being preferred. The computer programme by Dobson with its subsequent modification has been field-

tested in some conditions. It is yet to be tested for the Indian coastal waters.

The second approach is the spectral method where the modelling is done to get the shallow water spectrum from deep water spectrum. This has an advantage over the monochromatic method that it accounts for the randomness of waves. Compared to the monochromatic method, the number of models in this method are few. The computer models by Hurbertz (1980) and Shiau and Wang (1977) appears to be promising. Various contradicting views presently exist on the mode of transformation of wave spectra and particularly on the shape of the transformed shallow water spectra. However there is an agreement in literature regarding lower values for the slope of the high frequency side of the wave spectra in shallow waters. These aspects need to be confirmed from synchronized deep and shallow water measurements.

There is no consensus in literature regarding the friction factor to be used in transformation models. Factors ranging from values as low as 0.004 to as large as unity have been reported in literature.

The review also shows the need for more synchronized deep and shallow water wave measurements at different locations of the world oceans and evaluation and further improvements of the existing models based on such a data

base. No field evaluation of any of the wave transformation models has been carried out for the Indian coast.

CHAPTER 3

DATA COLLECTION AND ANALYSES

This chapter confines to the field programmes, method of data collection and analyses undertaken in connection with the present investigation. A brief description of the locations of field programmes and the reasons for the selection of these locations are given. Since two types of wave recording systems were used, a comparison of their relative performance was carried out and the results presented in this chapter.

3.1. Field Programmes

3.1.1. Location

The field programmes in connection with the proposed work were carried out at two different locations along the Kerala coast, viz. Trivandrum and Alleppey (Fig. 3.1.). These locations were particularly selected for this investigation because they present a wide range of field parameters,which help the evaluation of the prediction models for their applicability along the entire Kerala Coast.

The differences in shallow water wave climate between the two locations are discussed by Baba et al. (1983a,b and 1987). Trivandrum is a high energy coast

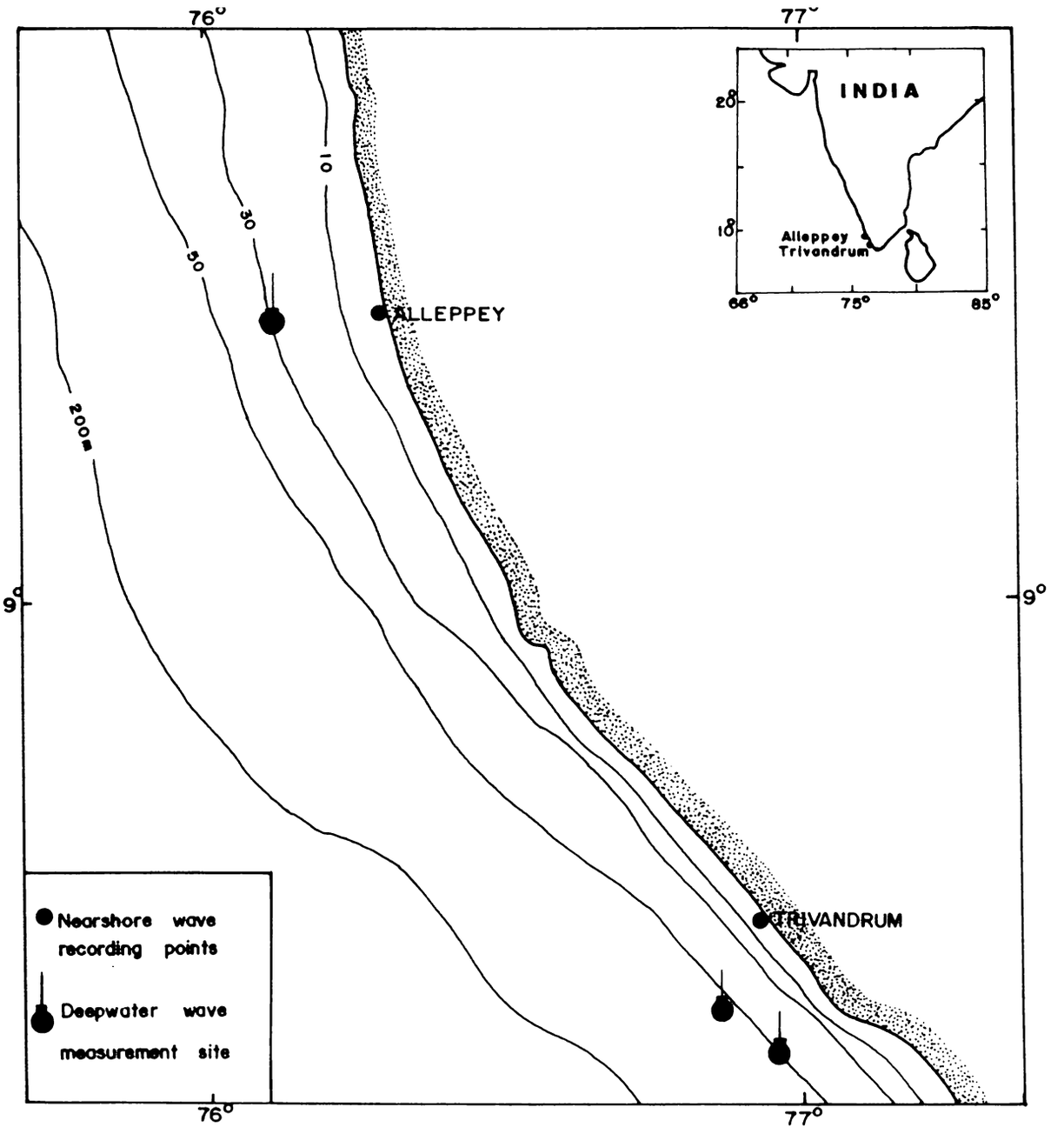

Fig.3.1 Location Map with Wave Recording Stations

compared to Alleppey. Significant wave heights of the fair-season (November-April) and rough season (May-October) for the year 1982 are reproduced from Baba et al. (1987) in Fig. 3.2. During the rough season, the significant wave heights (H_s) exceed 2.0 m at Trivandrum and 0.9 m at Allepey for 50% of time. During fair weather H_s exceed 1.0 m at Trivandrum and 0.6 m at Alleppey for 50% of time. The maximum nearshore wave heights reported during the period 1980-85 are 6m and 3.8 m respectively at Trivandrum and Alleppey (Baba, 1985).

While the coastline has approximately NW-SE orientation at Trivandrum, it has NNW-SSE trends at Alleppey (Fig. 3.1). Both the coastlines are more or less straight. Trivandrum is characterised by a steep inshore shelf gradient, while Alleppey is fronted by wide, and flat inshore profiles (Fig. 3.3). From a depth of 20 m offshore, though the slopes of both the profiles remain the same, the shelf at the same offshore distances is considerably deeper at Trivandrum than Alleppey.

The shelf sediment characteristics vary much at these two locations. Studies by Hashimi et al. (1981) have shown that the shelf sediments are having mean sizes of 346 μ and 31 μ respectively at Trivandrum and Alleppey. During the course of this study, size-characteristics of inshore sediments were further studied, which are discussed later.

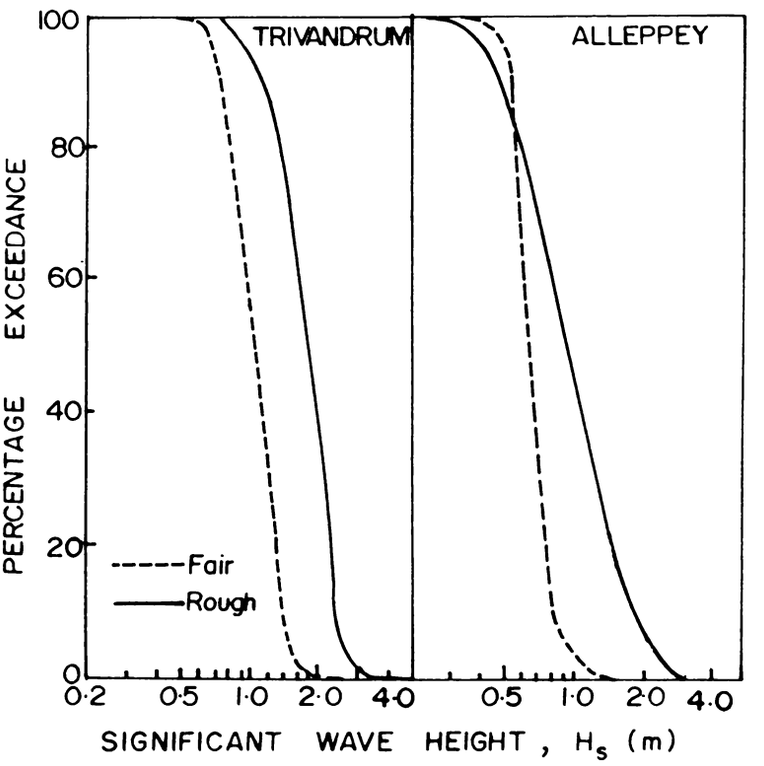

Fig.3.2 Percentage Excedance of Wave Height (after Baba et al, 1987)

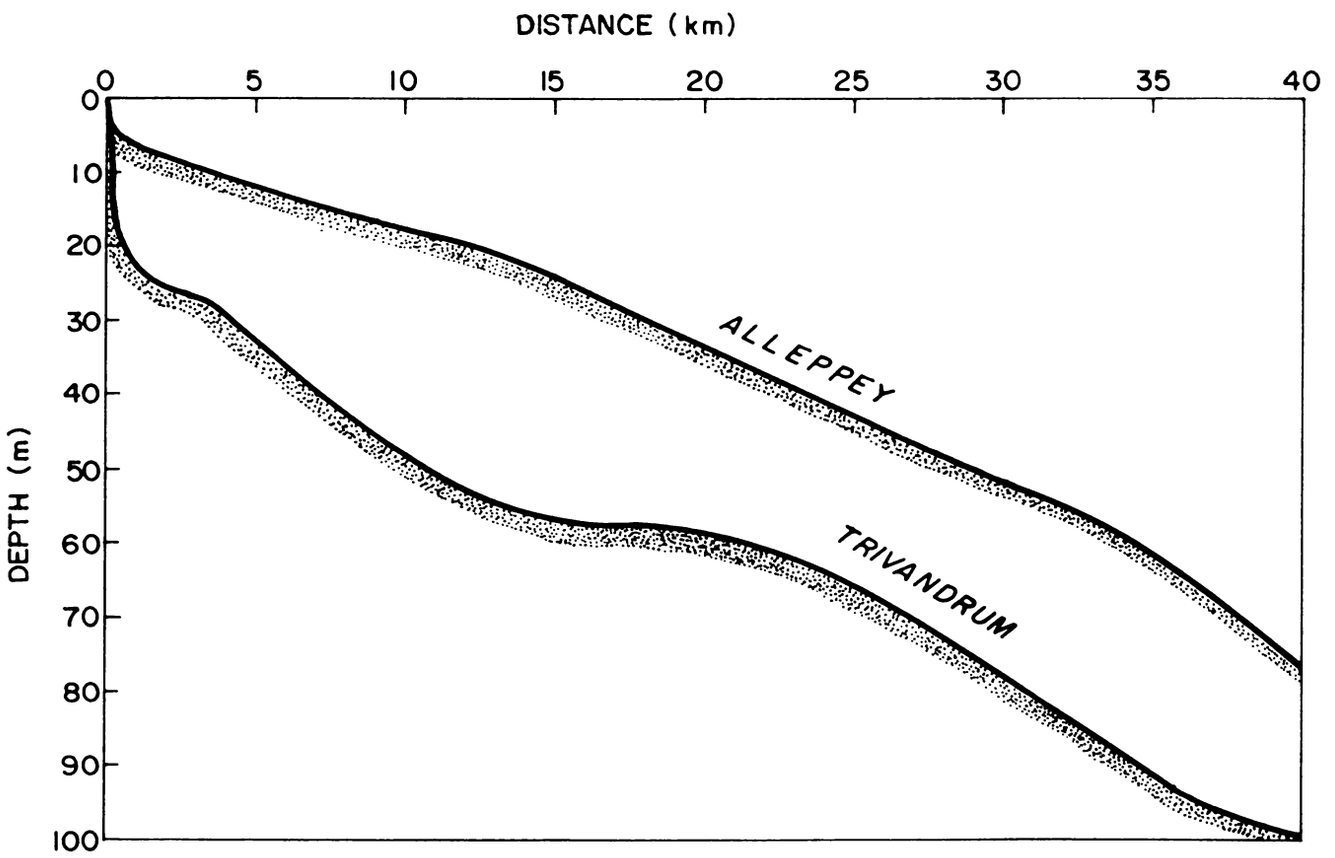

Fig.3.3 Shallow Water Bottom Profiles

Data on coastal currents is scanty for this coast. Current measurements off Cochin by Premchand (1987) indicate that the coastal currents are generally sluggish; hence currents may not play any significant role in the wave transformation off this coast.

3.1.2. Wave Recording

The wave measurement essentially involved the synchronised deep water and nearshore wave recording using wave recorders.

3.1.2.1. Deep water recording

For the measurement of deep water waves, a Datawell Waverider buoy was used. The description of the waverider system and details of its mooring are available in Nayak and Anand (1981). The sites of operation of the buoy at the two locations are indicated in Fig. 3.1. The buoy was operated off Trivandrum at depths of 60m during October 23-24, 1983 and 48m during May 19 -June 12, 1984. The buoy was operated off Alleppey at a depth of 30m during May 14-15,1984. The offshore depth covered at Alleppey was limited to 30m because of the greater width of the shelf there and the consequent logistic problems associated with the coverage of the distance. During all the operations, the WAREP receiver of the buoy was kept at shore and continuous wave recording was carried out, except during night hours, when the

recording was in the programme mode for half an hour durations at intervals of 1 h or 3 h. Deep water wave directions were measured using a Brunton Compass during attended operation of the buoy. During the unattended operation the ship observations of IDWR and the coastal observations were depended upon for wave directions.

3.1.2.2. Nearshore wave measurement

Nearshore waves at both the locations were measured using a pressure recorder. The description of the equipment and the mode of installation are given in Baba et al. (1983a). The sites of nearshore wave recording are shown in Fig. 3.1. Both the sites of measurement had a depth of 5.5m and the transducers of the system were at a depth of 3m from Mean Water Level (MWL). The wave recordings were carried out for 30 minutes duration at intervals of 3 h during the period of operation of the waverider buoy. Directions of nearshore waves were measured at least twice daily using a Brunton Compass at the measurement sites.

3.1.2.3. Synchronised recording at the same site

For a comparative study of the performance of the two systems, the pressure recorder and the waverider were operated simultaneously at the same site off Alleppey. This is achieved by deploying the waverider buoy at the nearshore wave recording site adjacent to the pressure recorder.

Simultaneous wave recordings were carried out in both the systems for a duration of two and half hours.

3.1.3. Bathymetric surveys

Accurate and updated bathymetric charts, especially for the inshore, were an essential requirement of the investigation. Detailed bathymetric charts of the inshore zones of the present study area had been prepared in Centre for Earth Science Studies based on the surveys carried out during 1981-82 (Baba et al., 1983b). These charts were updated with some more soundings during the course of the present field programmes. The 'Skipper' echosounder was used for the soundings. The position fixing was carried using a 'miniranger', which gives distances of offshore points from shore reference stations, at Trivandrum and theodolites at Alleppey.

3.2. Analyses

3.2.1. Analyses of Wave Records

The following analyses were carried out on the wave records collected.

3.2.1.1 Tucker-Draper method

Analyses of wave records were carried out using the Tucker-Draper Method as given in Silvester (1974) for the

deep water as well as nearshore wave records. Since the nearshore records were collected using the pressure recorder which has a pressure transducer, attenuation corrections had to be applied to the height parameters H_1 and H_2 derived from this analysis. The method of pressure attenuation correction followed is discussed in Section 3.3. The significant wave height (H_s) and zero-crossing period (T_z) derived from this analysis were used for the study of transformation of wave height and verification of models.

3.2.1.2. Wáve-by-wave method

The wave-by-wave zero-up-crossing method of analysis was carried out on the records, which were used for the comparison of the performance of buoy and pressure recorder. The H_s and T_z derived from this study were used for the comparisons.

3.2.1.3. Spectral analyses

The spectral analyses of wave records was carried out using the FFT method. The stability and accuracy of spectral estimates depend on many parameters such as record length, sampling interval, number of points etc. (Goda, 1974; Harris, 1974; Baba et al., 1986; etc).The digitisation and analysis were carried out, keeping the optimum conditions (Baba et al., 1986) given below in view, in order to get best and reliable results. Except for the few

records used for the study in Section 3.3., all waverider and pressure records were digitized at intervals of 0.5 s and 0.6 s respectively and the total number of data points were 2048 for each record. Since the chart paper speed could not be maintained uniform for both the types of records, the digitization intervals varied slightly in view of the convenience in the digitisation, which had to be carried out manually. The slight difference in the digitisation interval may not affect the comparability of the spectra (Baba et al., 1986). The digitisation interval was kept uniform at 1 s for both the types of records used in Section 3.3. and the number of data points were 1024.

The computer programme (Hameed, 1985, unpublished) used for the computation of spectra and spectral parameters has provision for correcting the pressure recorder data for pressure attenuation, which is again discussed in Section 3.3.

3.2.2. Analysis of Sediment Samples

Sediment samples collected from the inshore regions (5-15 m depth) of the locations of study during 1980-81 were used for the size-gradient analysis. The samples were chemically dispersed using sodium hexametaphosphate solution as per standard procedures and separated into sand fraction and fine fraction (clay and silt). Mechanical sieving was

carried out for sand fractions and pipette analysis for fine fractions. The results are presented in Table 3.1.

3.3. Comparison of Performance of Waverider and Pressure Recorder

3.3.1. Need for the Comparison

In the present investigation since data derived from two different systems were to be used for comparison and verification of the models, a comparison of the relative performance of the two systems was carried out first. The data collected as in subsection 3.1.2.3. were used for this study.

The major uncertainty in the use of pressure recorder data is related to the pressure attenuation correction required for the wave height. The pressure attenuation correction formula,

$$H = H' K_n \frac{\cosh(2\pi d/L)}{\cosh\left[\frac{2\pi d}{L}(1-z/d)\right]} \qquad (3.1)$$

where H and H' are the corrected and uncorrected waveheights respectively, z and d are the transducer and station depth respectively), consists of an instrument factor K_n which has been assigned values ranging from 1.1 to 1.5 by various researchers (Homma et al., 1966, Cizlak and Kowalzki, 1969;

Table 3.1 Average Size Characteristics of Nearshore Sediments (depth : 5-15 m)

Location	Sediment size (mm)	
	Median	D_{90}
Trivandrum	0.203	0.368
Alleppey	0.029	0.088

Dattatri, 1973; etc). Bergan et al. (1968) found from their laboratory tests that the spectral wave heights were well predicted without the empirical factor K_n for a pressure record.

To obtain the surface spectrum from the pressure spectrum, Black (1978) proposed the following relationship

$$S(f) = S'(f) \frac{\cosh^2 \frac{2\pi d}{L}}{\cosh^2 \frac{2\pi d}{L} (z+d)} \qquad (3.2)$$

where $S'(f)$ and $S(f)$ are the uncorrected and corrected pressure spectrum respectively. In the absence of a standard procedure for pressure attenuation correction, a comparison of the performances of the two systems used in the present investigation was felt very important.

3.3.2. Comparison of Wave Heights

The wave records collected from both the systems during the simultaneous operation were subjected to the Tucker-Draper, wave-by-wave and spectral methods of analyses. The height parameters H_1 and H_2 derived from Tucker-Draper method and H_s from wave-by-wave method for the pressure recorder were further corrected for pressure attenuation using equation (3.1) without instrument factor (i.e. $K_n = 1$) and with $K_n = 1.25$, as proposed by Dattatri (1973). In Fig. 3.4 the H_1 and H_2 values for the wave rider records

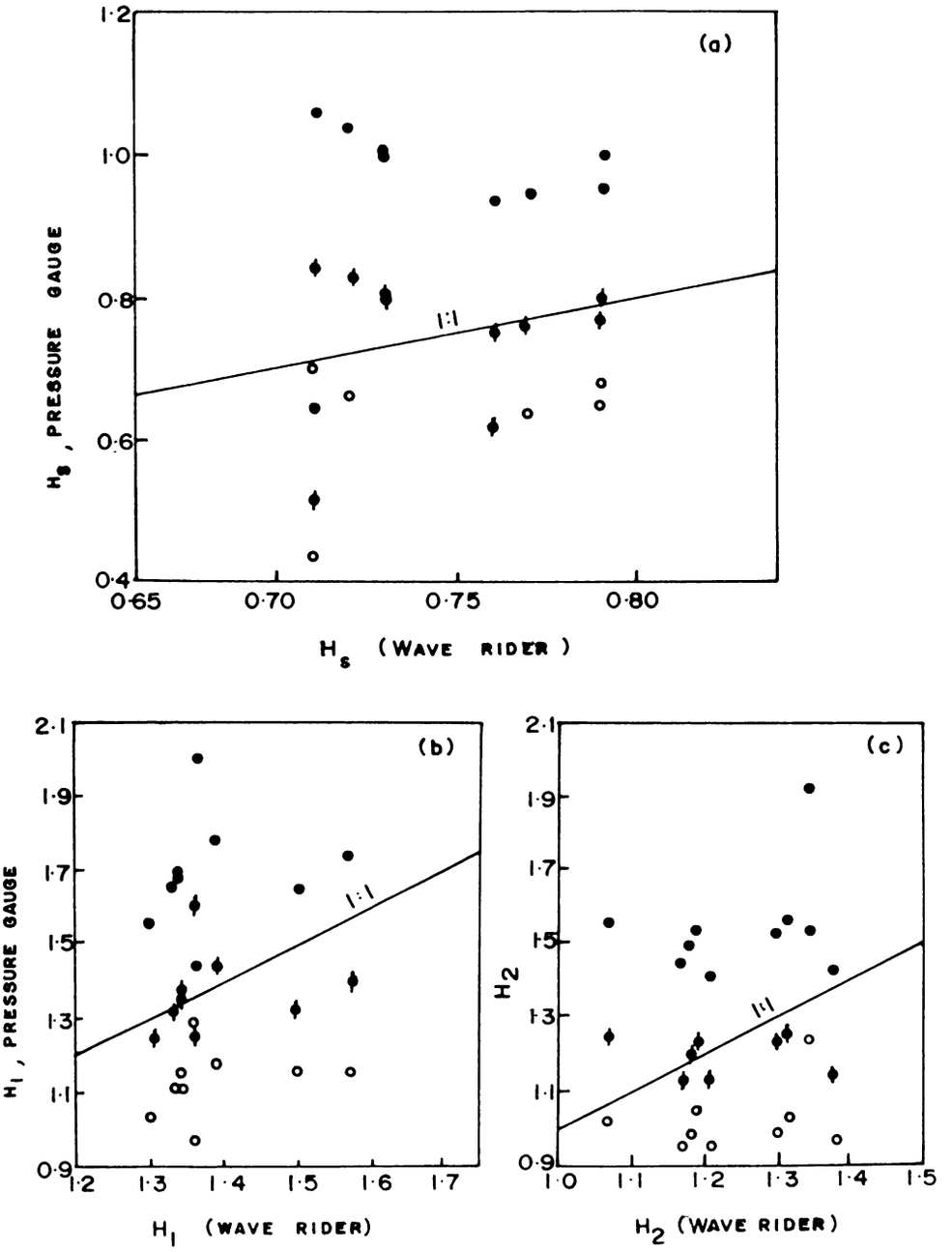

Fig. 3.4 Comparison of Wave Heights

• - Instrument factor = 1·25, ○ - No attenuation correction

♦ - No instrument factor

are plotted against the corresponding values for pressure recorder without attenuation correction, and with attenuation correction using K_n = 1.0 (i.e. no instrument factor) and K_n = 1.25. It is seen that there is good correlation between the wave rider and pressure recorder heights when the attenuation correction is applied to the latter without any instrument factor.

3.3.3. Comparison of Period Parameters

The plot of wave period parameters T_z and T_c of the pressure recorder against waverider is given in Fig. 3.5. The period parameters obtained from the pressure recorder are always higher than the corresponding ones for waverider. This is due to the differences in the response characteristics of the two systems. The pressure recorder used has 100% response only for periods above 5 s and the response is 95% for periods between 3 and 5 s (Baba et al, 1986). In the case of waverider the 100% response starts from a period of 3 s. Hence very short period components get filtered in the pressure record resulting in a shift of the period parameters towards higher period side.

3.3.4. Comparison of Wave Spectra

Spectral analyses were carried out for the wave records from the two systems. Pressure attenuation corrections using equation (3.2) were provided for the pressure recorder

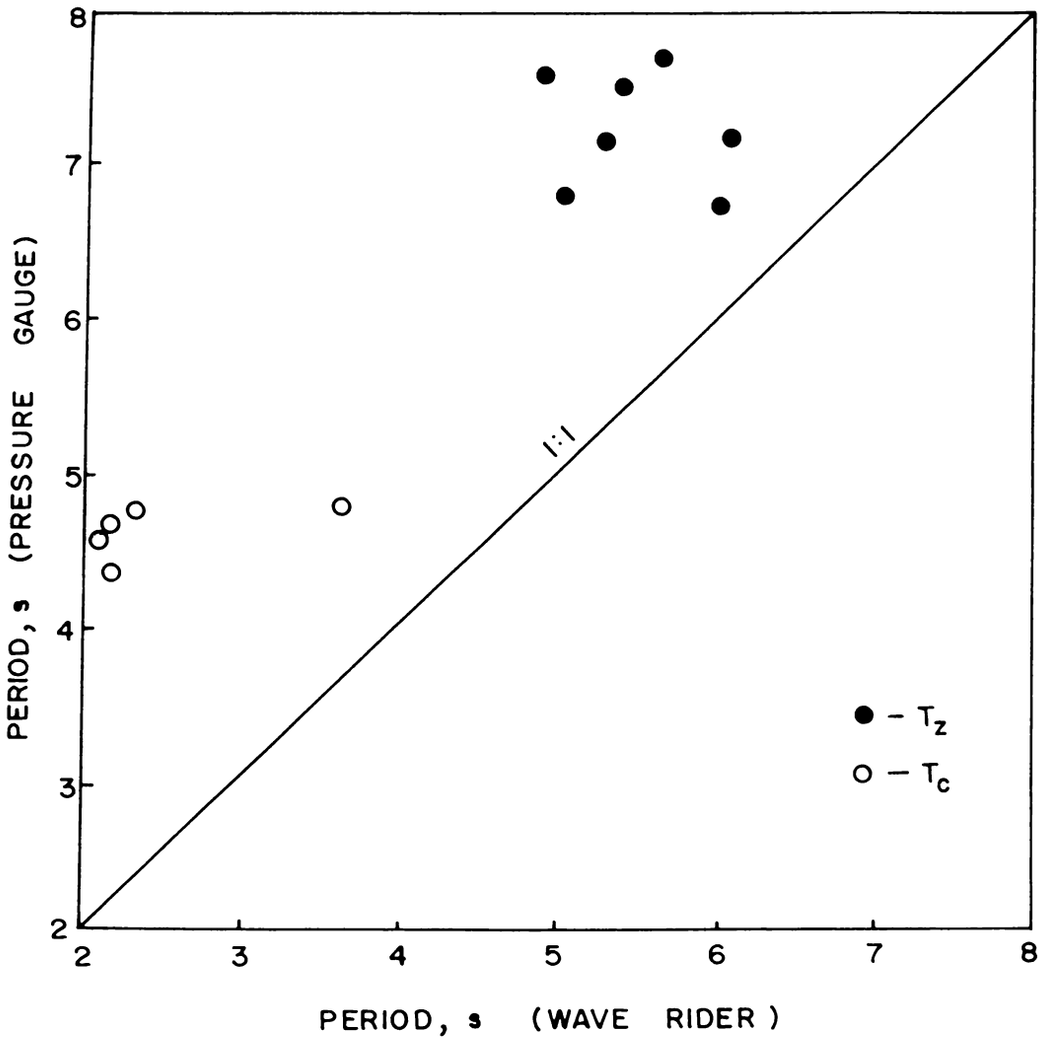

Fig. 3·5 Comparison of Period Parameters

spectra. Table 3.2 and Fig. 3.6 give a comparison of spectral parameters and spectra respectively from the records of both the systems. The spectra of wave records from the two systems compare well. In Table 3.2, the two values in sequence ~~against~~ given for each parameter are for 1205 and 1235 Hrs respectively. The spectral moments from both the systems nearly tally. The significant wave heights and the spectral peakedness parameter Q_p are also comparable. Like the other period parameters(T_z and T_c) the spectral peak period T_p of pressure recorder is higher than waverider when no smoothening of the spectral lines is done. However, when smoothening of spectral lines into spectral bands of frequency 0.0078 (which is used for plotting the spectrum in Fig. 3.6) is done, the peak periods are comparable as is seen in Table 3.2. The average periods are also comparable. Thus the results show that the periods derived from spectral analysis are more comparable.

3.3.5. Summary of Results of Comparison

Wave heights from pressure recorder corrected for pressure attenuation using equation (3.1) without any instrument factor gives good comparison with wave rider heights and Hence the pressure recorder heights so derived can be used along with waverider data for study of wave transformation and for verification of models. The spectra derived from pressure recorder after corrections using

Table 3.2 Comparison of Spectral Parameters

Parameter	Waverider	Pressure Recorder
m_o	0.042	0.050
	0.035	0.039
m_1	0.006	0.007
	0.005	0.005
m_2	0.001	0.001
	0.001	0.001
H_s(m)	0.82	0.88
	0.75	0.79
$\overline{T}$ (s)	7.0	6.9
	6.9	7.4
T_p(s)	16.0	16.0
	14.0	16.0
Q_p	1.6	1.5
	1.7	1.6

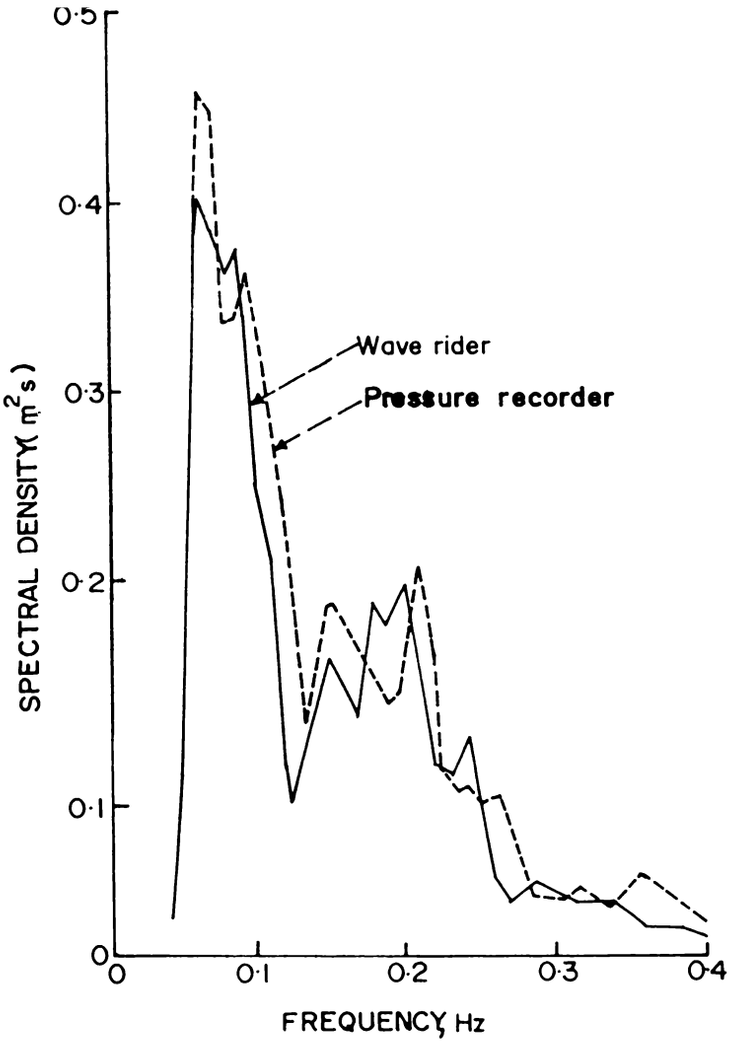

Fig. 3.6 Comparison of Spectra

equation (3.2) compare reasonably well with waverider spectra and hence both can be used together for study of spectral transformation. While wave period parameters from Tucker-Draper analysis are always higher for the pressure recorder, the spectral analysis gives comparable values.

CHAPTER 4

OBSERVED WAVE TRANSFORMATION

4.1. Introduction

Before proceeding to the prediction of wave transformation, it is intended to study the major features of wave height and spectral transformation along this coast based on a comparative study of synchronised deep and nearshore wave data. Studies on wave transformation based on synchronised data are lacking for the Indian coasts, and are few for the other parts of the world. Such a study would enable in delineating the various processes at work.

For this study, measured wave data off Trivandrum and Alleppey are used. However, off Alleppey, since the measured deep water waves did not cover the higher range of wave characteristics, ships observations of IDWR were also depended upon to get a wider range. In this chapter, the deep water and nearshore wave characteristics including their spectral forms are discussed first and then the features of transformation are studied by comparing the synchronized deep water and nearshore wave data.

4.2. Characteristics of Deep Water Waves

4.2.1. Height, Period and Direction

The deep water wave characteristics used for the study

covered a broad spectrum in terms of the wave characteristics. The significant wave heights ranged from 0.5 to 4.5 m and the period (zero-crossing) from 5 to 11 s. The highest values are shipbased observations off Alleppey. The direction varies from 220° to 320° N off Alleppey and from 185° to 300° N off Trivandrum. Fig.4.1a. is a scatter diagram of the deep water height (H_s) and period occurrences. Waves with height 1.0-2.0 m and period 5 - 7 s dominate . The wide range in the height, period and direction were possible because the data corresponded to the premonsoon and monsoon seasons. As can be seen from the scatter diagram, the wave steepness exceeded 1:50, which is expected during the rough weather conditions. The occurrence of rough, steep wave conditions in the deep water with advance of season is clearly seen in Fig.4.2 where the daily (1200 Hrs) variations in deep water wave height and period off Trivandrum are presented. The H_s reaches the maximum value of 2.7 m in the first week of June.

4.2.2. Deep Water Wave Spectra

4.2.2.1. Spectral characteristics

Literature on deep water wave spectra is particularly lacking for this coast. The deep water wave spectral characteristics and wave spectra are given in Table 4.1 and Fig. 4.3 respectively. The spectral peaks before the onset of

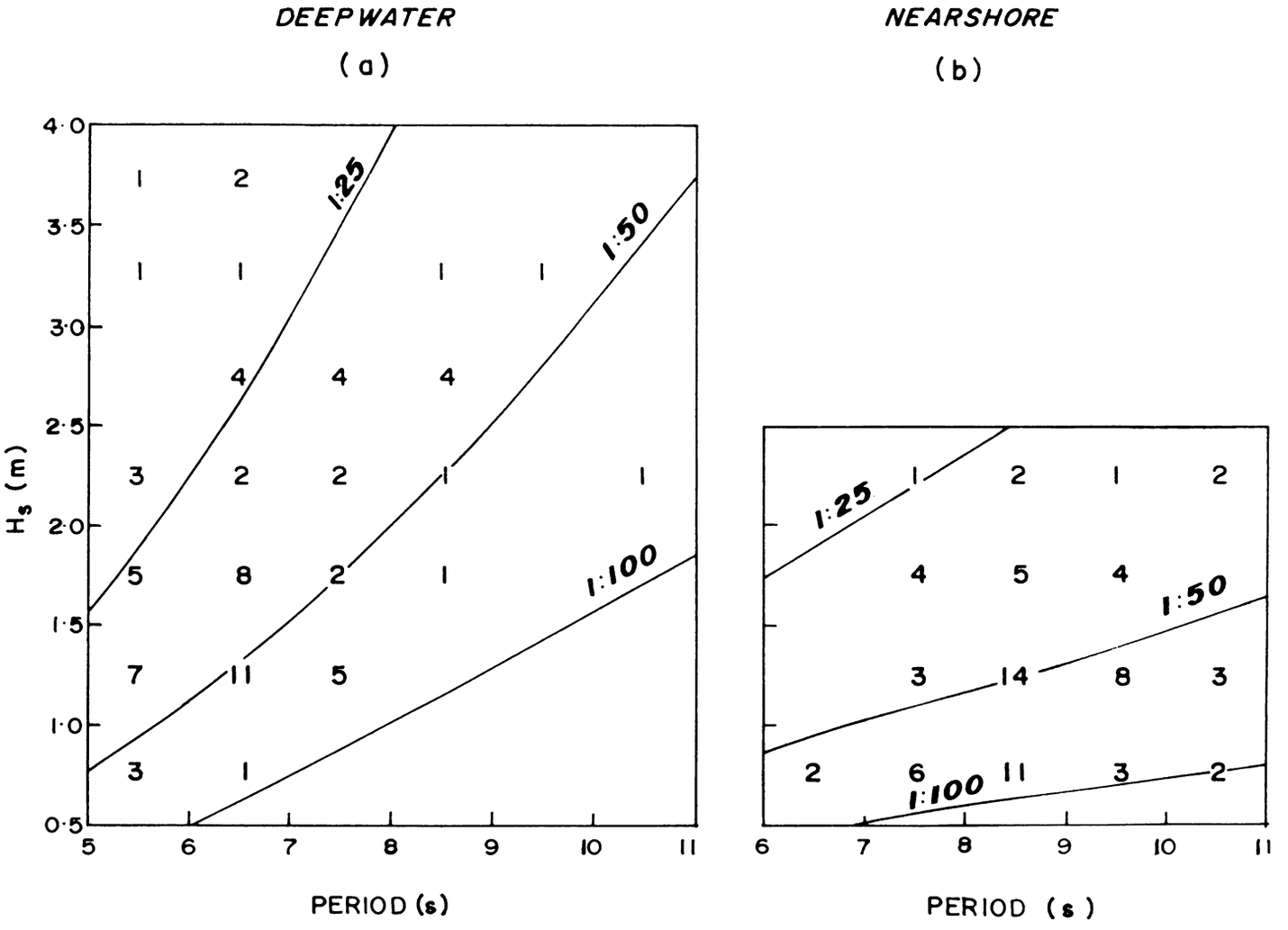

Fig. 4.1 Scatter Diagram of Deep Water and Nearshore H_s & T_z

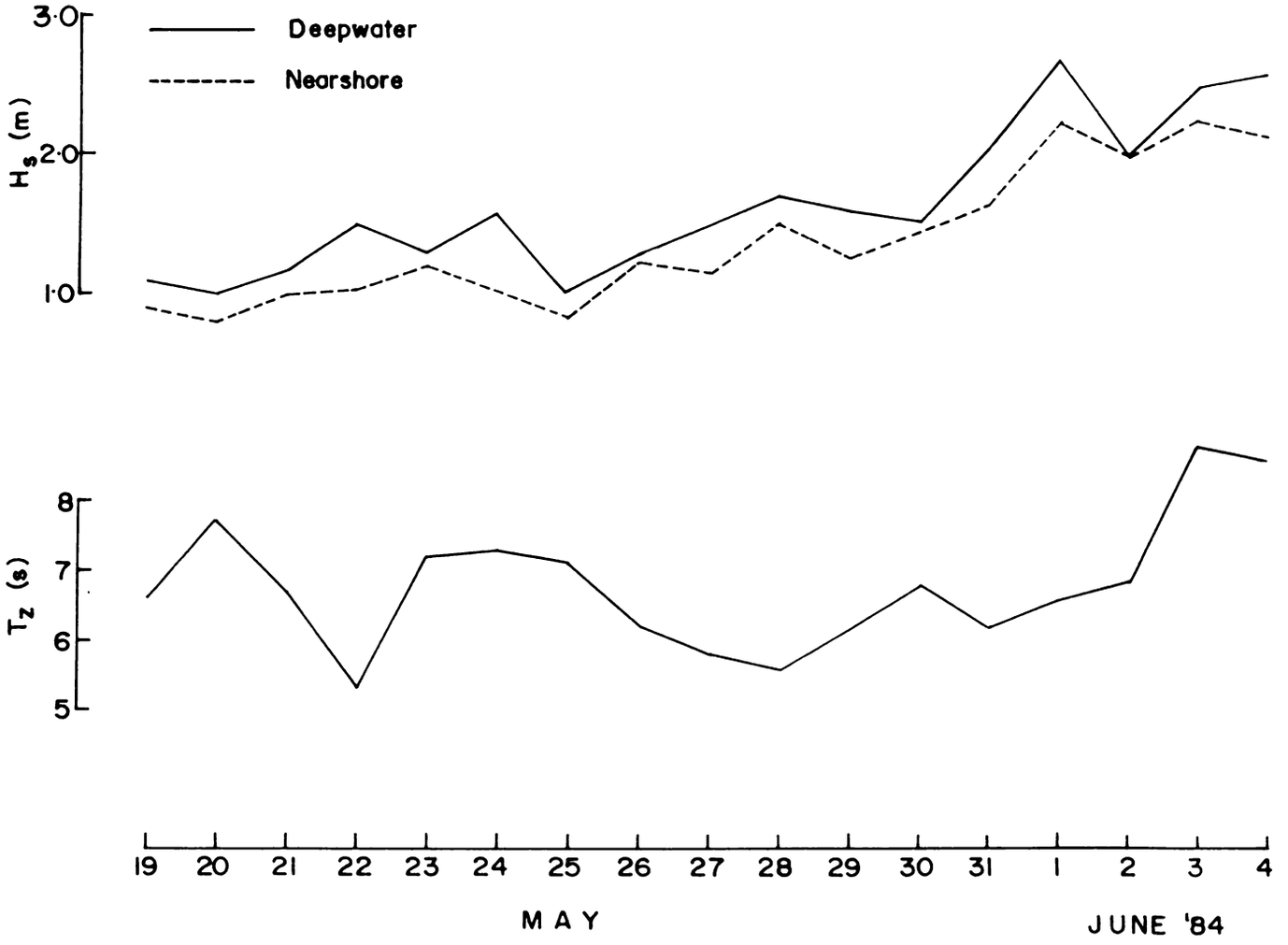

Fig.4.2 Daily Variation of Deep Water and Nearshore H_s & T_z

Table 4.1

Spectral Characteristics of Deep Water Waves

Location	Date	Time Hrs. IST	m_o (m^2)	m_1 (m^2)	H_s (m)	Q_p	ϵ	Ist peak		2nd peak	
								T_{p1} (s)	S_{p1} (m^2s)	T_{p2} (s)	S_{p2} (m^2s)
TVM	19.5.84	1200	0.06	0.01	0.96	1.69	0.7	11.1	0.46	7.1	0.38
TVM	20.5.84	1300	0.08	0.01	1.13	1.74	0.7	10.2	0.65	---	----
TVM	21.5.84	1200	0.08	0.01	1.13	1.94	0.7	12.8	0.80	6.4	0.38
TVM	22.5.84	1200	0.11	0.02	1.32	1.39	0.7	12.8	0.87	6.4	0.59
TVM	23.5.84	1200	0.11	0.01	1.30	1.59	0.7	11.7	0.86	6.4	0.59
TVM	24.5.84	1200	0.12	0.02	1.39	2.21	0.7	7.0	1.17	12.8	0.89
TVM	25.5.84	1200	0.07	0.01	1.05	1.60	0.7	12.8	0.63	5.3	0.31
TVM	26.5.84	1200	0.08	0.01	1.16	1.76	0.7	12.8	0.6	7.1	0.50
TVM	28.5.84	1200	0.13	0.02	1.44	1.68	0.7	6.0	0.93	9.1	0.76
TVM	29.5.84	1200	0.18	0.03	1.69	2.54	0.6	6.9	2.15	---	----
TVM	30.5.84	1200	0.15	0.02	1.53	1.94	0.7	12.8	1.04	7.1	1.03
TVM	31.5.84	1200	0.17	0.02	1.64	1.69	0.7	12.8	1.53	6.4	0.94
TVM	2.6.84	1200	0.25	0.03	1.99	2.29	0.7	8.3	2.93	---	----
TVM	3.6.84	1200	0.43	0.05	2.63	1.93	0.8	11.1	5.45	---	----
TVM	4.6.84	1200	0.32	0.04	2.24	2.79	0.7	11.6	4.86	---	----
ALP	14.5.84	1500	0.05	0.01	0.89	1.93	0.6	4.9	0.33	10.2	0.30
ALP	15.5.84	0900	0.06	0.01	0.98	1.52	0.7	12.8	0.40	5.0	0.30

TVM - Trivandrum, ALP - Alleppey.

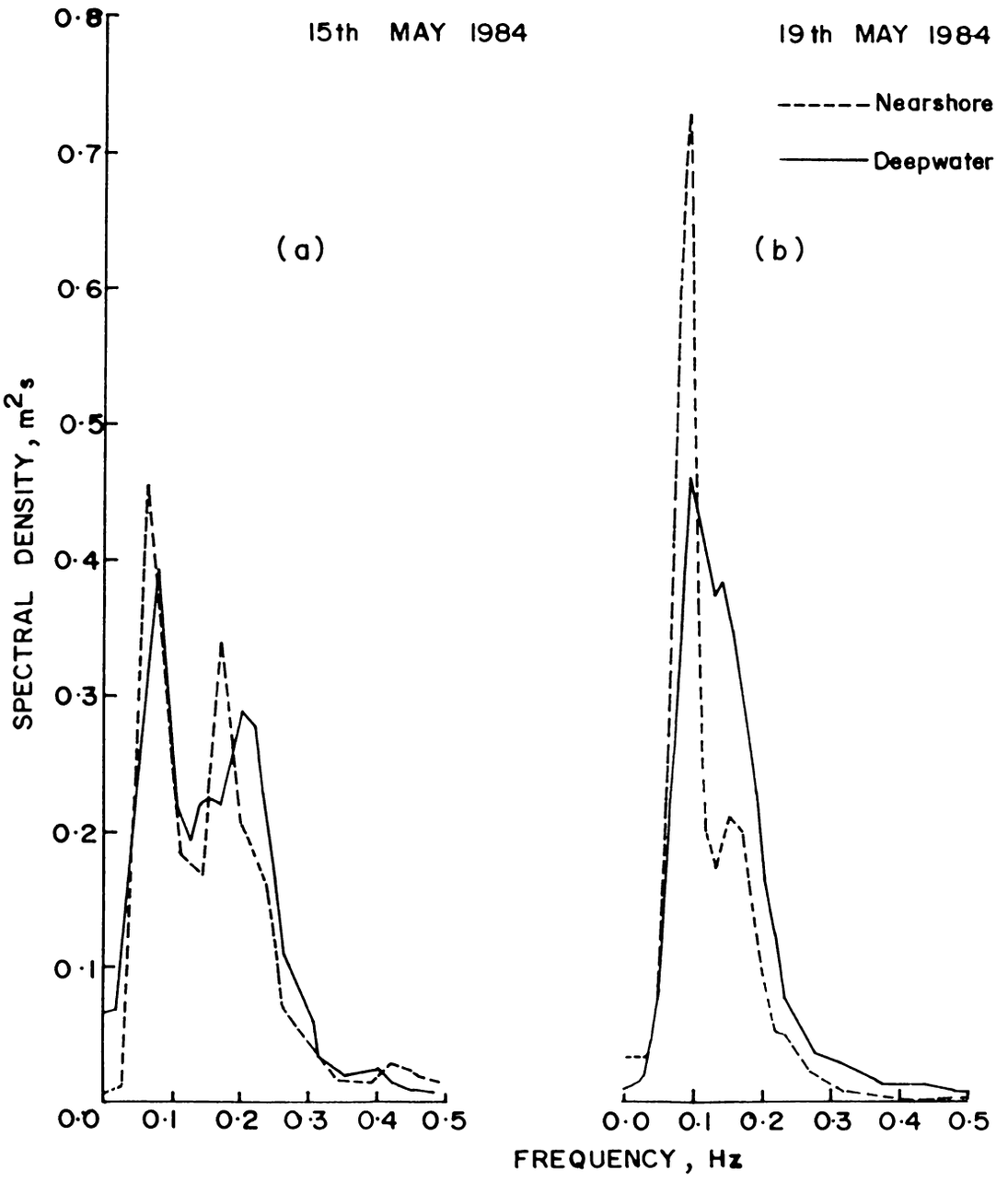

Fig.4.3 Comparison of Deepwater and Nearshore Wave Spectra

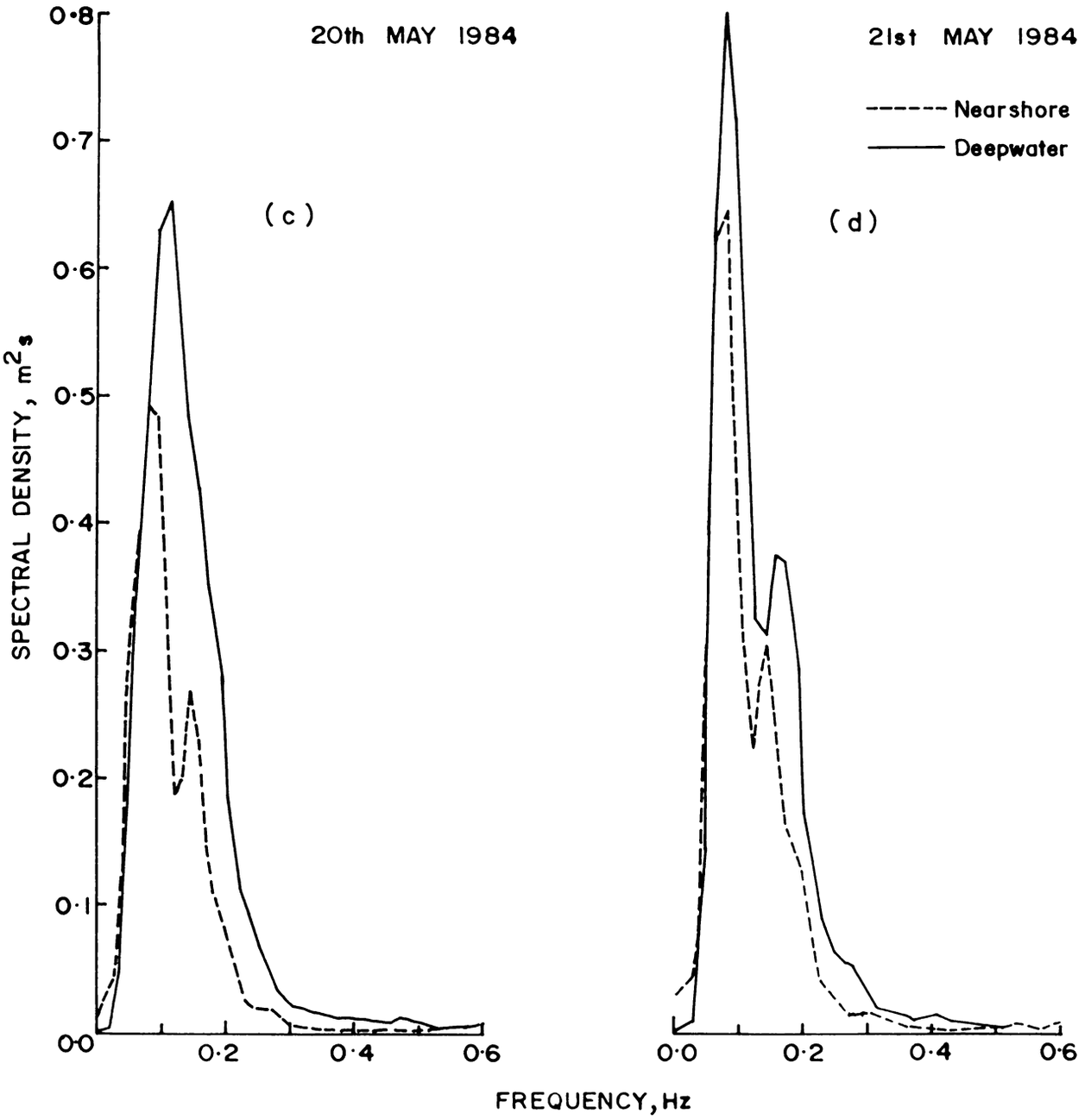

Fig. 4.3 Comparison of Deepwater and Nearshore Wave Spectra (contd

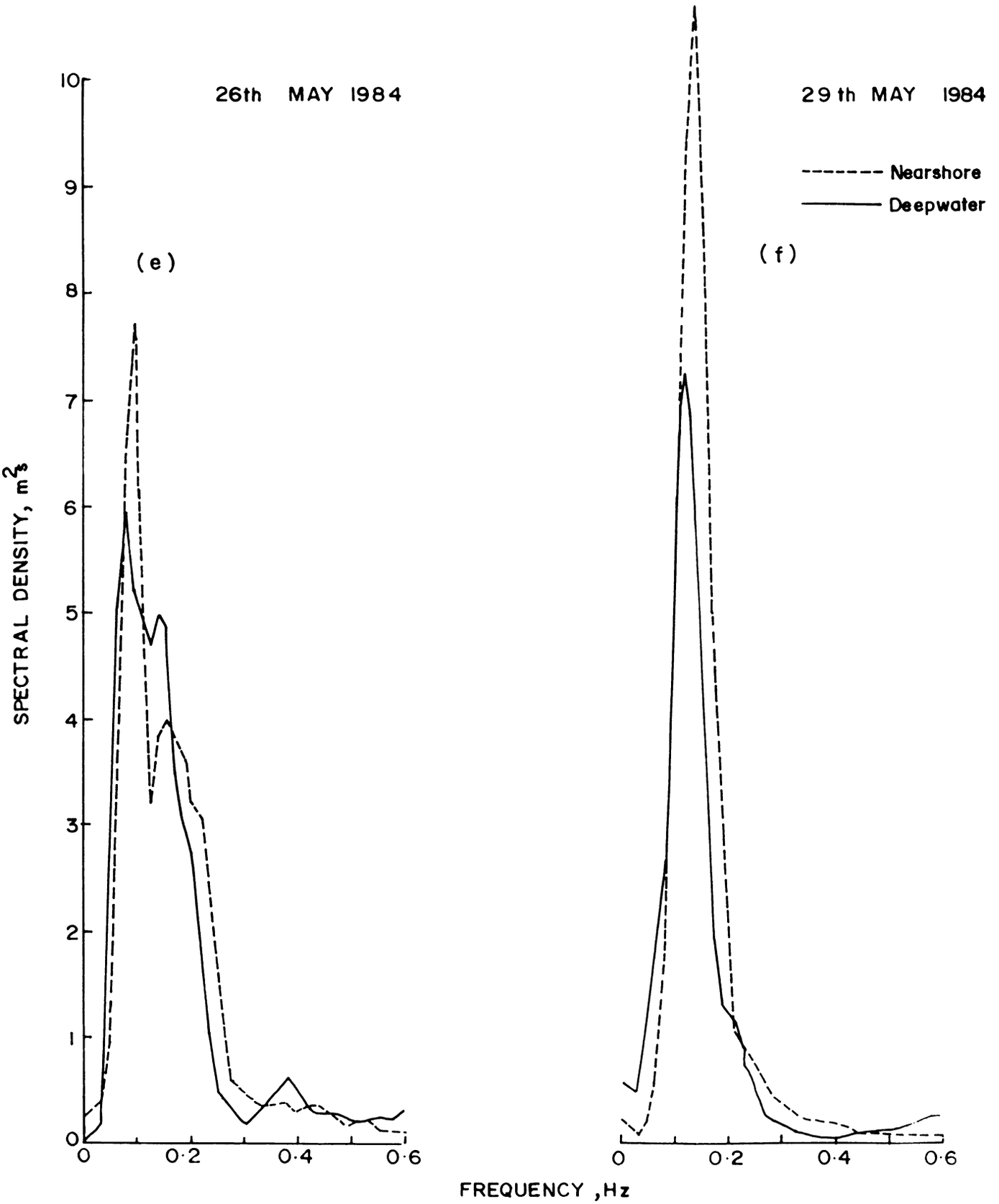

Fig.4.3 Comparison of Deepwater and Nearshore Wave Spectra (contd.....)

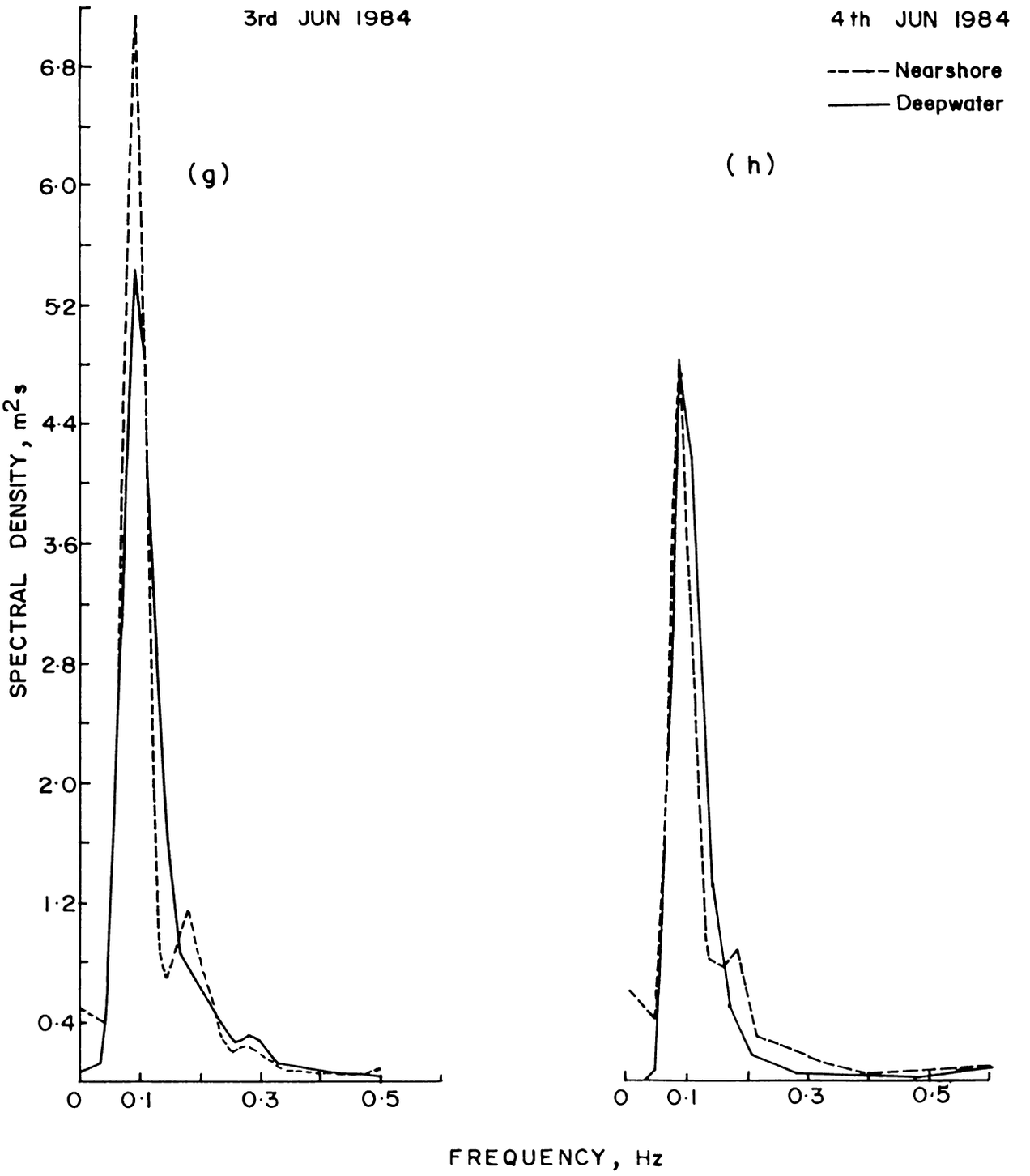

Fig. 4.3 Comparison of Deepwater and Nearshore Wave Spectra (contd.....)

the rough conditions are mostly in the period range 10- 13 s and the energy density is rarely above 1.0 m^2s. However, towards the end of May, the energy level, which is indicated by the spectral moment 'm_o' increases till June 3, when it is maximum with m_o = 0.43 m^2 . The peak spectral density is as high as 5.45 m^2s at a period of 11 s on June 3

Most of the spectra are multipeaked indicating the presence of different wave trains (Bretschneider, 1964; Goda, 1974). The spectral characteristics also reveal information regarding the dominance or absence of sea or swell. Soares (1984) suggested that if the secondary peak of a spectrum is to the low frequency side of the main peak, the spectra can be considered to be wind-dominated and if the secondary peak is to the high frequency side of the main peak, the spectrum can be considered to be swell-dominated. In the present case, since the majority have their secondary peaks in the high frequency side, it can be concluded that the waves are swell-dominated. In a few cases, the spectra are single-peaked and the peak occurs in the low frequency side indicating swells.

This observation was confirmed from the distribution of wind and wave speed during the above period. In Table 4.2 the wind velocities recorded at the offshore stations (as reported in IDWR)and the corresponding wave phase velocities calculated from the peak period are presented. It is seen

Table 4.2. Comparison of wind and wave velocities at offshore locations.

Date	Location	Wind Speed U_w (kmph)	Wave phase velocity, C (kmph)	$\frac{C}{U_w}$
14.5.84	Alleppey	16	29	1.8
15.5.84	Alleppey	13	72	5.5
19.5.84	Trivandrum	5	61	12.0
20.5.84	Trivandrum	14	56	4.0
21.5.84	Trivandrum	--	72	---
22.5.84	Trivandrum	14	72	5.1
23.5.84	Trivandrum	--	67	---
24.5.84	Trivandrum	--	40	---
25.5.84	Trivandrum	23	72	3.1
26.5.84	Trivandrum	18	72	4.0
28.5.84	Trivandrum	--	34	---
29.5.84	Trivandrum	36	40	1.1
30.5.84	Trivandrum	27	72	2.7
31.5.84	Trivandrum	--	72	---
2.6.84	Trivandrum	29	45	1.6
3.6.84	Trivandrum	32	61	1.9
4.6.84	Trivandrum	22	67	3.0

that the speeds are comparable only in few cases which account for wave spectra with high frequency peaks. All other cases are swell-dominated. However, as can be seen from this table, there must be the contributions from sea components because the wind speed picked up from May 25 onwards.

The spectral peakedness parameter Q_p has a range from 1.39 to 2.79, while the spectral width parameter ϵ has a value of 0.7 most of the time. Hence no relation is indicated between these two parameters. It has been observed by some authors (Dattatri and Nayak, 1976; Goda, 1983) that the spectral width parameter does not reflect the spectral shapes and hence is not a reliable parameter. The present data also seem to confirm these observations.

4.2.2.2. Comparison with theoretical spectra

Though many spectral models have been proposed, no model has been universally accepted as to represent all environmental conditions. Some of the commonly used and recommended (Scott, 1963; Pierson and Moskowitz, 1964; Hasselmann et al., 1973) theoretical spectra have been compared with the measured spectra in the present case. The spectra considered for comparison are:

(i) Scott spectrum which is based on Darbyshire's frequency spectrum, and is given by

$$E(f) = 3.424 \times 2\pi m_o \exp\left\{-\left[\frac{96.66(f-f_m)^2}{(f-f_m+0.041)}\right]^{1/2}\right\} \quad (4.1)$$

(ii) Pierson-Moskowitz (P-M) spectrum, which is meant for fully developed sea conditions and is given by

$$E(f) = 5.00153 \times 10^{-4} f^{-5} \exp\left[-1.25\left(\frac{f_m}{f}\right)^4\right] \quad (4.2)$$

(iii) JONSWAP spectrum, which is based on a considerable amount of wave data obtained under the Joint North Sea Wave Project and represents partially developed sea conditions. It is expressed as

$$E(f) = E(f)_{P-M}\, \gamma^{\exp\left[\frac{-(f-f_m)^2}{2\sigma^2 f_m^2}\right]} \quad (4.3)$$

where

$$\sigma = \begin{cases} \sigma_a = 0.07, & f \leq f_m \\ \sigma_b = 0.09, & f > f_m \end{cases}$$

γ is the ratio of the maximum JONSWAP spectral energy to that of the corresponding P-M spectrum, and is usually taken as 3.3 (Hasselmann et al., 1973).

Fig. 4.4 (a-f) give examples of comparison of these theoretical spectra with the measured ones. It is seen that the Scott spectrum gives reasonably good fit with the data.

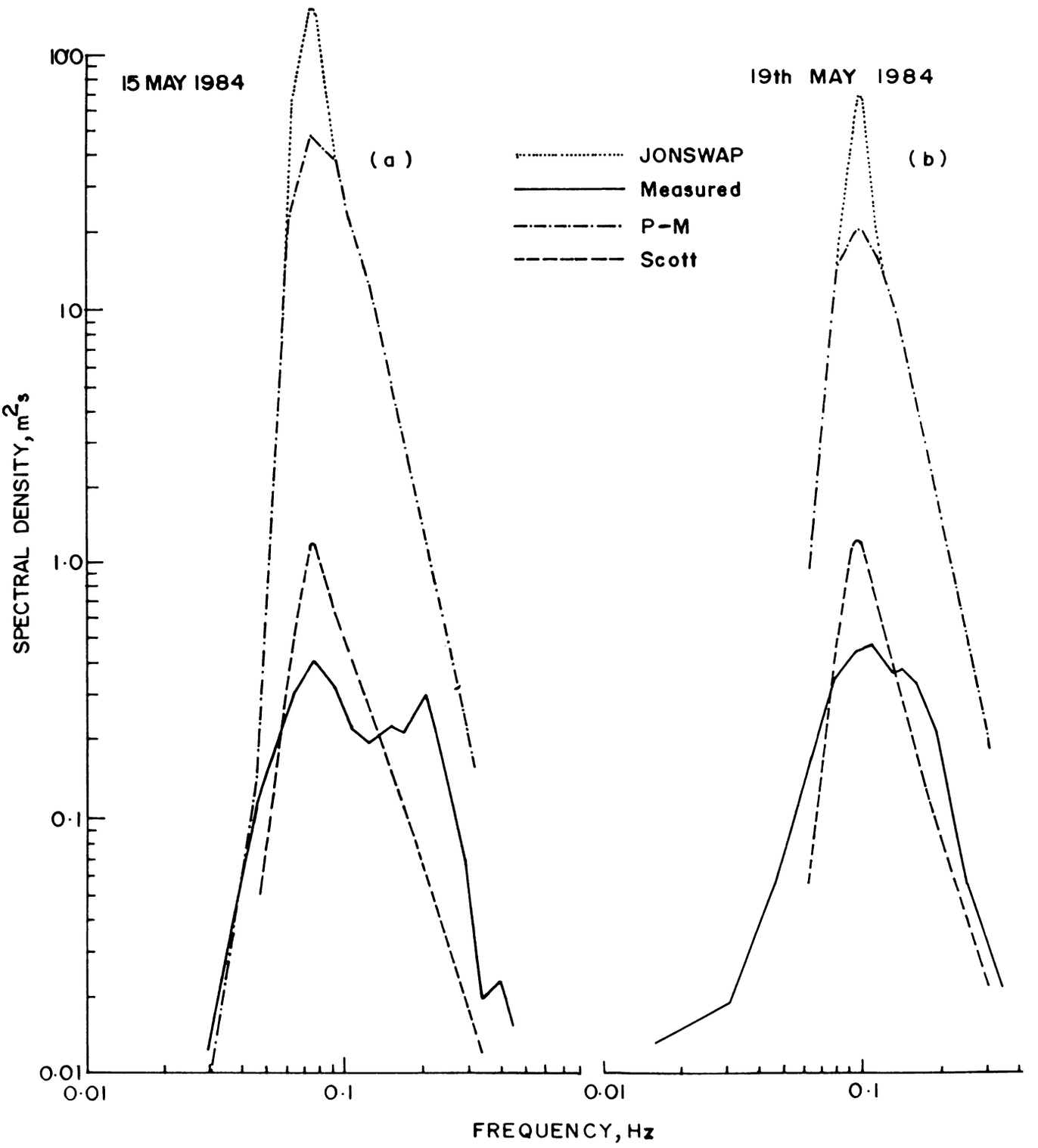

Fig.4.4 Comparison of Deepwater Spectra with Theoretical Models.

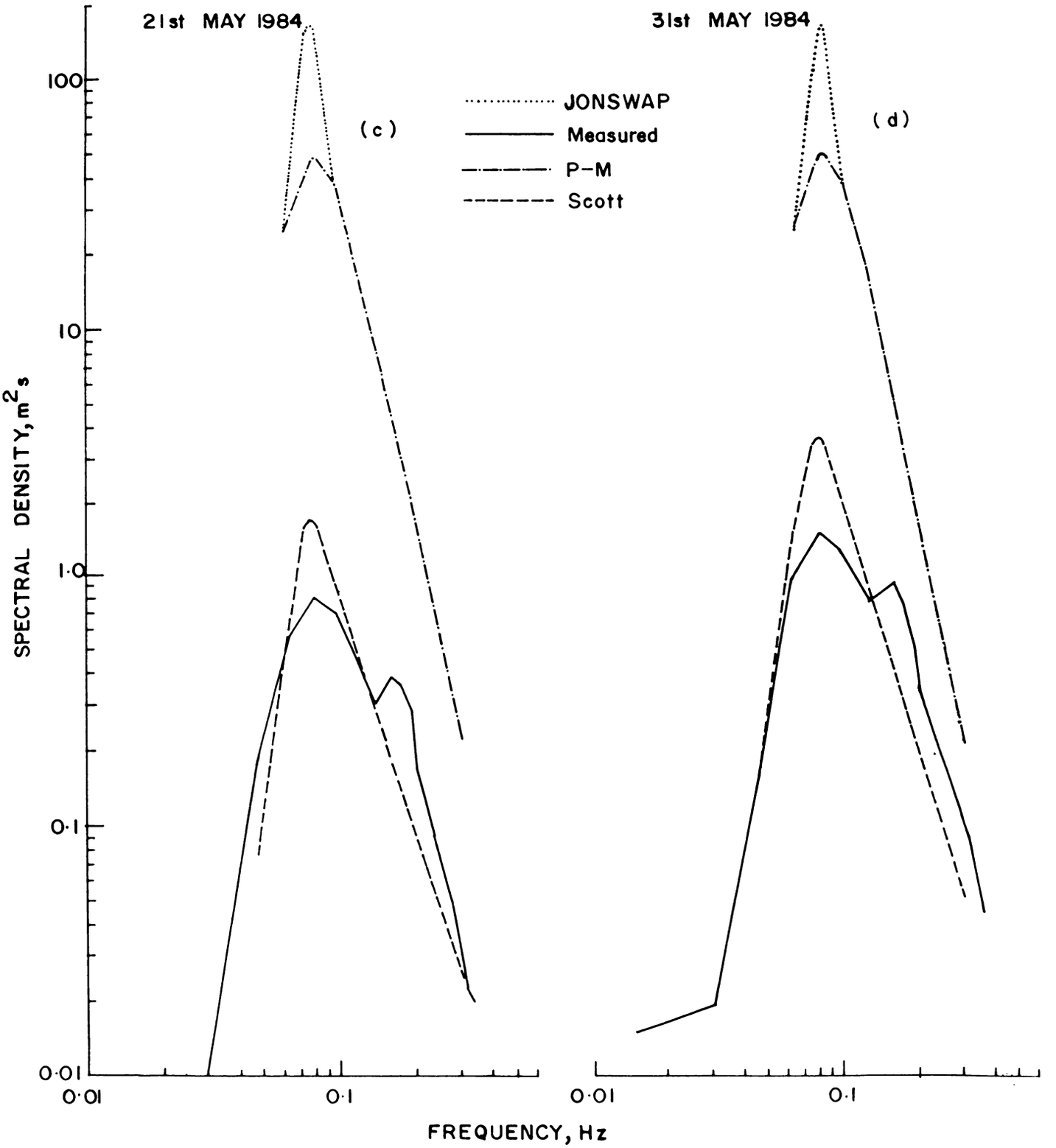

Fig. 4.4 Comparison of Deepwater Spectra with Theoretical Models (contd.....)

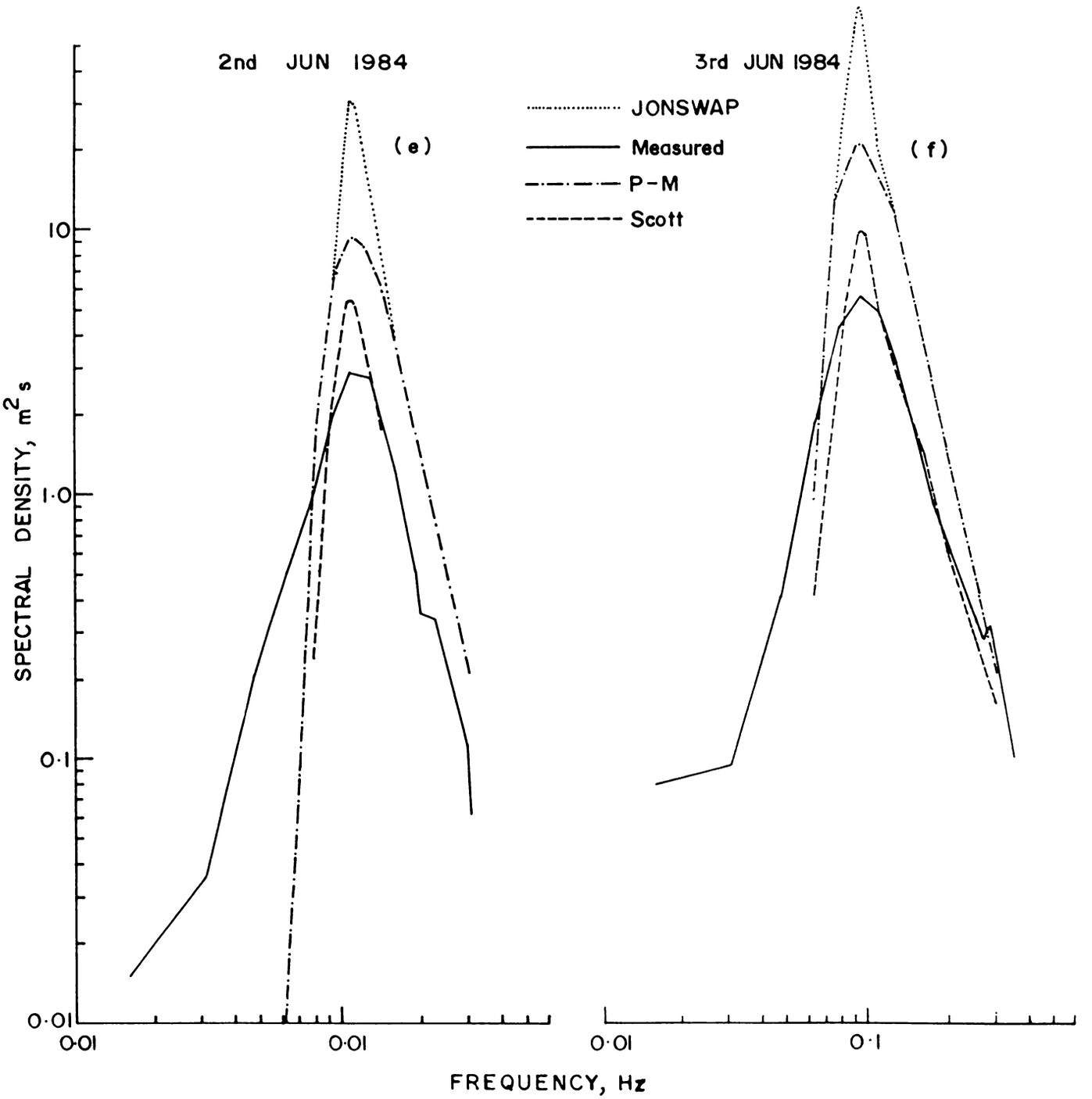

Fig. 4.4 Comparison of Deepwater Spectra with Theoretical Models (contd....)

The P-M and JONSWAP spectra give overestimates of the energy density. Based on deep water data from the west coast of India various workers (Narasimhan and Deo, 1979b; Bhat, 1986; etc.) reported the suitability of Scott spectrum.

4.3. Characteristics of Nearshore Waves

4.3.1. Height, Period and Direction

The significant wave heights range from 0.5 to 2.5 m and the zero-crossing period from 6 to 11 s, thus covering almost the complete range of H_s and T_z reported for this coast (Baba et al., 1983b, and 1987). From the scatter diagrams of H_s and T_z (Fig. 4.1b) it is seen that the predominant groups have heights in the range 0.5 - 1.5 m and period 8 - 9 s. The steepness of the nearshore waves range between 1:100 and 1:25.

As in the case of deep water wave charecteristics, the nearshore waves got intesified towards the end of May. The daily variation in the H_s of nearshore waves off Trivandrum is superimposed in Fig.4.2. The variations follow the deep water pattern well. The maximum H_s measured is 2.25m.

The nearshore wave directions range from 235°to 275°N off Alleppey and 200°to 255°N off Trivandrum.

4.3.2. Nearshore Wave Spectra

4.3.2.1. Spectral characteristics

The results of spectral analysis carried out for nearshore wave records are given in Table 4.3 and Fig. 4.3. The spectral peaks are mostly observed at a period of 13 s before the onset of the rough conditions and the peak shifts to the lower periods with further roughening of the sea. The peak spectral density varies from 0.3 $m^2 s$ during normal conditions to a high value of 7.2 $m^2 s$ during rough conditions. Correspondingly the spectral moment m_o range from 0.03 to 0.42 m^2. Secondary peaks are observed for nearshore spectra for all but two cases (Fig 4.3). Since multipeakedness is seen in some cases which were singlepeaked in deep water, other processes also seem to be involved. These aspects are discussed separately.

The spectral peakedness parameter has a wide range between 1.56 and 2.89. The spectral width parameter has a value of 0.7 in a majority of the cases, but it occasionally goes upto 0.8. Though the variability of ϵ is relatively more here, no relation is indicated between Q_p and ϵ

4.3.2.2. Comparison with theoretical spectra

The spectral models discussed in sub-section 4.2.2.2. may not represent shallow water conditions. Kitaigorodskii

Table 4.3

Spectral Characteristics of Nearshore Waves

Location	Date	Time Hrs.	m_o (m^2)	m_1 (m^2)	H_s (m)	Q_p	ϵ	1st Peak T_{p1} (s)	1st Peak S_{p1} ($m^2 s$)	2nd Peak T_{p2} (s)	2nd Peak S_{p2} ($m^2 s$)
ALP	14.5.84	1400	0.03	0.00	0.69	1.56	0.7	12.8	0.32	5.5	0.11
ALP	15.5.84	0900	0.06	0.01	0.98	1.52	0.7	15.3	0.48	5.9	0.36
TVM	19.5.84	1200	0.05	0.01	0.88	2.66	0.7	11.0	0.73	6.4	0.21
TVM	20.5.84	0900	0.05	0.01	0.86	1.75	0.7	12.8	0.49	7.0	0.27
TVM	21.5.84	1200	0.06	0.01	0.94	1.78	0.8	12.8	0.64	7.0	0.31
TVM	22.5.84	1200	0.08	0.01	1.14	2.00	0.7	12.8	0.95	5.9	0.38
TVM	23.5.84	1200	0.07	0.01	1.03	1.59	0.7	12.8	0.74	7.0	0.29
TVM	24.5.84	1200	0.07	0.01	1.06	1.66	0.8	12.8	0.76	7.0	0.40
TVM	25.5.84	1200	0.05	0.01	0.90	2.09	0.7	12.8	0.69	7.0	0.22
TVM	26.5.84	1200	0.08	0.01	1.12	1.60	0.8	12.8	0.88	7.7	0.43
TVM	28.5.84	1200	0.13	0.02	1.46	2.04	0.7	6.4	1.36	11.0	0.96
TVM	29.5.84	1200	0.13	0.02	1.43	2.10	0.7	8.5	1.45	——	——
TVM	30.5.84	1200	0.14	0.02	1.52	1.78	0.7	12.8	1.27	7.0	1.18
TVM	31.5.84	1230	0.18	0.02	1.69	2.13	0.7	12.8	2.28	7.0	0.97
TVM	2.6.84	1200	0.25	0.03	1.99	1.92	0.7	9.6	3.08	——	——
TVM	3.6.84	1200	0.42	0.05	2.60	2.89	0.8	11.0	7.15	5.9	1.15
TVM	4.6.84	1200	0.32	0.04	2.28	2.07	0.8	11.0	4.76	5.5	0.87

TVM - Trivandrum, ALP - Alleppey.

et al. (1975) proposed a spectral form for shallow water:

$$E(f) = Ag^2 (2\pi)^{-4} f^{-5} \phi \omega_d \qquad (4.4)$$

where ϕ is a dimensionless function varying from 1 in deep water to 0 in depth d = 0 and

$$\omega_d = 2\pi f \left(\frac{d}{g}\right)^{1/2} \qquad (4.5)$$

The measured nearshore spectra are compared with this and also with the theoretical spectra already mentioned in Section 4.2.2.2. Fig.4.5(a-f) give examples of the comparison of the measured spectra with the theoritical. Among all the spectra compared the Scott spectrum gives reasonably good fit for shallow water also. Dattatri (1978), Abraham (1987) and Rachel (1987) have also found the suitability of Scott spectrum for shallow water waves. Baba and Harish (1986) have reported that the Scott's peak spectral estimate holds good in all the cases except high energy conditions. The Kitaigorodskii et al., spectrum shows good fit for the high frequency part of the observed spectrum in almost all cases. This is also in conformity with the results of Baba and Harish (1986).

4.4. Characteristics of Observed Wave Transformation

The characteristics of wave transformation in these coastal waters can be studied from a comparison of deep

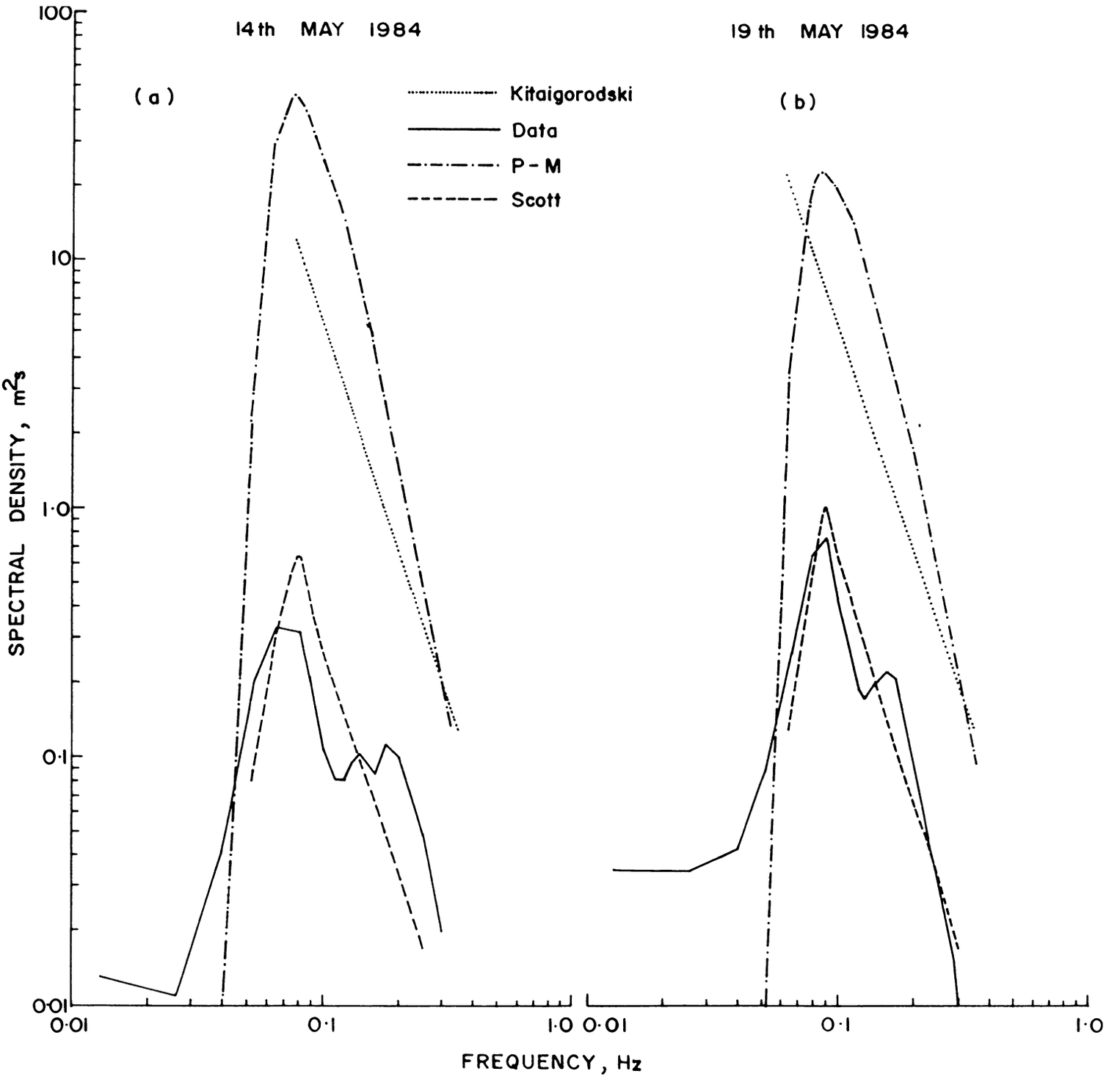

Fig.4.5 Comparison of Nearshore Spectra with Theoretical Models.

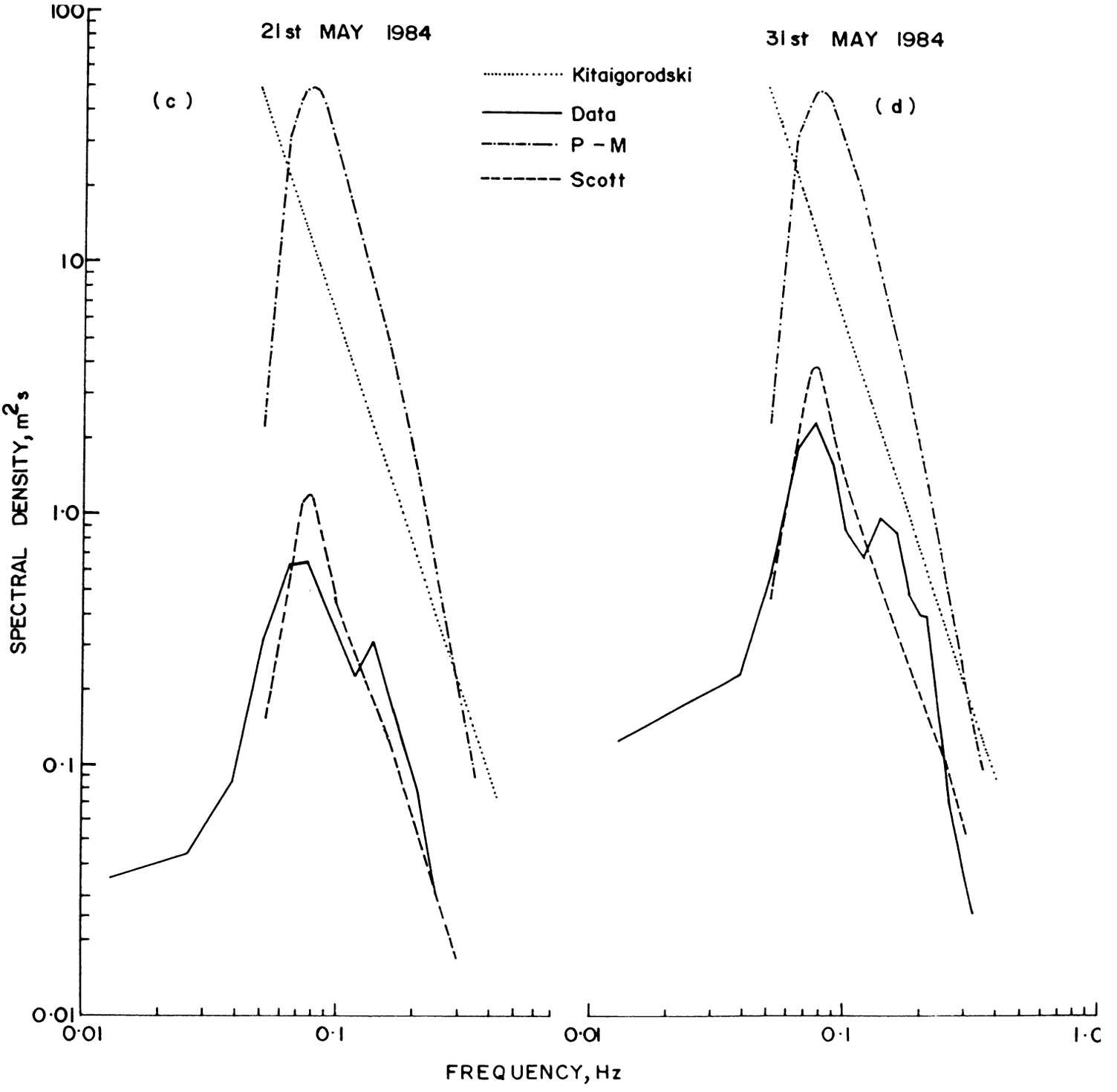

Fig. 4.5 Comparison of Nearshore Spectra with Theoretical Models (contd.....)

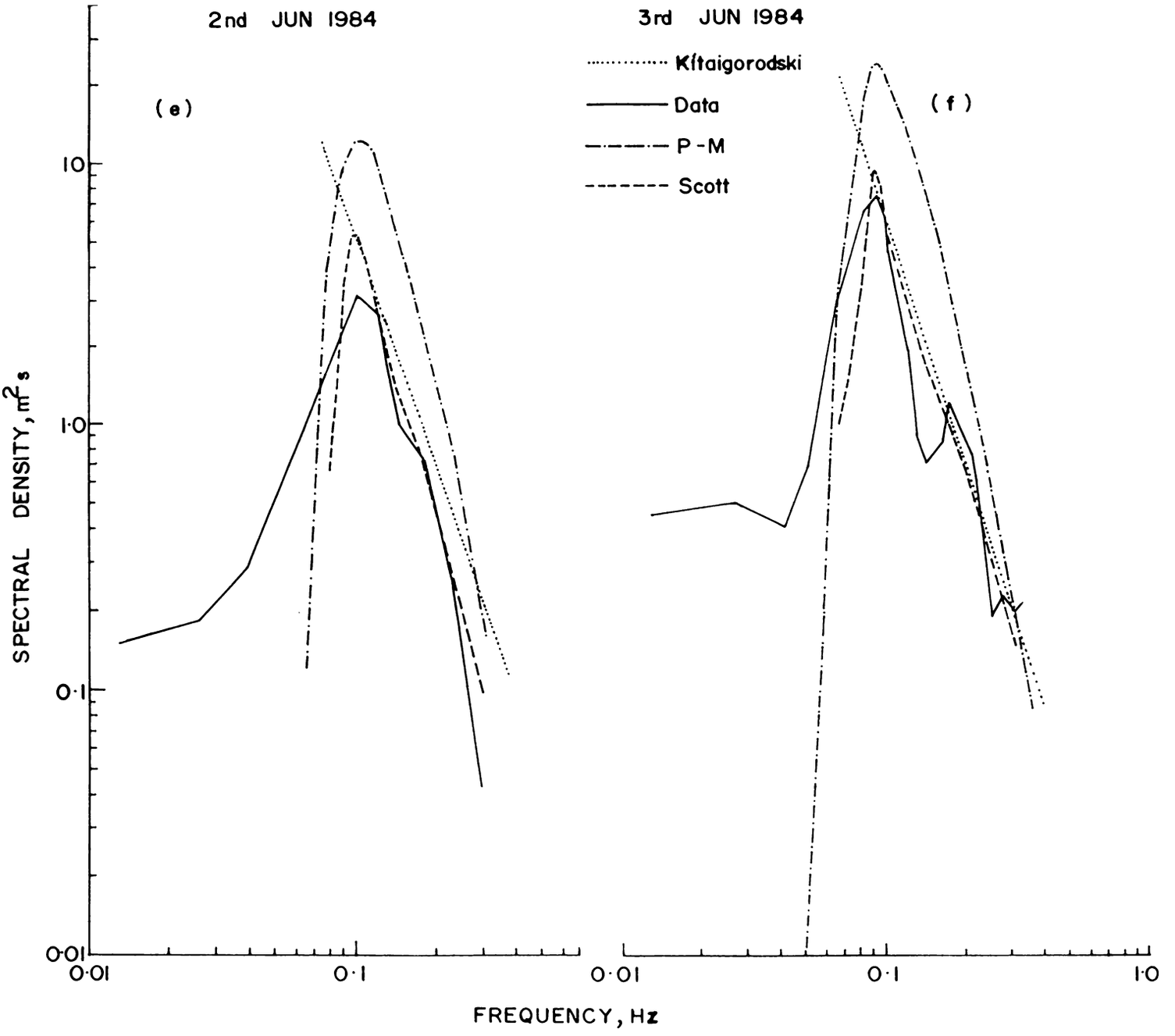

Fig. 4.5 Comparison of Nearshore Spectra with Theoretical Models (contd.....)

water and nearshore wave data. The results of the present study are discussed with reference to those of other researchers.

4.4.1. Transformation of Wave Height

The major features of wave height transformation is obtained by comparing the synchronised deep water and nearshore wave height. For the purpose of comparison of wave heights, the significant wave heights (H_s) derived from Tucker-Draper analysis is used. It has been shown by Harish and Baba (1986) and Abraham (1987) that the height parameters H_s and $\overline{H}$ derived from Tucker-Draper method is quite comparable to that derived from spectral method.

For the study of transformation, the time of nearshore data must be chosen incorporating the lag in time due to the propagation of waves from the offshore to the nearshore. In the present case, the farthest offshore recording station is at a distance of about 21 km. For a wave period 10 s it is seen from refraction and shoaling computations that the time required to reach the nearshore point from this offshore point is about 45 minutes. For the ship based observations, the time lag may be more because some of them are reported in very deep waters. It was difficult to account for this lag and even if it was calculated, there was problem of non-availability of nearshore data at the required time. This

problem was solved to a great extent because of the stationarity of waves which has already been reported by Thompson and Harris (1972).

The stationarity of waves of this coast was studied here by making use of continuous recorded data for the nearshore zone off Alleppey, as given in Table 4.4. The wave heights preceding and succeeding the time of deep water observation are given for some cases in this table. It is seen that the nearshore wave heights show more or less stationary conditions for a fairly long time. Hence for the present study, the nearshore data at the time of deep water measurements were chosen. In some cases where such data were not available, the data nearest in time to the deep water data were considered.

Sixty seven data sets are used for the present comparison. Fig.4.6 gives a plot of the transformed significant wave heights (nearshore) against the corresponding deep water heights. It is found that the transformed wave heights are very rarely greater than the deep water heights indicating the attenuation of wave heights irrespective of location. It is also interesting to note that the data points for the two locations, Alleppey and Trivandrum, fall around two different lines. Regression analyses for the data set (24 at Alleppey and 43 at Trivandrum) give the following relations:

Table 4.4

Stationarity of Nearshore Waves*

Date	Deep water Time (Hrs GMT)	Deep water Wave Ht (m)	Nearshore Wave heights (m) measured H_{-09}	H_{-06}	H_{-03}	H_{oo}	H_{+03}	H_{+06}	H_{+09}	H_{+12}	S.D
26.5.81	0000	2.5	1.04	0.91	1.16	1.12	1.06	1.21	1.44	1.42	0.18
27.5.81	1200	2.0	1.45	1.36	1.56	1.53	1.69	1.61	1.44	1.33	0.12
28.5.81	0600	2.5	1.44	1.33	1.33	1.52	1.37	1.46	1.44	1.61	0.10
1.6.81	0600	3.0	1.59	1.72	1.92	1.57	1.59	1.50	1.39	1.40	0.17
8.6.81	0000	2.5	1.93	1.96	1.86	1.62	1.93	1.56	1.48	1.65	0.19
25.7.81	0000	2.5	1.55	1.54	1.56	1.59	1.56	1.93	1.75	1.73	0.14
8.9.81	0600	3.0	1.91	1.95	1.89	1.82	1.75	1.53	1.52	1.28	0.24
20.9.81	1800	2.0	1.68	1.61	1.37	1.47	1.52	1.46	1.46	1.48	0.10
23.9.81	1800	2.0	0.96	0.94	1.00	1.00	1.00	0.99	0.95	0.91	0.03

* H_{-09}, H_{-06} etc. denotes the measured heights at 3-hour interval. The subscript indicates the time in hours preceding or succeeding the time of deep-water observation depending on whether the sign is negative or positive

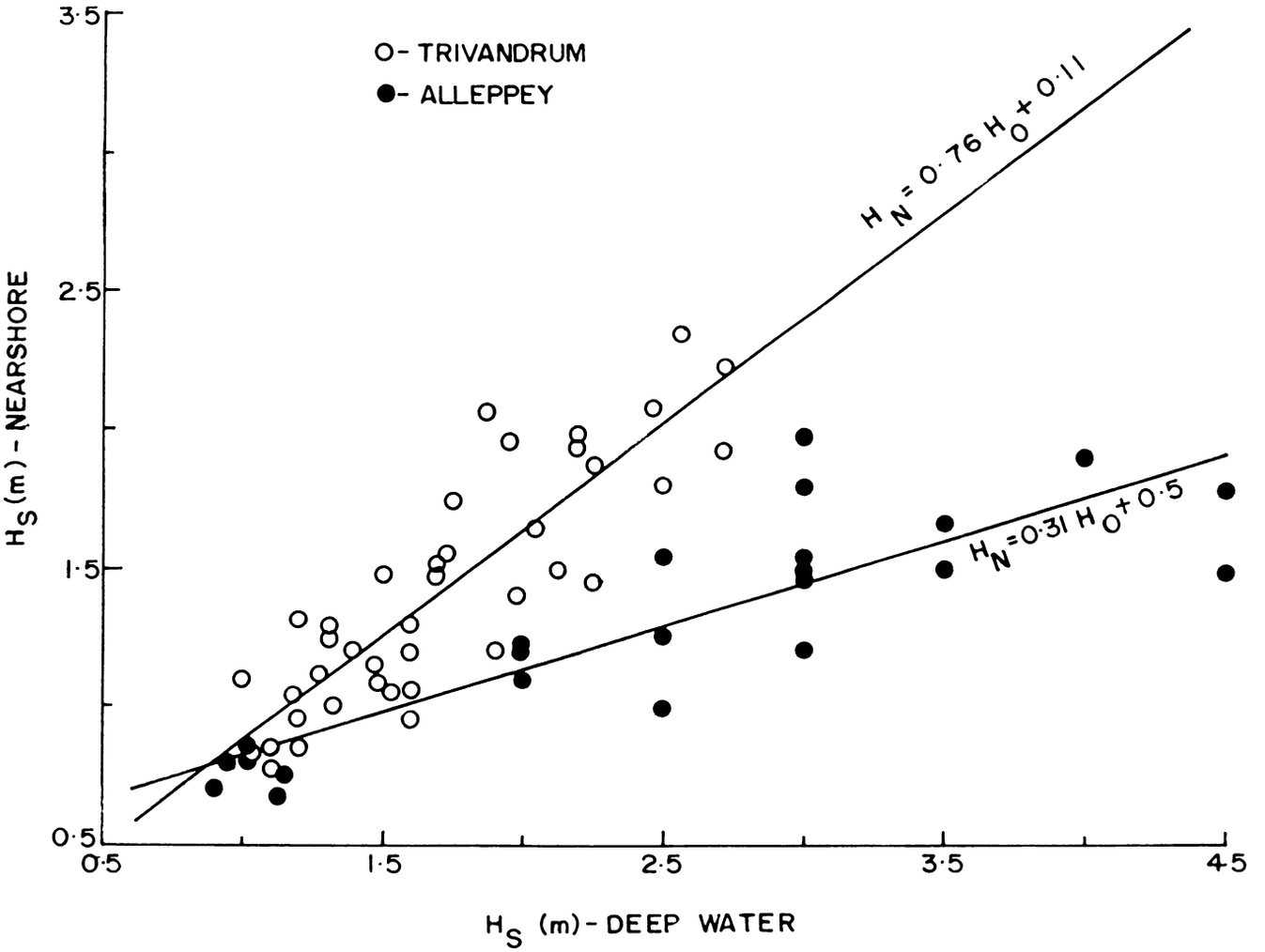

Fig. 4.6 Relation between Significant Heights in Deepwater and Nearshore

$$H_N = 0.81\ H_o + 0.05 \text{ at Trivandrum} \qquad (4.6)$$

and

$$H_N = 0.29\ H_o + 0.41 \text{ at Alleppey} \qquad (4.7)$$

where H_N is the transformed nearshore wave height and H_o is the corresponding deep water height. The standard error estimates are 0.30m and 0.21m respectively at Alleppey and Trivandrum. The higher error estimate at Alleppey could be obviously attributed to the errors associated with ship-based observations, which constitute the major part of the data there.

The above equations show that for waves of deep water height in the range 1 - 3m, the transformed wave heights are correspondingly 87 - 80% of deep water height at Trivandrum and 81 - 48% of deep water height at Alleppey. In other words, the attenuation of wave height due to propagation in shallow waters is insignificant at Trivandrum, whereas it is as much as 50% for waves of 2 - 3m height at Alleppey.

Provis and Steedman (1986) found a halving of significant wave height due to the propagation of waves over a distance of 280 km from 1150 m depth to 26 m depth. The shelf profile they selected was very gentle. In contrast, Le Mehaute (1982) studied transformation over waters with very steep profile and obtained attenuation in wave heights ranging from 33 to 71% for wave propagation from 210m to 18m

depth. Since these authors have not covered the nearshore zone, where the transformation is expected to be maximum the results are not exactly comparable.

As already discussed, the transformed wave heights are dependent on the various transformation processes, viz. refraction, shoaling and the nonlinear dissipation. While the shoaling may not cause a decrease in wave height at these nearshore points, except for short period waves, refraction may tend to increase or decrease the wave height depending on the convergence or divergence of wave energy, which depends on the wave direction. Hence refraction and shoaling together may not lead to attenuation of wave height in all cases and the observed attenuation could be significantly contributed by the nonlinear dissipation processes. Since the cases considered here are mostly swell-dominated, the possible factors are bottom friction and percolation. Among these percolation may not be of much significance, according to the results of Beach Erosion Board (1953), Bretschneider and Reid (1954) and considering the fact that the sea beds in the locations of study are constituted by fine sands, silt and clay. Thus bottom friction may be the only deciding factor which brings about this dissipation.

The observed difference in the attenuation between the two locations could be again attributed to the differences

in the frictional dissipation. For the same wave conditions, bottom roughness determines the rate of frictional dissipation, which is expressed in terms of the friction factor C_f . Since the bottom sediment is coarser at Trivandrum, the rate of frictional dissipation is expected to be higher there. However, the total frictional loss due to the propagation from deep water to nearshore is decided by the slope of the sea bottom, which in turn decides the duration over which the wave effectively feels the bottom. While the 30 m contour is only 4 km from the shoreline at Trivandrum, it is at a distance of 1 8 km at Alleppey (Fig. 3.3). The inshore profile, where maximum transformation takes place, is very steep at Trivandrum. This difference in the shelf width results in higher attenuation at Alleppey when compared to Trivandrum. The fact that the attenuation is considerably higher at Alleppey than Trivandrum indicates the over-riding effect of bottom slope over bottom roughness for the range of slope and sediment textures encountered here. Thus the bottom slope plays the major role in the attenuation of wave heights along this coast.

4.4.2. Transformation of Wave Spectra

As in the case of wave height comparisons, the nearshore spectra at the time of deep water recording, or nearest in time to it, were selected for the comparisons

here (Fig.4.3 a-h). The spectral parameters are compared in Table 4.5.

4.4.2.1. Spectral energy

The most conspicuous aspect is the reduction in the spectral energy (indicated by m_o). Off Trivandrum, energy losses, except in a few cases, are in the range 0 - 43%. Of the two observations available at Alleppey one shows loss of 39%. The other case, for which the nearshore spectrum gives a significant high frequency secondary peak, shows no loss of energy. The higher attenuation of wave height, especially for higher waves discussed in Section 4.4.1 indicates corresponding energy losses also. Since only two spectral comparisons are available at Alleppey, and that too are confined to the low energy level, the extent of energy loss as deduced from results of wave height attenuation in Section 4.4.1 cannot be confirmed.

At Trivandrum, however, during the period 19-25 May, the observed energy losses are of the order as expected from the attenuation of wave heights discussed earlier. It is seen that with further roughening of the seas as seen from May 25 onwards (Table 4.2) the energy loss is reduced. During most of the high energy conditions, the nearshore energy level is the same as the deep water ones. Sometimes even an enhancement of energy is observed on such

Table 4.5 Comparison of Nearshore and Deep Water Spectral Characteristics and Energy Loss

Location	Date	Energy loss %	$\frac{T_p}{T_{p_o}}$	$\frac{S_p}{S_{p_o}}$
Alleppey	14.5.84	39.4	2.6	1.0
Alleppey	15.5.84	1.2	1.2	1.2
Trivandrum	19.5.84	17.2	1.0	1.6
Trivandrum	20.5.84	42.5	1.3	0.8
Trivandrum	21.5.84	30.0	1.0	0.8
Trivandrum	22.5.84	26.0	1.0	1.1
Trivandrum	23.5.84	38.0	1.1	0.9
Trivandrum	24.5.84	42.5	1.8	0.7
Trivandrum	25.5.84	27.5	1.0	1.1
Trivandrum	26.5.84	6.0	1.0	1.5
Trivandrum	28.5.84	-3.4	1.1	1.5
Trivandrum	29.5.84	28.5	1.2	0.7
Trivandrum	30.5.84	2.0	1.0	1.2
Trivandrum	31.5.84	-6.0	1.0	1.5
Trivandrum	2.6.84	0.0	1.2	1.1
Trivandrum	3.6.84	2.0	1.0	1.3
Trivandrum	4.6.84	-0.3	1.0	1.0

occassions. This may be due to the increased wind wave generation from May 25 onwards. Thus the attenuation of wave energy during propagation in shallow waters is compensated by the input of energy in the shallow waters, which is indicated by the growth of the high frequency secondary peaks (Fig.4.3 e&g).This is true for Alleppy also on May 15. From spectral comparisons, Forristall (1980), Le Mehaute (1982) and Provis and Steedman (1986) found very high losses of energy due to propagation in shallow waters.

4.4.2.2. Peak frequencies

The peak frequencies are found to coincide in a majority of the cases and the spectral peakedness parameter Q_p are also more or less comparable. These indicate that there is no appreciable change in the shape of the spectra due to their propagation in shallow waters. Similar results are obtained by Provis and Steedman (1986). However, these differ from the observations of Thompson (1974) and Le Mehaute (1982), who found that the spectra become narrow-banded as a result of transformation.

4.4.2.3. Peak spectral density

There is a general reduction in the peak spectral density due to transformation during normal conditions, as indicated by the ratio of spectral densities S_p / S_{p_o}. However, they are found to be higher in magnitude for the

nearshore during the rough conditions. Vincent (1982) discusses the roles of nonlinear transfer (wave-wave interaction), frictional dissipation and white-capping/breaking mechanisms in the modification of wave spectra in shallow water. While bottom friction losses should be expected to be biased towards the peak and lower frequencies, nonlinear transfer and white-capping/breaking should produce growth on the forward face of the spectrum with a loss at the peak frequencies and above. According to him, the pattern of low frequency gain and high frequency loss is pronounced under active wind growth and wave-wave interaction dominates when the energy is large. It is quite possible that these mechanisms would have played a role in the growth of the spectral peaks during the rough conditions. The effect of bottom friction, which gives higher attenuation in the low frequency side is not seen because the spectra presented here mostly belong to Trivandrum, where the effect of bottom friction is not pronounced and the spectra off Alleppey belonged to the low energy conditions.

4.4.2.4. Multipeakedness

Another feature of interest is the multipeakedness of the spectra. Secondary peaks occur for a majority of deep water spectra and all but two of nearshore spectra. These peaks occur at frequencies about 1.5 to 2 times of the

frequency of primary peak. Similar observations are made by Dattatri (1978), Namboothiri (1985), Baba and Harish(1986), Abraham (1987), etc. It is seen that even some nearshore cases, for which the deep water spectra are not multipeaked, have secondary peaks.

According to Thompson (1980) multipeakedness is a typical characteristic of shallow water spectra and it is pointed out that this may be due to a single train of steep waves rather than independent wave trains. This multipeakedness for a single train is explained to be due to the shifting of some energy from the main peak to the higher frequencies. Lee and Black (1978) also explained the transfer of energy from the main peak to the higher harmonics as the reason for multipeakedness in shallow waters. This does not seem to be true for the present cases. Here the deep water spectra itself are mostly multipeaked. The growth of the high frequency secondary peaks observed in the nearshore is well correlated with the increasing wind speed in the latter half of the field observations. As seen already, the low frequency spectral peaks are also found to grow, which is attributed to the wave-wave interaction. Hence it appears logical to conclude that there is no transfer of energy from the peak to the higher harmonics and the secondary peaks are only due to separate wave trains (in this case sea waves). Abraham

(1987) and Rachel (1987) explain the multiple peaks observed in shallow water spectra to be due to swell and sea waves.

4.5. Summary

From a comparison of synchronised deep water and nearshore wave data, it is found that attenuation of wave height and energy takes place during the propagation of waves in shallow water. The extent of attenuation is less at Trivandrum, whereas it is very pronounced at Alleppey, particularly for the high energy conditions. The difference in attenuation between the two locations is attributed to the bottom frictional dissipation, which can be high at Alleppey because of the gentle slope of the bottom, when compared to Trivandrum. Two regression equations connecting deep water and nearshore heights are obtained for these locations.

The spectra of deep water and nearshore fit the Scott spectrum reasonably well. The Kitaigorodskii et al. spectrum is found to simulate the high frequency part of the nearshore spectrum.

Multipeakedness is observed both in the deep water and nearshore wave spectra. During transformation, a spectral energy loss upto 43% has been observed. In general, there is no shift in the peak of the spectrum during transformation. The spectral peaks are found to grow during

rough conditions and this may be due to nonlinear transfer of energy. It is concluded that the high frequency secondary peaks observed are due to sea waves only.

CHAPTER 5

PREDICTION OF WAVE HEIGHT TRANSFORMATION

5.1. Introduction

The deep water waves are generally represented by characteristic height, period and direction. For most coastal applications, the wave heights predicted from these using relatively simple numerical models will suffice. In such cases models based on the wave ray approach can be used. Though this method may not truly represent the natural conditions, it has the greatest advantage of being comparatively simple and hence may not require much of computational time and advanced computer facilities. As seen already (Ch.2) a computer programme by Dobson has been evaluated for some coastal conditions. The field evaluation of this programme carried out for the Kerala Coast is presented in this Chapter.

5.2. Principles of Wave Ray Computer Models

Most of the computer models with the wave ray approach, like the graphical methods, are based on the geometrical optics approximation. The initial position and characteristics of the wave ray are given as input and the subsequent path of the wave ray is computed based on a grid of depths or wave celerity. The earlier workers (Griswold, 1963; Harrison and Wilson, 1964; etc.) calculated the path of the

wave ray from a grid of wave celerities, which are estimated separately each time when waves of different periods are considered. This involved unnecessary labour and enhanced the probabilities for committing error. Wilson (1966) used a grid of depths, which is advantageous in this context. However, the limitation with his method is that a linear surface is used to compute the depth at intermediate points. Dobson (1967) was the first to come out with a successful wave refraction model, in which a grid of depths was used with a quadratic surface to describe the local variation of depth within the grid. Hence it was possible to apply the equations governing the wave height transformation. The programme by Dobson with its subsequent modification by Coleman and Wright (1971) has been modified further during the course of this investigation.

5.3. Computer Programme and Governing Equations

5.3.1. Computer Programme by Dobson (1967) and Coleman and Wright (1971)

The programme by Dobson defines the transformed wave height in terms of the shoaling and refraction coefficients. Coleman and Wright introduces the friction coefficient (K_f) also so that the transformed wave height is given by

$$H = K_r \cdot K_f \cdot K_s \cdot H_o$$

The programmes when combined consist of a main

programme WAVES.S and nine subroutines. The flow chart for the programme is given in Fig.5.1. The functions of the main programme and subroutines are discussed below.

Programme WAVES.S : This programme reads the input data viz. grid parameters, depth grid, co-ordinates of ray starting point, etc. After reading the data for the first ray, the control passes to the subroutine RAYCON.

Subroutine RAYCON : This subroutine controls each individual ray as it progresses across the grid. Initially, it calculates the second point on the ray assuming that the wave is still in deep water, and then calls subroutine DEPTH to find the depth at this new point. If the depth is greater than the refraction depth then the subroutine WRITER is called which prints the wave details at this point. If the wave has reached shoaling water the subroutine CURVE is called to calculate the initial value of the ray curvature. With this value the subroutine REFRAC is called to calculate the next point on the wave ray. The ray may also be stopped by this subroutine for reasons such as lack of convergence in calculation of curvature, wave breaking, ray reaching the boundaries, etc. The criteria for wave breaking is the one suggested by Munk (Eq.2.13).

Subroutine REFRAC : This subroutine solves the following refraction equations (Dobson, 1967) iteratively to find the

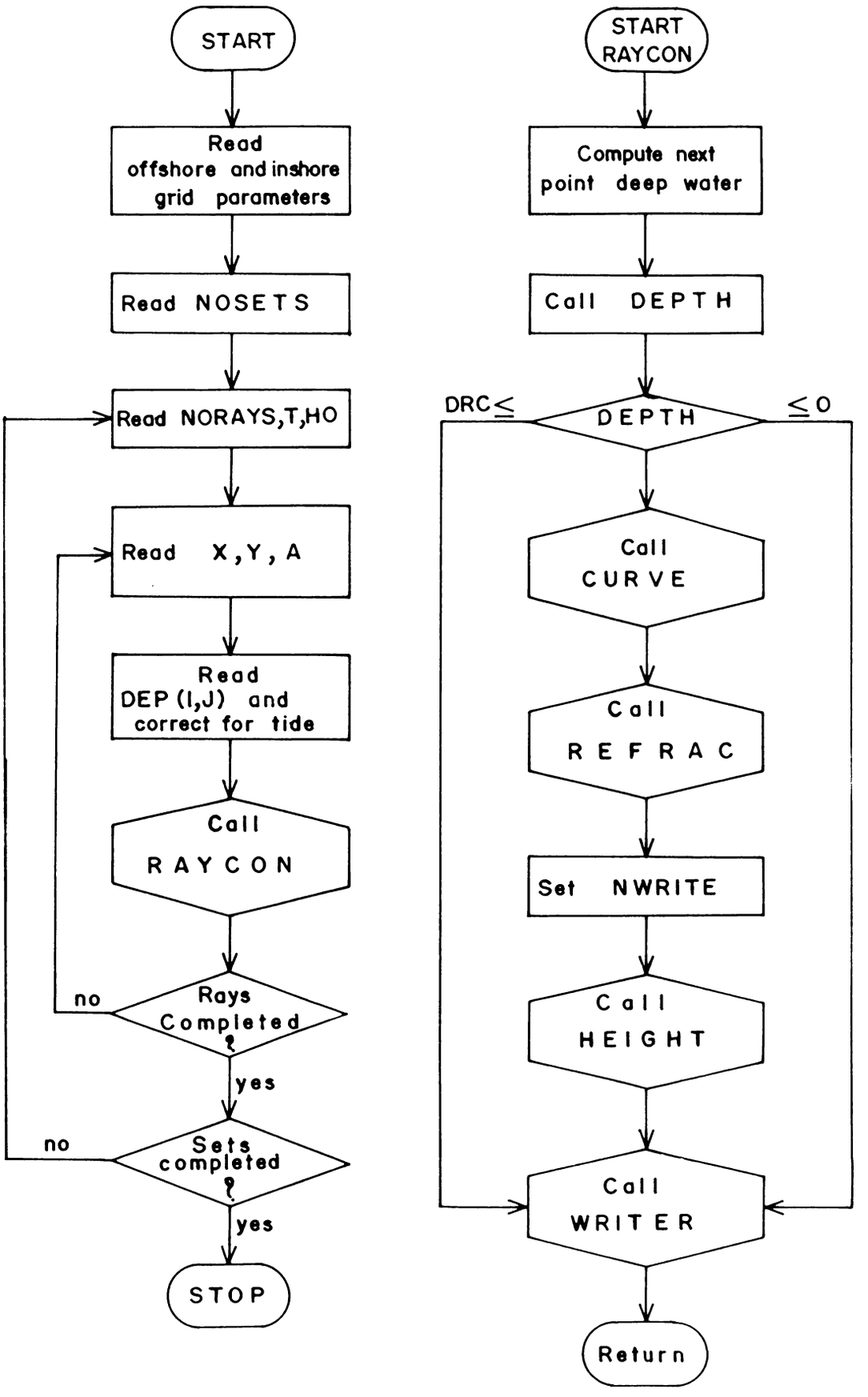

Fig.5.1 Flow Chart for Wave Ray Transformation Model

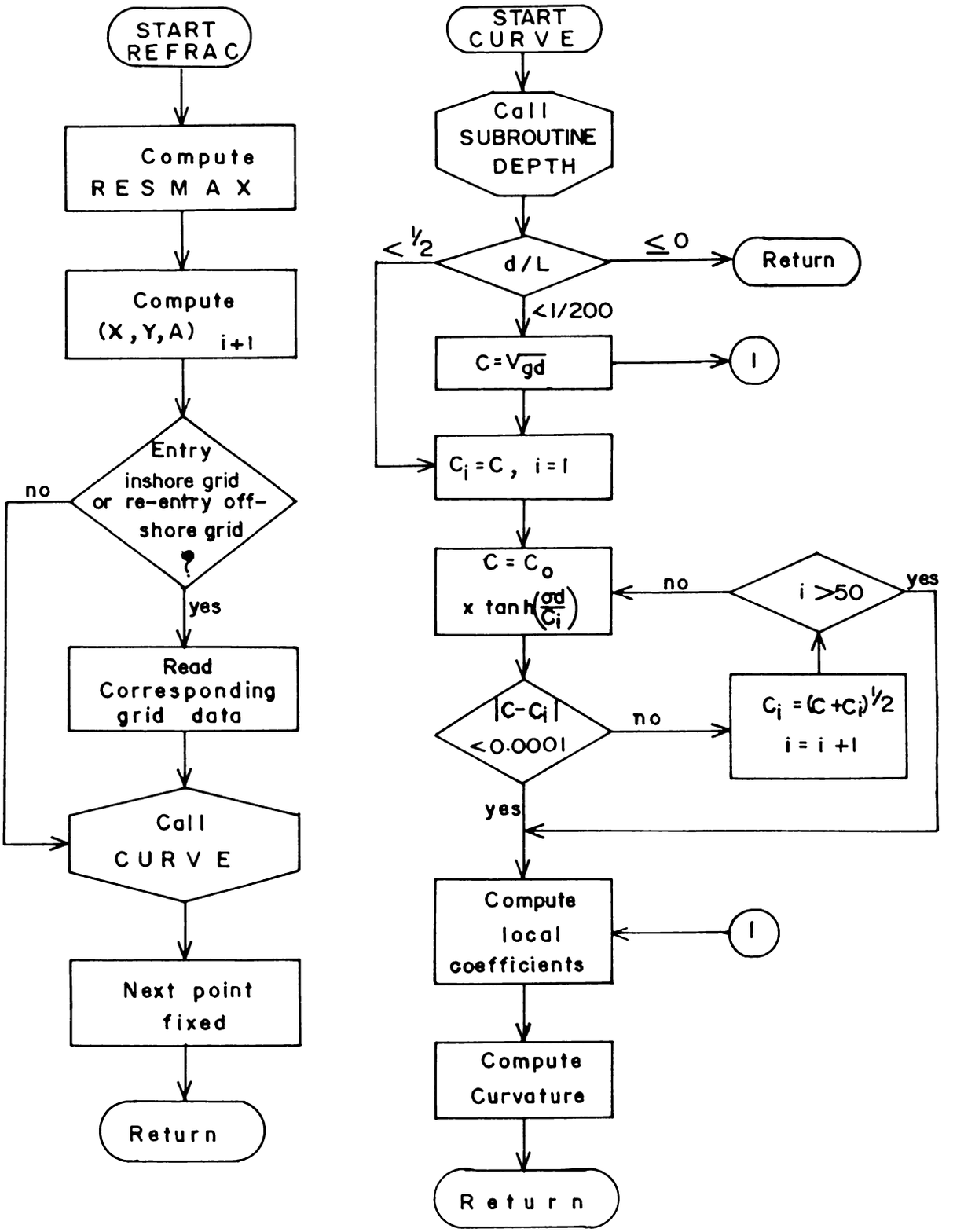

Fig.5.1 Flow Chart for Wave Ray Transformation Model (contd.....)

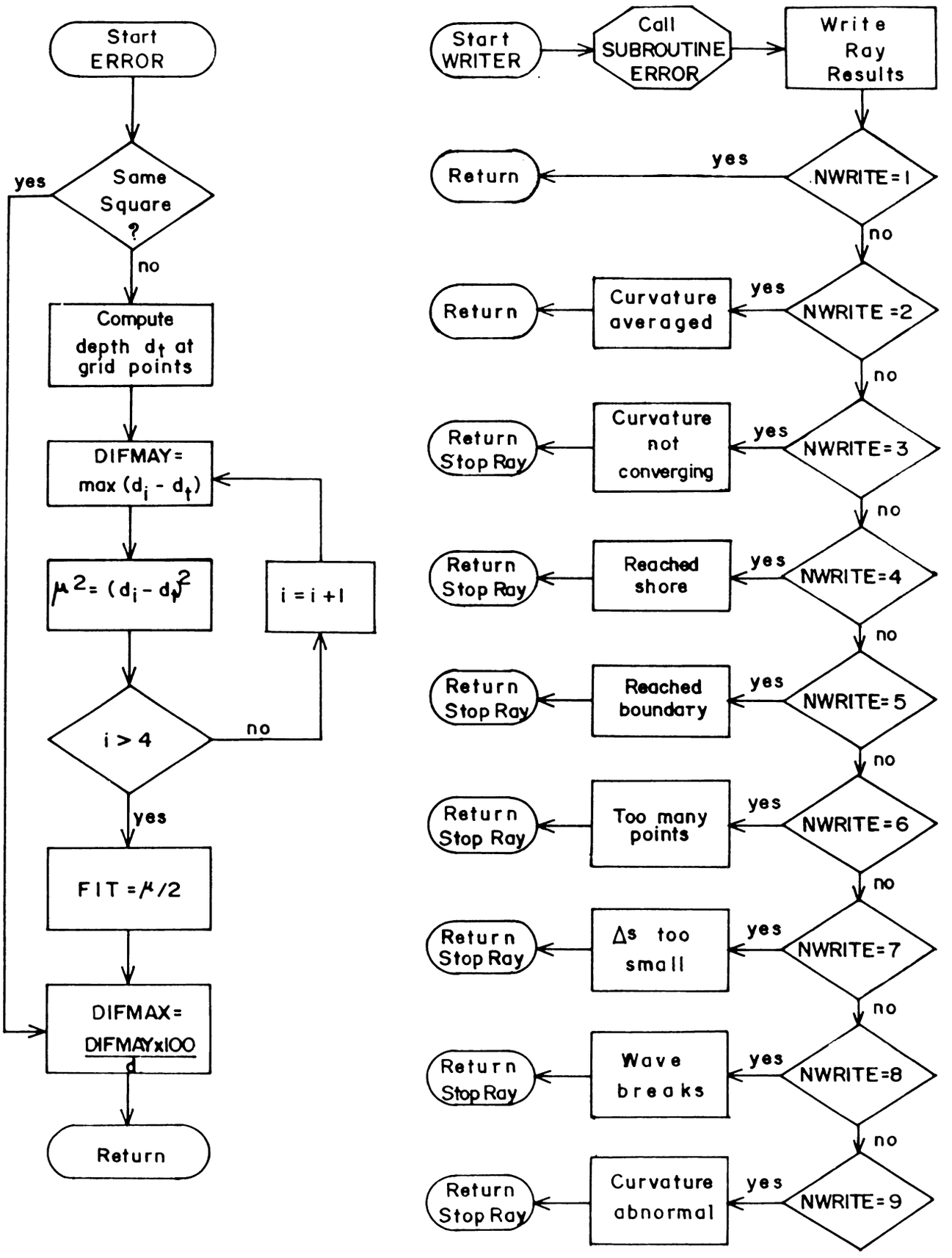

Fig·5.1 Flow Chart for Wave Ray Transformation Model. (contd.....)

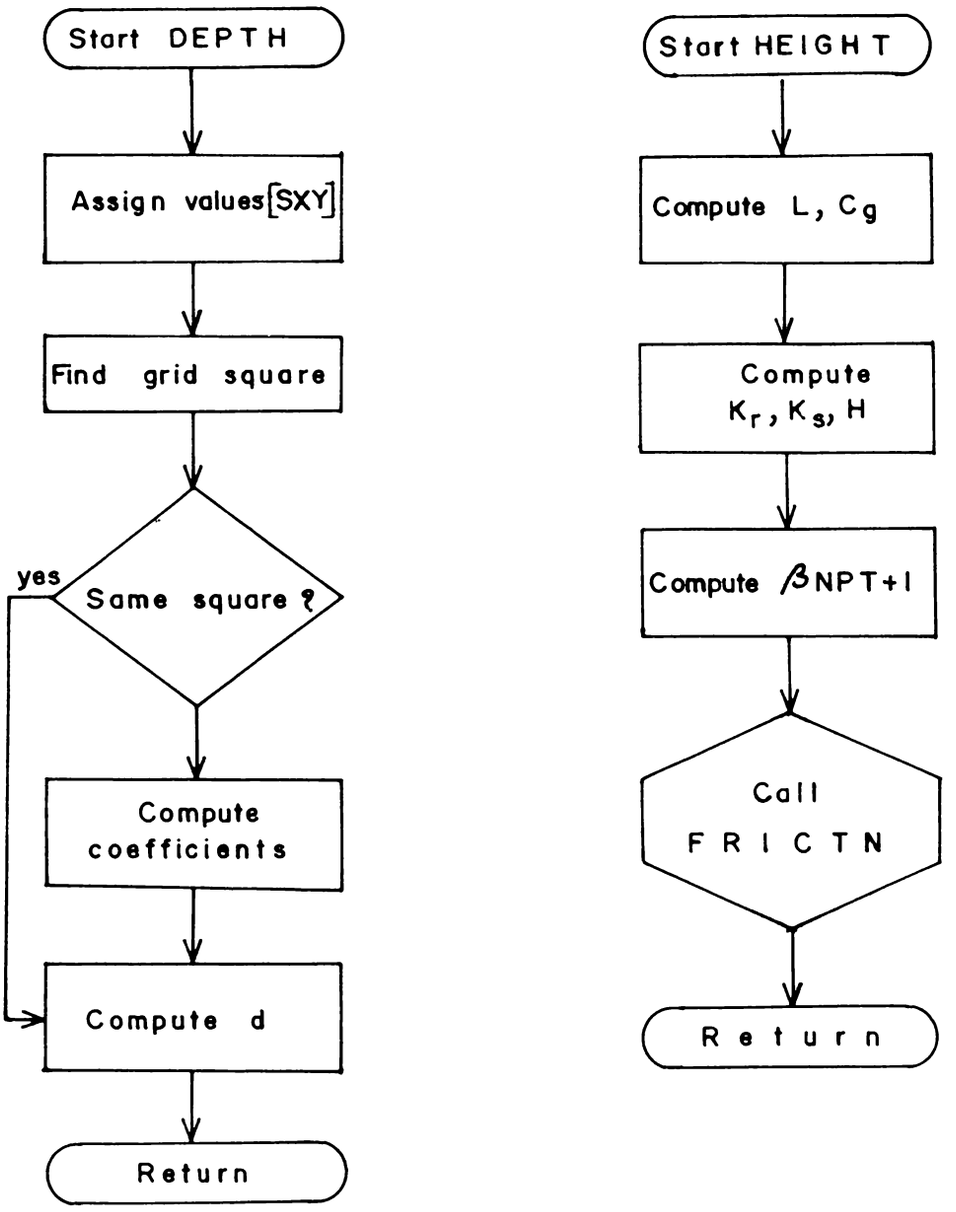

Fig. 5.1 Flow Chart for Wave Ray Transformation Model. (contd.....)

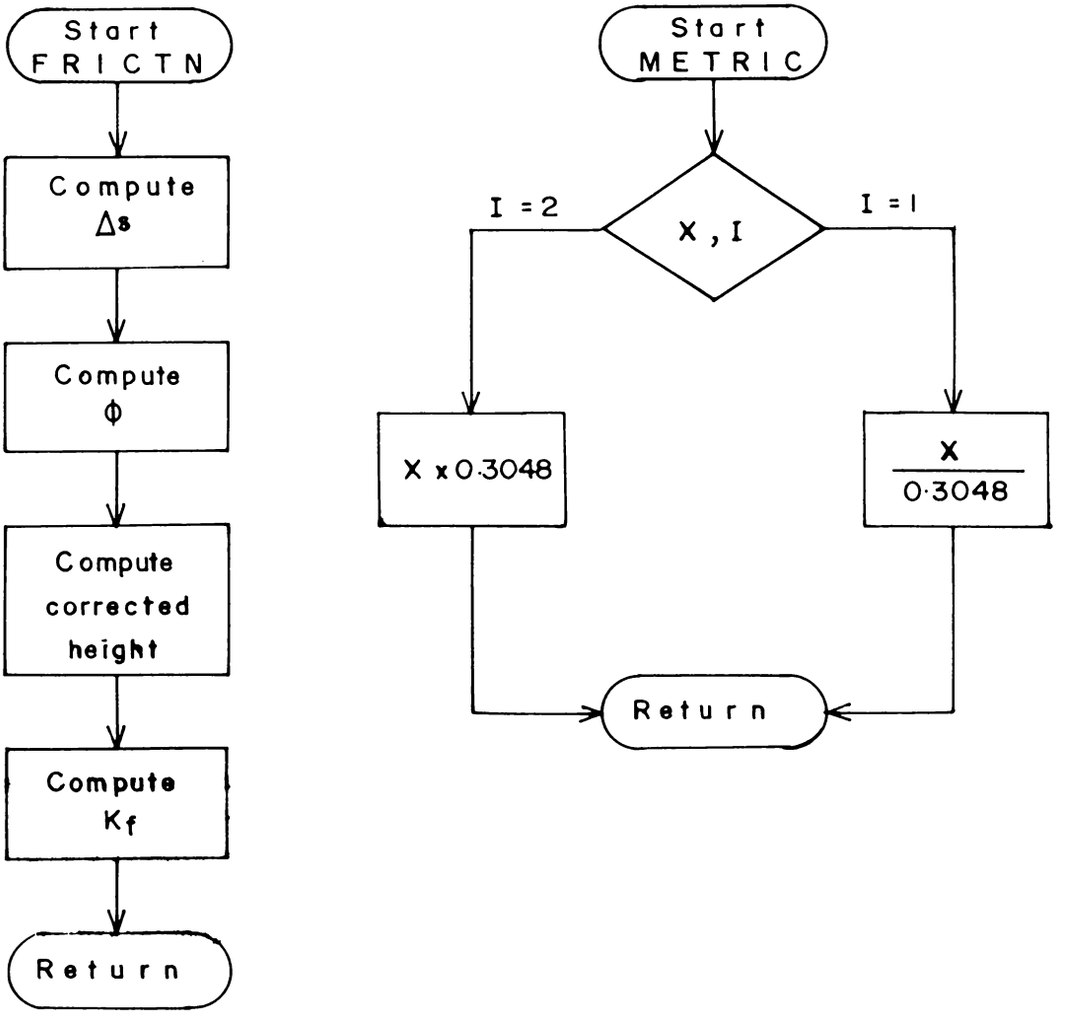

Fig. 5.1 Flow Chart for Wave Ray Transformation Model

(contd.....)

next point on the ray.

$$\Delta\alpha = \bar{\gamma}_s \Delta S \tag{5.2}$$

$$\bar{\gamma}_s = \frac{1}{2}\left[(\gamma_s)_i + (\gamma_s)_{i+1}\right] \tag{5.3}$$

$$\alpha_{i+1} = \alpha_i + \Delta\alpha \tag{5.4}$$

$$\bar{\alpha} = \frac{1}{2}(\alpha_i + \alpha_{i+1}) = \alpha_i + \frac{\Delta\alpha}{2} \tag{5.5}$$

$$x_{i+1} = x_i + \Delta s \ \text{Cos} \ \bar{\alpha} \tag{5.6}$$

$$y_{i+1} = y_i + \Delta s \ \text{Sin} \ \bar{\alpha} \tag{5.7}$$

Subroutine CURVE : This subroutine tests to discover whether the wave is in shallow water or at an intermediate depth, and then computes the local speed using the appropriate equation. Having calculated the speed, it finds the curvature of the ray at the point by use of the equation

$$\gamma = \frac{\sigma(1-R_c^2)}{CR_c + \sigma d(1-R_c^2)} \left[\text{Sin}\alpha(e_2 + 2e_4 x + e_5 y) - \text{Cos}\,\alpha\,(e_3 + e_5 x + 2e_6 y)\right] \tag{5.8}$$

where x and y are values of the co-ordinates in the local grid system and

$$R_c = \frac{C}{C_o} \tag{5.9}$$

Subbroutine DEPTH : This subroutine determines the local origin for the point on the ray and then calculates the local co-ordinates. Before computing the coefficients of the equation for the surface of best fit, it tests to determine whether the point lies within the same mesh square

as the previous point. In the case that it does, the subroutine calculates the new depth using the new local co-ordinates. Otherwise, it calculates the coefficients for the surface equation and then finds the depth.

Subroutine HEIGHT : The shoaling coefficient and refraction coefficient are calculated here. Using these two coefficients, the wave height is calculated as

$$H = K_r K_s H_o \tag{5.10}$$

Subroutine ERROR : A measure of the error involved in calculating depths by using a least sqare surface is estimated here.

Subroutine WRITER : This subroutine controls the printed output for the programme. Depending on the values of the branching identifier NWRITE, the ray may be stopped.

Subroutine FRICTN : The correction for the attenuation due to bottom friction is applied to the computed wave height from subroutine HEIGHT. The equations used, are

$$Hf_j = \frac{Hf'_{j-1}}{\left[(C_f \phi \Delta s Hf_{j-1})/(K_{sj} T^4)\right] + 1.0} \tag{5.11}$$

$$Hf'_{j-1} = Hf_{j-1}(K_{sj}/K_{sj-1})(K_{rj}/K_{rj-1}) \tag{5.12}$$

$$\phi = (\rho \pi^3/3g^2)\left[(K_{sj}/\sinh[2\pi d/L])^3\right] \tag{5.13}$$

where Hf_j and Hf_{j-1} are the wave heights after frictional attenuation at points j and j-1 on the orthogonal and Δs is the distance between the points.

Subroutine METRIC : The programme by Dobson is in terms of FPS units. This subroutine converts the input and output to metric units.

5.3.2. Modifications for Simultaneous use of Offshore and Inshore Grids

The above programme has provision for input of only one depth grid which extends from the deep water to the shore. The grid size will be normally coarse since it is practically not possible to give a fine grid for such a wide zone due to limitations of computer memory and time. Moreover, such a fine grid is not required for the intermediate waters where the wave transformation is not pronounced. At the same time it is essential to use a fine grid which depicts the topography in detail for the inshore where the effects of transformation are very pronounced. Hence considering all aspects, it is advisable to use two grids, one coarse offshore and another fine inshore grid, for obtaining best results. Bryant (1980) has modified the above programme such that the grid parameters of an inshore grid also is accommodated in the input. As soon as the wave ray enters the inshore grid from the offshore, the

corresponding wave parameters with inshore grid co-ordinates are printed out and this is further used as input for a second set of computations using the inshore grid.

This approach has been improved during the course of the present investigation. The programme is modified such that it permits the simultaneous usage of two grids. The wave orthogonal travelling from the deep water over the offshore grid propogates towards the shallow waters and once it enters the inshore grid, the computations and propogation of the orthogonal are continued based on the inshore grid of depths. Necessary modifications to achieve this are provided in the main programme and subroutines RAYCON and REFRAC. Provision has also been made for the re-entry of the ray into the offshore grid as may happen in some cases.

In addition to the above, some minor modifications have also been made in the programme. Provision is made for incorporation of water level changes due to tide or storm surge into the depth grid. Another modification is the facility to select rays during computations. This facility will be useful when the computations have to be repeated for some selected rays with change in wave parameters, friction factor, etc.

The complete computer programme with all the above modifications is given in Appendix-I.

5.4. Depth Grids

Two depth grids, one coarse offshore and another fine inshore are used at both Alleppey and Trivandrum. The offshore grids at both the locations have a grid element of 1.8 km. While the grid at Alleppey has a size of about 3600 km^2, the grid at Trivandrum has a size of about 6000 km^2. Naval Hydrographic Charts (No. 220, 221 and 222) are used for the preparation of these grids. The inshore grids are prepared from the bathymetric charts available in the Centre for Earth Science Studies updated during the present study. The inshore grid elements are 100 m and 200 m respectively at Trivandrum and Alleppey. A relatively finer inshore grid has been taken at Trivandrum because of the steep inshore. The inshore grids have areas of 8.5 km^2. and 13 km^2 at Alleppey and Trivandrum respectively.

The interpolation of depths at grid intersects from irregularly spaced soundings in bathymetric charts was done as follows. The grids are aligned with the x-axis in the south-north direction as per the programme logistics (Fig.5.2). A set of values at each grid intersect is obtained first by linear interpolation from the available data points. A second set of values is obtained by proceeding along the y-axis. Since most of the data points may not lie along the grid lines, the available points were transferred to the grid lines for the interpolations. The

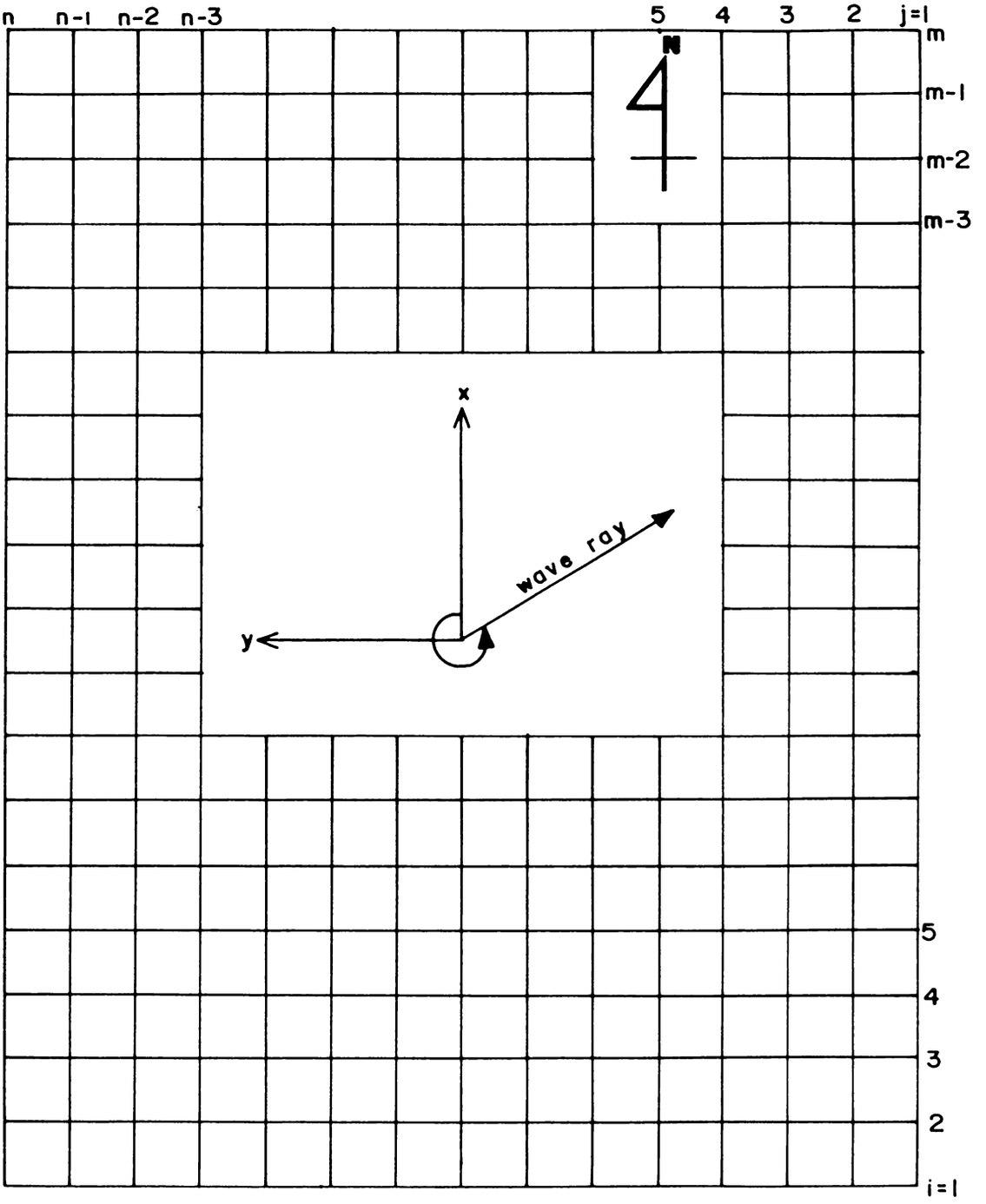

Fig.5.2 Grid System used in the Wave Ray Model.

averages of the two sets of data at each grid intersect constituted the depth grid.

5.5. Computational Procedure

5.5.1. Check for Deep Water Conditions

One of the stipulations of the computer programme employed is that the input wave data must correspond to the deep water, i.e. $d/L > 0.5$, according to linear wave theory. An attempt was made first to ascertain whether the offshore wave data in the present case fulfil this condition. For this, the deep water wave lengths were calculated for the different recorded zero-crossing periods using the relation

$$L = 1.68T^2 \qquad (5.15)$$

It was found that except few cases all others correspond to deep water. Even for the few shallow water cases computation with true deep water positions showed that the shoaling, refraction and friction coefficients are near unity at these recording stations and hence the error involved in the assumption of deep water is negligible.

5.5.2. Friction Factor

As seen in Table 2.1, there is a wide spectrum of values for the friction factor, which has been computed or used in transformation models by various authors. Different methods available for the computation of friction factor and

the problems encountered have already been discussed. It was decided to see the order of values computed by these formulations for the present area of study.

The simple formula of Kajiura (Nielsen, 1985) ~~(1968)~~, the friction factor diagram of Kamphuis (1975), which is most popular and the recent equations by Jonsson (1980) were selected for the computations. The sediment size values given in Table 3.1 for these coastal locations were used.

For the determination of C_f using the friction factor diagram, the Reynolds number, Re and the relative roughness height A/K_s were calculated as per the following equations in Grosskopf (1980):

$$R_e = \frac{U_b A}{\nu} \tag{5.16}$$

$$U_b = \frac{\pi H_s}{T \sinh kd} \tag{5.17}$$

$$A = \frac{H_s}{2 \sinh kd} \tag{5.18}$$

$$K_s = 2D_{90} \tag{5.19}$$

ν, the kinematic viscosity of sea water is taken as 6.25×10^{-7} m/s.

For the methods of Kajiura and Jonsson, the hydraulic roughness 'r' was assumed as 2.5 D (Nielsen 1983).

As the sediment size reported was for the 5-15 m depth zone, a mean depth of 10 m, and a representative wave of height 1.5 m and period 10 s were chosen for the calculations. The calculations for Alleppey derived C_f much less than 0.005 by the method of Kamphuis and a value of 0.0057 by the method of Jonsson. The corresponding values at Trivandrum were 0.005 and 0.0083 respectively. The equation by Kajiura was not applicable since the limiting condition of $r/a > 0.02$ was not applicable for these zones.

Lack of detailed sediment size information does not permit the calculations for the other depth zones. Moreover, the calculations were done based on the flat bed assum ption which does not represent the natural conditions, especially in the inshore waters, because of bed ripples. Recent studies (Hsiao and Shemdin, 1978; Nielsen, 1983, 1985; etc.) have shown that the formation of ripples in the bottom causes additional energy dissipation and depending on the bed geometry, the friction factor may be considerably high.

In view of ~~the~~ this, the values obtained above might only show the order of values rather than the actual ones. Hence an empirical approach was felt more practical. It is pertinent to note that some authors (Wright, 1976; Bryant,

1979) arbitrarily selected the values of friction factor. In the present study, it was decided to use different C_f values like 0.005, 0.010, 0.015 etc. and fix the factor empirically.

5.5.3. Results of Computations

The input data corresponding to different deep water conditions, along with the depth grid was fed to the computer and wave orthogonal positions and heights computed. Samples of input and output data are given in Appendix I. Examples of computed orthogonals are given in Fig. 5.3(a-b).

The computed orthogonals were checked for extreme refraction effects. According to Le Mehaute and Wang (1980) refraction coefficients less than 0.5 and greater than 1.5 must be doubted. Extreme refraction effects and crossing of orthogonals were found in some deep water cases of high obliquity and high period. A limiting refraction coefficient of 2.0 was used following Mogel et al. (1970). Computations were carried out for each data set with friction factors of 0.005, 0.010, 0.015 and 0.020. The range of values of K_r, K_s, K_f, (for C_f = 0.02) is given in Table 5.1

5.6. Comparison of Wave Heights

For the purpose of comparison, the nearshore wave height at the wave recording point had to be obtained from

Table 5.1 Range of values of Refraction (K_r), Shoaling (K_s), and Friction (K_f) Coefficients (with C_f = 0.02) at the Nearshore Points.

Location	K_r	K_s	K_f
Alleppey	0.67 - 1.34	0.90 - 1.40	0.43 - 0.92
Trivandrum	0.30 - 1.34	0.92 - 1.07	0.92 - 1.00

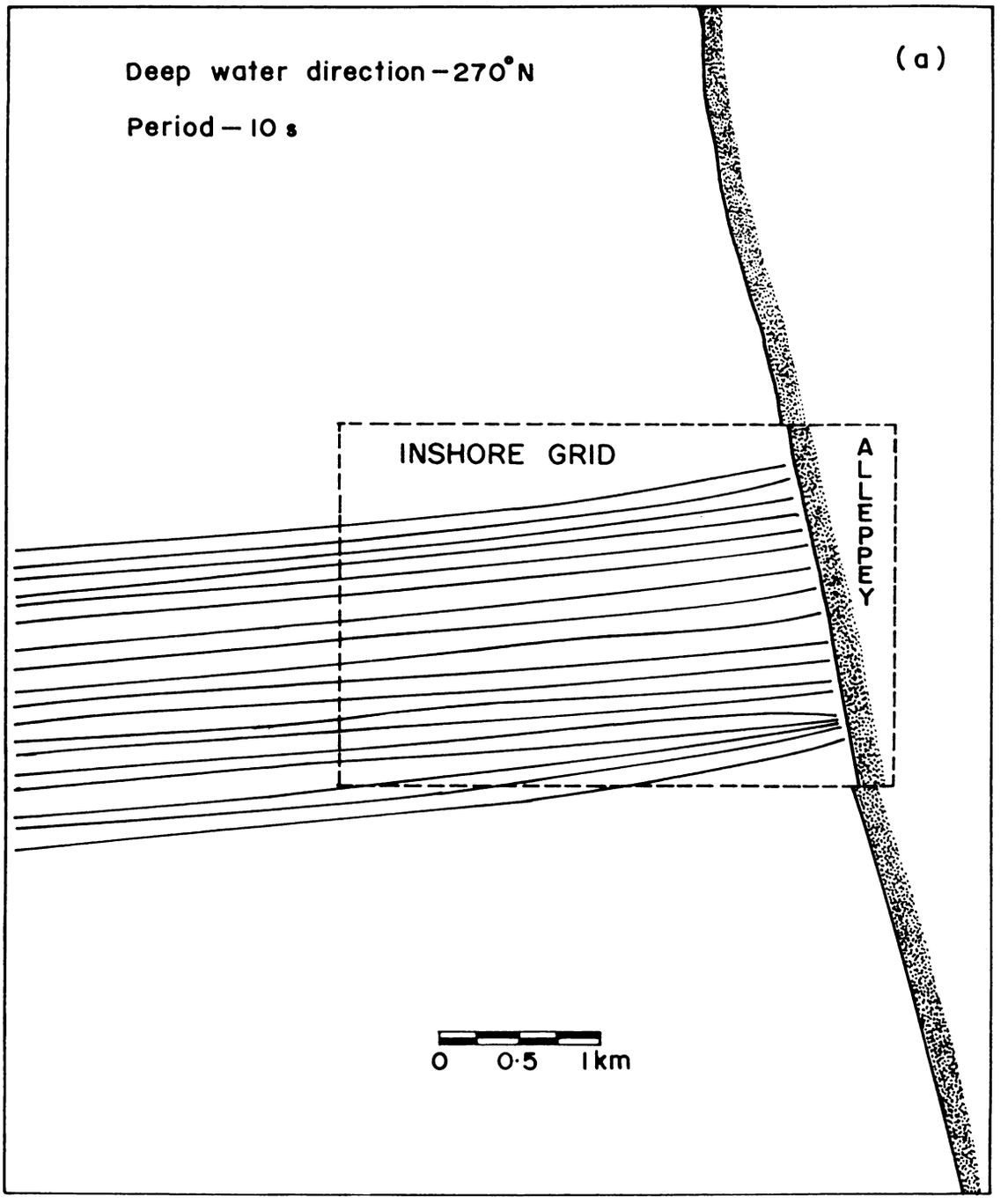

Fig. 5.3 Examples of Computed Orthogonals

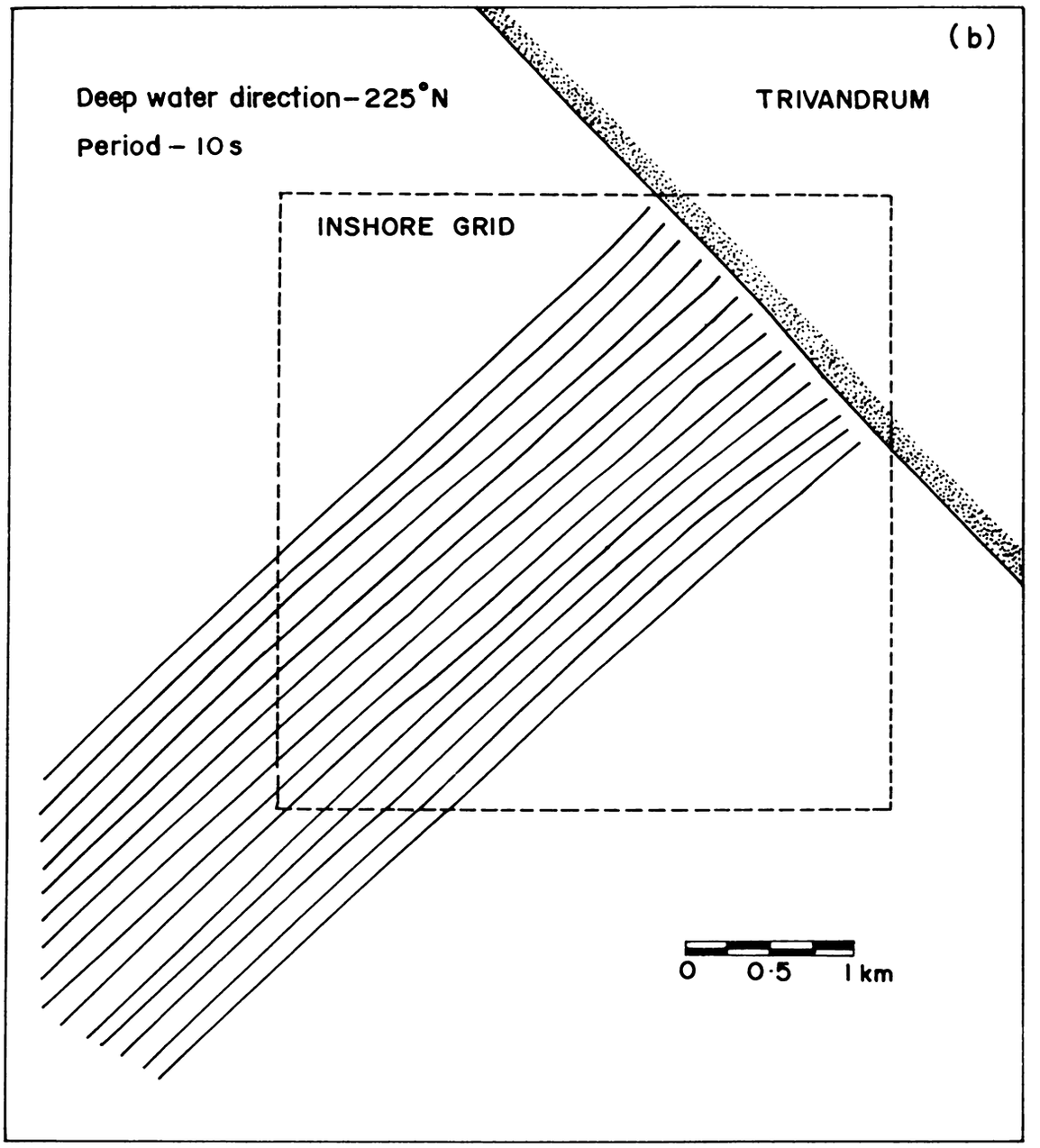

Fig. 5.3 Examples of Computed Orthogonals

the computations. As the wave rays did not pass through the nearshore point exactly in all cases, those orthogonals which pass by the point within 30 m distance were selected for the comparison of results. In some cases, the computations were repeated to make it pass by the nearshore point.

The computed results for different friction factors were compared with the measured data. For the cases with friction factor C_f = 0.02, good comparison was obtained with the measured as shown in Fig. 5.4. Parametric linear regression analysis was carried out to evaluate the correlation between the measured and computed heights. A correlation coefficient of 0.8 was obtained indicating high degree of correlation between the measured and computed heights.

The correlation obtained in the present case could have been still higher, but for some wide deviations as seen in Fig. 5.4 due to the following reasons:

(i) The input deep water data at Alleppey comprises mostly of ship-based observations, which have an accuracy of $\pm$0.5 m. Hence the computed results suffer from this limitation of deep water data.

(ii) As has already been discussed in Chapter 4, the data comprises high conditions with generating areas over the shallow waters. Because of this input in the

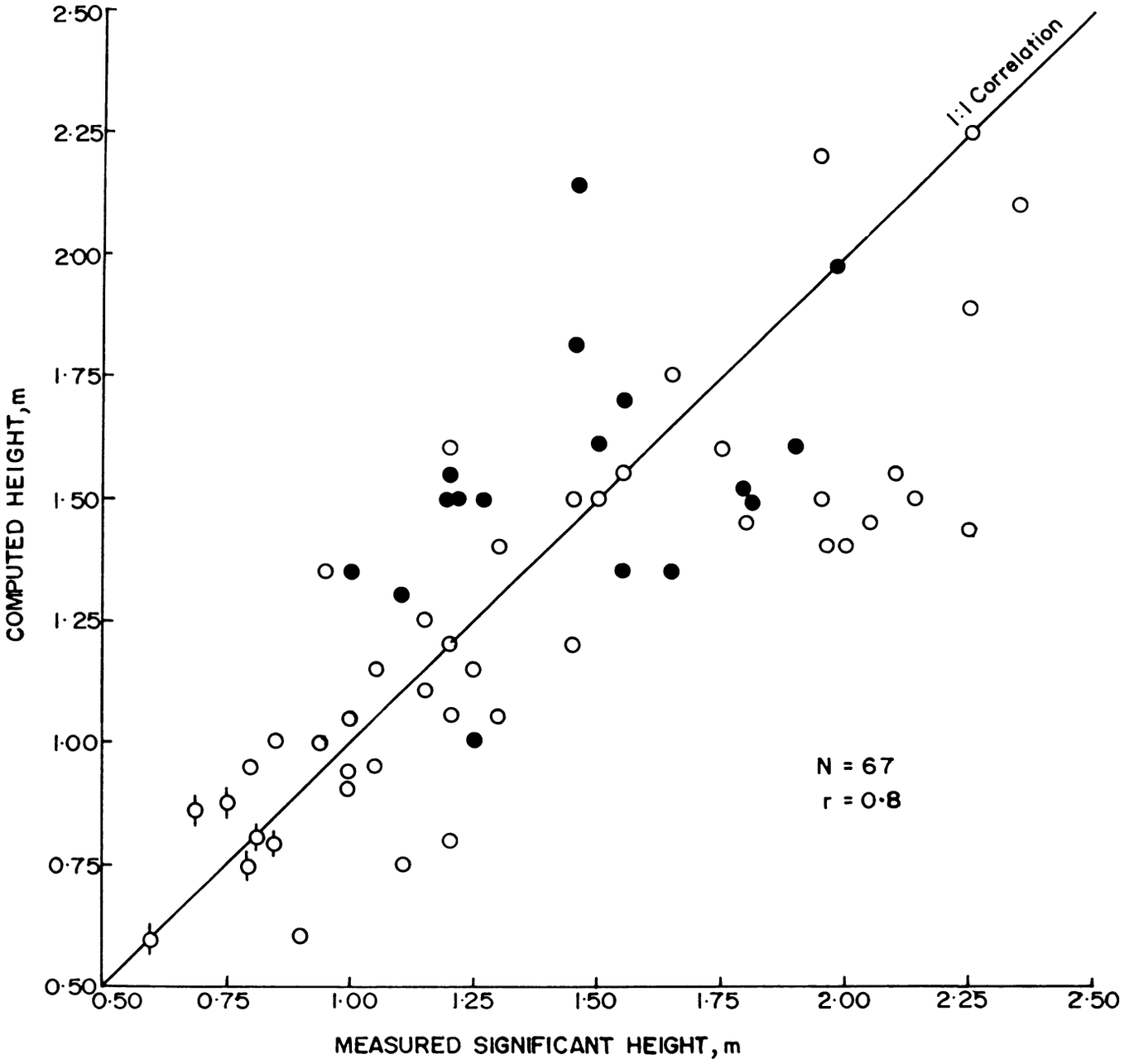

Fig. 5.4 Comparison of Measured and Computed Heights

● – Alleppey — Shipbased Deepwater Data

ϕ – Alleppey — Measured Deepwater Data

○ – Trivandrum — Measured Deepwater Data

shallow waters, the computed data happen to be underestimates in those cases. Grosskopf (1980) also has reported under prediction of nearshore heights in conditions of wave generation.

Due to the aforesaid reasons, it can be summed up that the wider deviations in the computed results in some cases may be due to the limitations of the data set rather than the model.

Since the present evaluation has been carried out for two coastal environments having different sediment, wave and shelf slope characteristics, which are representative of the Kerala coast, it can be concluded that the present model with a friction factor of 0.02 can be successfully used for the prediction of shallow water wave heights along the Kerala coast.

The present results are significant in terms of the applicability of the model for other coastal waters of the world. The model has been field tested by Bryant (1979) for the shelf waters of New South Wales, which is one of the steepest in the world. In the present case, the model has been field tested for two different environments, as already discussed. Hence the results of Bryant (1979) and the present study indicate the universal applicability of the present model.

5.7. Attenuation of Wave Heights

Since the programme is field tested, the results of computation could be used to study the extent of the bottom frictional attenuation. The computational results can be used to study the influence of refraction and shoaling also, but since their characteristics are already known, it does not require a further study.

For evaluating the influence of bottom friction, the friction coefficient K_f , which is derived in the wave orthogonal computation itself could be used. The value of K_f at the nearshore point indicates the total energy expended due to bottom friction during the passage of the wave from deep water to this point. The friction coefficients at the nearshore points range from 0.92 to 1.0 at Trivandrum and from 0.43 to 0.92 at Alleppey (Table 5.1). This does not enable a true comparison of the frictional effect at the two locations since the range of wave heights and periods used are different at both the locations.

For this purpose, computations for the same deep water height and period approaching normal to the coastline at each location are obtained and the values of K_f compared.The percentage attenuation in terms of the deep water height are obtained (Table 5.2). It can be seen that the frictional attenuation is quite high reaching as much as 52% at

Table 5.2. Attenuation of Wave Height due to Bottom Friction.

Location	Percentage attenuation of waves* (in terms of deep water height)					
	Height (m)	1			2	
	Period (s)	6	9	12	6	9	12
Trivandrum		1	2	4	1	3	7
Alleppey		18	27	34	30	43	52

* Deep water direction normal to the coastline at each location.

Alleppey. This validates the conclusion drawn in Chapter 4 that bottom slope plays the major role in deciding bottom frictional attenuation and consequently the shallow water wave heights.

5.8. Extension of the Results to Other Parts of the Kerala Coast

Having seen that bottom slope is the dominant factor that determines the transformation and consequently the shallow water wave climate, it can be taken as a criterion for classification of the coastal waters into zones of different wave intensity.

The widths of the shelf at different depth levels for a few locations along the Kerala coast are given in Table 5.3. The characteristic feature of the Trivandrum coast is the steep and very narrow shelf (Fig. 5.5). Towards north, the isobaths, especially the inshore, move away from the coastline indicating a decrease in the slope of the bottom. This trend is continued till Cochin. In the coastal zone around Ponnani, a slight reduction in the width of the shallow zone is seen. However, further north, the slope again decreases and the bottom is most gentle off Calicut. North of Cannanore, the coast is characterized by an increase in the slope.

The possible wave height distribution along the Kerala

Table 5.3. Shelf Width at Different Locations Along the Kerala Coast.

Location	Distance (km) from shoreline of isobaths (m)					Sector
	10	20	30	50	100	
Trivandrum	0.3	0.5	4.0	11.0	40.0	A
Quilon	1.8	3.2	5.7	17.7	39.0	B
Alleppey	3.5	11.5	18.0	29.0	46.0	C
Cochin	4.8	11.1	20.7	37.5	46.0	D
Ponnani	2.7	8.1	17.4	26.9	45.6	C
Calicut	4.8	10.2	14.7	42.0	73.5	D
Tellicherry	4.5	8.7	15.0	35.1	75.0	D
Kasargode	2.7	7.5	10.4	24.0	58.0	B

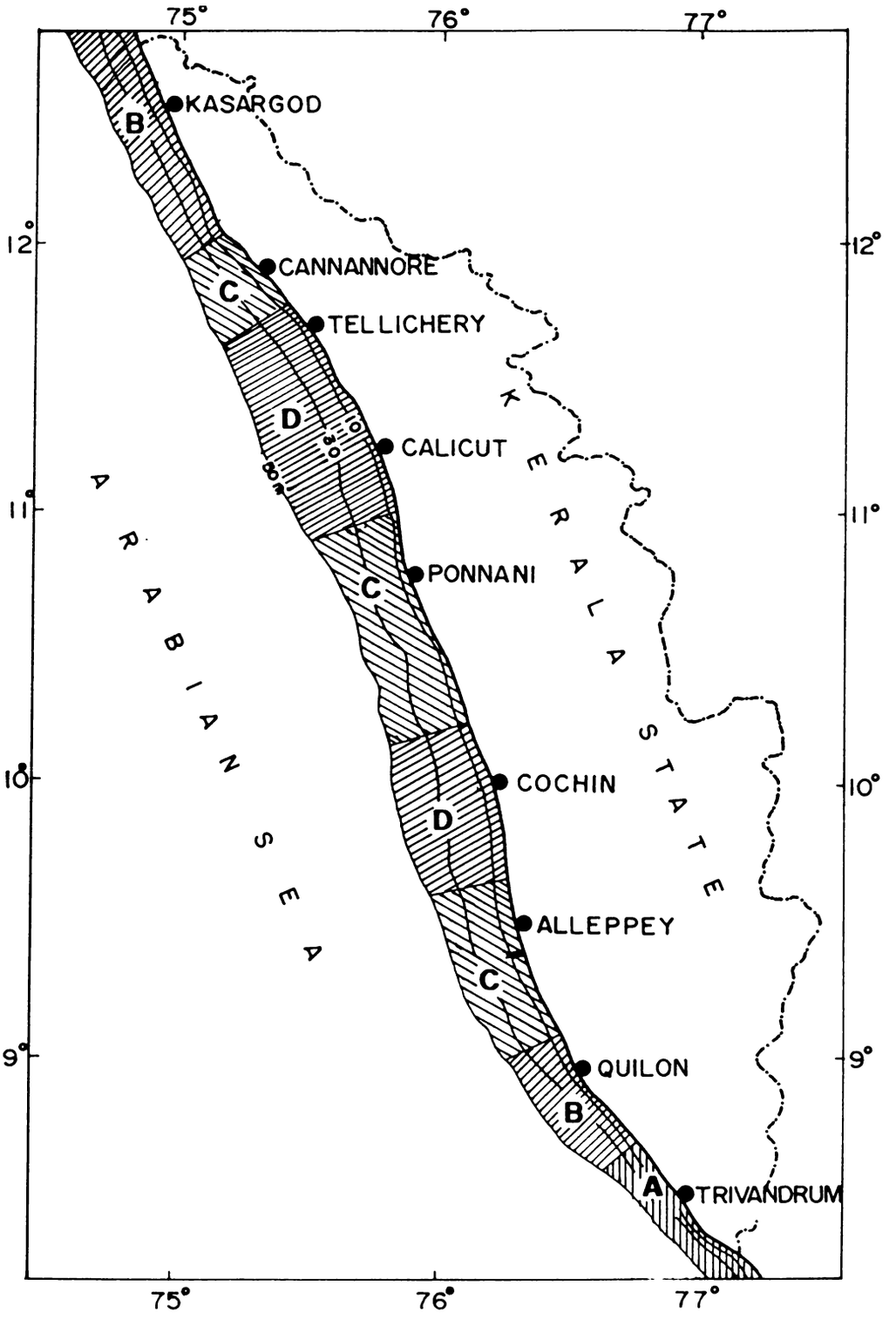

Fig.5.5 Different Wave Transformation Sectors along Kerala Coast

coast may be deduced from the distribution of bottom slope as given in Table 5.3 (last column) and Fig. 5.5. The shallow water wave intensity should be maximum at the zone off Trivandrum (Sector A). The zone around Quilon and the northernmost stretch of the coast beyond Cannanore (Sector B) follows Trivandrum in intensity. The zone around Ponnani and Alleppey will have moderate wave conditions (Sector C). The wave intensity is expected to be the least off Cochin, Calicut and Tellicherry (Sector D).

The above prediction for Calicut was checked using the present computer programme. For the computations, offshore and inshore grid elements of 1.8 km and 200 m respectively were chosen. A deep water wave of height 2 m approaching normal to the coastline was selected for the study. For wave periods of 6, 9 and 12 s, frictional attenuations of 43, 60 and 74% respectively in terms of deep water height were obtained. These results for Calicut may be true for Cochin and Tellicherry also, but with the following difference. The zone 50 - 100m depth is exceptionally wide off Calicut and Tellicherry, unlike Cochin (Table. 5.3). Hence high period waves will start feeling the bottom much earlier at Calicut and Tellicherry than Cochin, resulting in higher losses for these wave components at the above locations. Thus the exceptionally high percentage of loss obtained in the above computations may not be just the same for Cochin.

The measured wave data at different parts of Kerala coast also seem to support the deductions of the present study. Baba et al., (1983a,b and 1987) and Baba (1985) based on nearshore wave measurements at Trivandrum, Alleppey, Calicut and Tellicherry conclude that there is a general reduction in the wave intensity from south to north. The only discrepancy in the present results is that while they find lower wave heights at Tellicherry when compared to Calicut, the present study shows more or less similar conditions at these two locations. This discrepancy for Tellicherry could be due to the peculiarity of the wave measurement site, which happens to be in a bay with offshore stacks (Baba et al. 1983 a,b), where the transformation processes are different. Hence the results are not comparable with those of Calicut or the other stations, where the measurements are in nearshore waters with more or less straight and parallel bottom contours. The moderately high wave conditions deduced from the present study for the northernmost stretch of the Kerala coast is confirmed by the results of Dattatri (1973) for Mangalore.

Thus based on the factors responsible for wave transformation (the bottom slope being the dominant) it is possible to categorize the Kerala coast into different zones of wave intensity as indicated in Fig. 5.5.

5.9. Summary

The study shows that the Dobson's model, with the suggested modifications for the simultaneous use of offshore and inshore depth grids, frictional attenuation, etc., can be successfully used for the prediction of shallow water wave heights along the Kerala coast. The present results in conjunction with that of Bryant (1979) tend to establish the universal applicability of this model. A friction factor of 0.02 which was determined empirically is recommended for use in this model for this coast. Friction factors calculated using available formulations proved to be underestimates of the empirically determined. This points to the necessity of including bed ripple geometry in the calculations of friction factor.

The present model cannot be justifiably used in cases dominated by sea conditions or where the sea waves make a significant contribution towards the energy spectrum.

The study of the frictional coefficients validates the conclusions made in Chapter 4 regarding the dominance of bottom frictional attenuation in shelf waters with gently sloping bottom . Based on the distribution of bottom slope different wave transformation zones are proposed for the Kerala coast. Available literature on wave climate for this coast well supports this categorisation.

CHAPTER 6

PREDICTION OF WAVE SPECTRAL TRANSFORMATION

6.1. Introduction

Of late most coastal engineering applications require the wave spectral information in the shallow waters. The model suggested in Chapter 5 is based on the monochromatic approach and will not give this information. Wave spectral transformation models which can predict the shallow water spectrum become a useful tool under such circumstances. These models, unlike the ray models, are more complex and require better computer facilities and more computational time.

As seen in literature, the number of models available are few in this method. The models by Shiau and Wang (1977) and Hubertz (1980), which have the same computational procedure, appear to be promising, since field evaluation of these for some conditions have already been done. Based on the results of this field evaluation and the observed wave transformation characteristics (Ch.4), this model has been further modified. These modifications and the field evaluation of this revised model along with the recommendations are reported in this Chapter.

6.2. Theoretical Background

The total energy of a random sea wave can be expressed as the summation of energy content in the wave number and frequency domain such that

$$E = \iint \phi(k,f)\, dk\, df \tag{6.1}$$

From this the wave number spectral density function, F(k) and wave spectral density functions, S(f) can be obtained as follows:

$$F(k) = \int_0^{\infty} \phi(k,f)\, df \tag{6.2}$$

and

$$S(f) = \int \phi(k,f)\, dk \tag{6.3}$$

Equations have been developed connecting the spatial variation of S(f) with the spatial variation of $dE(k,\theta)$ and k where dE is the incremental wave energy over the wave number band dk and a directional angle θ.

The basic equation to compute the spatial variation of k is the conservation equation for wave number, which for steady cases reduces to the simple form

$$\nabla f = 0 \tag{6.4a}$$

or

$$f = \text{Constant} = \sigma_o \tag{6.4b}$$

In the presence of a steady current U,

$$f = \sigma(k,d) + K\,U \tag{6.5}$$

According to linear wave theory, the dispersion relation is

$$\sigma^2 = gk \tanh kd \tag{6.6}$$

Combining equations (6.4), (6.5) and (6.6),

$$(gk \tanh kd)^{1/2} + uk \cos\theta + vk \sin\theta = \sigma_o \tag{6.7}$$

where u and v are current velocities in the x and y directions respectively with x direction normal to the shoreline and y direction along the shoreline.

From the assumption that the wave-number vector in space is irrotational, it follows that

$$\frac{\partial(k \cos\theta)}{\partial y} + \frac{\partial(k \sin\theta)}{\partial x} = 0 \tag{6.8}$$

Since equations 6.7 and 6.8 are coupled through k and θ, they can be solved simultaneously to get k and θ.

To determine the variations of $dE(k,\theta)$, the assumption made is that the wave energy associated with a certain frequency band stays within this band so that the principle of conservation of energy is applicable to each frequency band under consideration. This assumption denies energy transfer among different frequencies and is valid when nonlinear effects are negligible. According to Longuet-Higgins and Stewart (1960, 1961), the energy equation for the fluctuating motion of waves with a superimposed current system is

$$\frac{\partial}{\partial x}[dE(k)(u + C_g \cos\theta] + \frac{\partial}{\partial y}[dE(k)(v + C_g \sin\theta)] + S_{xx} \frac{\partial u}{\partial x}$$

$$+S_{xy} \frac{\partial v}{\partial x} + S_{yy} \frac{\partial v}{\partial y} + S_{yx} \frac{\partial u}{\partial y} = - \phi_d \tag{6.9}$$

where

$$\left.\begin{aligned} S_{xx} &= dE(k)\left[\left(2n-\tfrac{1}{2}\right)\cos^2\theta + \left(n-\tfrac{1}{2}\right)\sin^2\theta\right] = dE(k)\ \sigma_{xx} \\ S_{yy} &= dE(k)\left[\left(2n-\tfrac{1}{2}\right)\sin^2\theta + \left(n-\tfrac{1}{2}\right)\cos^2\theta\right] = dE(k)\ \sigma_{yy} \\ S_{xy} &= S_{yx} = \frac{dE(k)}{2}\, n \sin(2\theta) = dE(k)\ \sigma_{xy} \end{aligned}\right\} \quad (6.10)$$

are the radiation stresses and ϕ_d is the rate of energy dissipation per unit area.

Equation (6.9) permits the computation of the spatial variations of dE(k) for given boundary conditions and dissipation function. Hubertz (1980) and Shiau and Wang (1977) apply the shallow water breaking criteria (Divoky et al., 1970)

$$\left(\frac{H_s}{L}\right)_b = 0.12\ \tanh(kd)_b \quad (6.11)$$

to restrict the wave height in the nearshore.

The theory given above is the basis of the models of Hubertz (1980) and Shiau and Wang (1977).

6.3. The Computer Programmes

6.3.1. Programme by Hubertz

This programme calculates refraction and shoaling effects on wave spectra due to bathymetry and currents in a

horizontal two dimensional region using a finite differnce solution of equations given above. The programme consists of a main driver programme and nine subroutines (Fig. 6.1). The grid system used in the computations is given in Fig. (6.2). A brief functional description of the programme and its subroutines are given below:

Programme MAIN : This is the driver programme. It reads the input data, sets constants, executes a loop which calculates wave angle and height for different frequencies and prints out the results.

Subroutine DEPTH : The x and y derivatives of the depths at each grid point using the values adjacent in the respective x or y directions are calculated.

Subroutine SMOOTH : In case the input bathymetry varies too greatly in space, for a stable solution this is used as an option.

Subroutine CURRENT : This subroutine calculates the x and y derivatives of the current components at each grid point using the values adjacent in the respective x or y direction. This subroutine is not considered in the present study due to the reasons already cited.

Subroutine SNELL : The initial wave height and angle at each grid point using the input data without current effects is

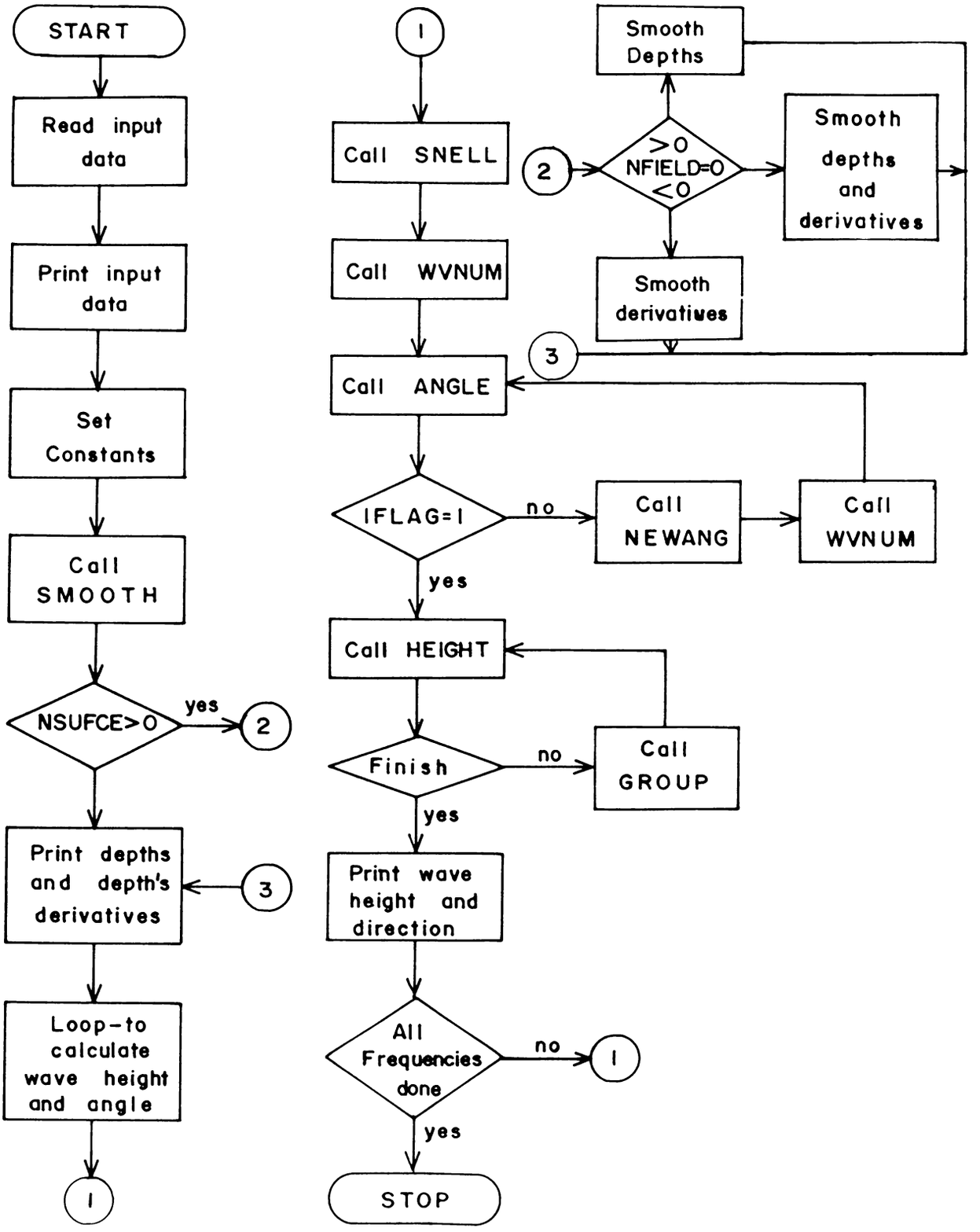

Fig.6.1 Flow Chart for Spectral Transformation Model

calculated. By calling the subroutine WVNUM, an initial wave number is calculated which is used for calculation of an initial wave height.

Subroutine ANGLE : This subroutine sets values of wave angle on the boundary and determines sweep direction based on wave approach angle and then calls subroutine NEWANG to determine wave angle at each grid point as affected by bathymetric and current refraction.

Subroutine NEWANG : The wave number determined in WVNUM and the equation (6.8) are used to calculate a wave angle at each grid point.

Subroutine WVNUM : The wave number at a grid point is calculated through interaction of the dispersion relationship including current terms.

Subroutine HEIGHT : This subroutine uses the wave number and angle calculated previously and the equation (6.9) to calculate through iteration wave height at each grid point.

Subroutine GROUP : Various terms used in subroutine HEIGHT are calculated using this subroutine.

6.3.2. Modifications to Incorporate Bottom Frictional Attenuation

Modifications were made in the above programme during

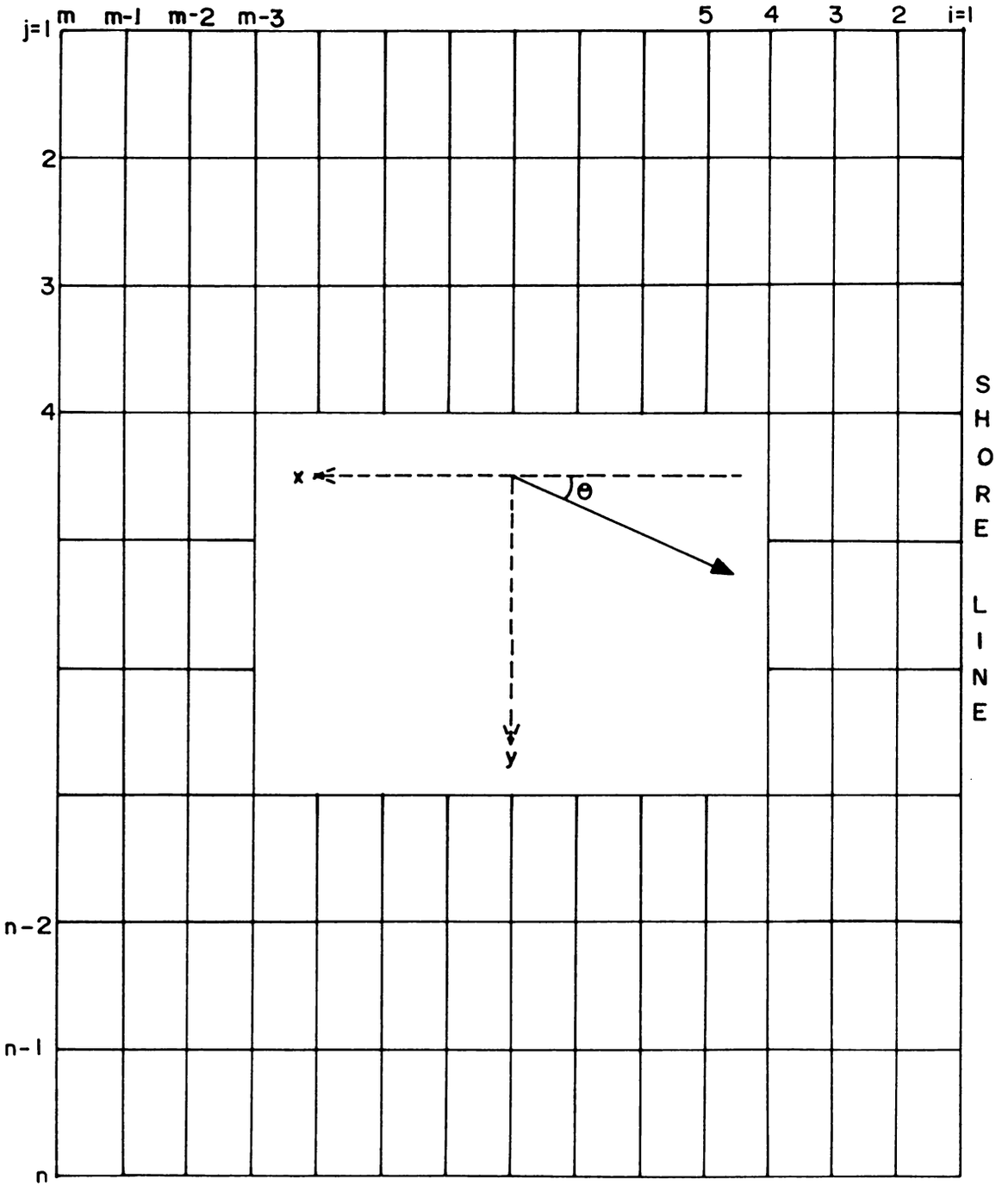

Fig. 6.2 Grid System used in the Spectral Model

the course of the present study to incorporate bottom frictional attenuation. The bottom frictional dissipation function given by Collins (1972) was used for bottom frictional correction. It may be noted that Wang and Yang (1981) used the dissipation function of Collins to incorporate bottom frictional attenuation in the model of Shiau and Wang (1977) and carried out its field evaluation. Since the computer programme of Wang and Yang (1981) is not available, modification was carried out independently in the present study.

The frictional dissipation function according to Collins (1972) is

$$\phi = \frac{C_f g k C_g}{2\pi\sigma^2 \cosh^2 kd} S(f)\langle u\rangle \qquad (6.12)$$

where

$$\langle u\rangle = \left[\Sigma S(f) \frac{g^2k^2}{\sigma^2 \cosh^2 kd} \Delta f\right]^{1/2} \qquad (6.13)$$

The original programme was modified to incorporate the above equations. The equation for the dissipation function was introduced in the subroutine GROUP. This dissipation function is introduced in the wave energy equation of subroutine HEIGHT. Modifications were made in the MAIN programme to calculate $\langle u\rangle$ and other additional terms.

The final programme with all the modifications is given

in Appendix II.

6.4. Depth Grids

Two depth grids, as in the case of wave ray model, were prepared. The basic sounding data used remained the same at both the locations. However, as the orientation of the axes are different in the programme logistics as shown in Fig. 6.2, the depth grids were prepared again according to this grid orientation.

Since for the stability of the calculations of wave number and wave angle, the condition

$$\frac{\Delta y}{\Delta x} > \tan \theta_m \qquad (6.14)$$

is recommended (Wang and Yang, 1976), the grid sizes were selected accordingly. The offshore grids have size elements of 1260 x 2515 m and 865 x 1725 m respectively at Trivandrum and Alleppey. The inshore grids have size elements of 71 x 142 m and 100 x 200 m respectively at Trivandrum and Alleppey.

6.5. Computations

The deep water spectral data and parameters of offshore grid were given as input. The computations were carried out in the offshore grid. Since the programme is not modified

to accommodate both offshore and inshore grids at the same time due to certain limitations in computer time, computations in the inshore grid were done subsequently. For this, the output from the offshore grid at the boundary of the inshore grid was given as input.

The same empirical approach as in Chapter 5 was followed for selection of friction factor. Computations were carried out with friction factors of 0.005, 0.010, 0.015 and 0.020 for each data set. The total number of data sets were 17 consisting of 2 at Alleppey and 15 at Trivandrum.

Samples of the computer inputs and outputs are given in Appendix II.

6.6. Comparisons

The different sets of observed wave spectra for comparison purposes were selected with the following consideration. The cases of deep and shallow water spectra, where the shallow water part is under active generation were excluded. As seen earlier the nearshore spectra for such cases show the same energy level as the deep water or sometimes even higher energy level than the deep water. These cases have clearly shown underpredictions in the wave ray method as well. The cases before May 25 at Trivandrum presents more or less near ideal conditions for comparisons.

Comparison of the measured spectra with computed spectra for different friction factors shows that the computations with C_f = 0.01 give the best results. Examples of the comparisons are given in Fig. 6.3(a-d). The results obtained are reasonably good in the context of the complexity of the problem and the assumptions made in the programme.

The computed spectrum follows the deep water spectrum in shape since the nonlinear wave-wave interaction processes are not considered. Hence discrepancies occur wherever the nearshore spectrum is influenced by such processes. An example is the computed spectrum for May 24 (Fig. 6.3d). While the computed and measured peak spectral densities tally, the frequencies do not. This is because the high frequency spectral peak in deep water has changed to low frequency peak in shallow water possibly due to wave-wave interaction.

Barring this discrepancy it may be concluded that the present model successfully predicts shallow water spectrum and can be used for the shallow waters of Kerala coast.

Like the wave ray prediction model, this model cannot be justifiably used for prediction of shallow water spectra in cases where the shallow water zone is under atmospheric energy input. Examples of the computations in such cases is

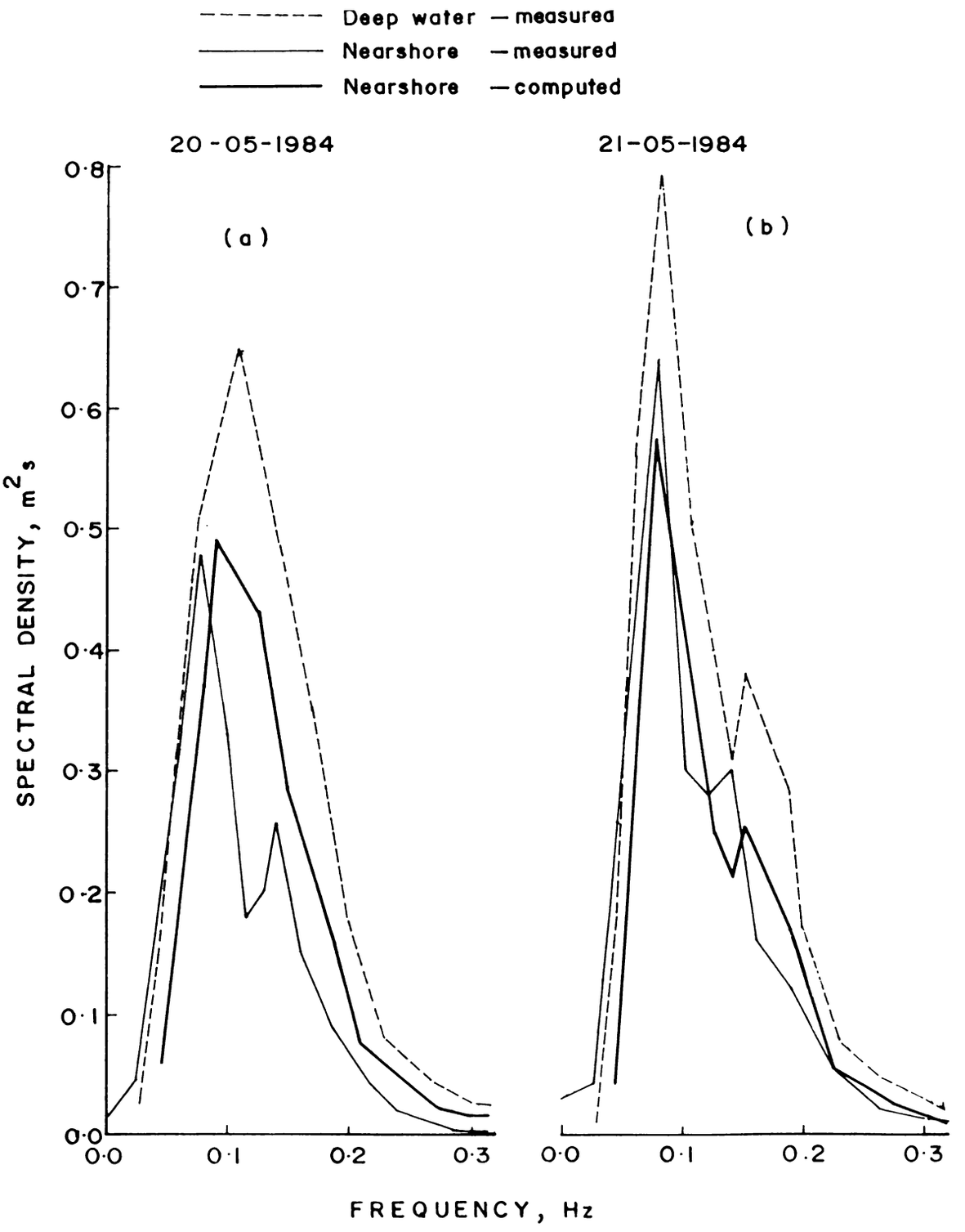

Fig.6.3 Comparison of Measured and Computed Spectra (C_f=0·010)

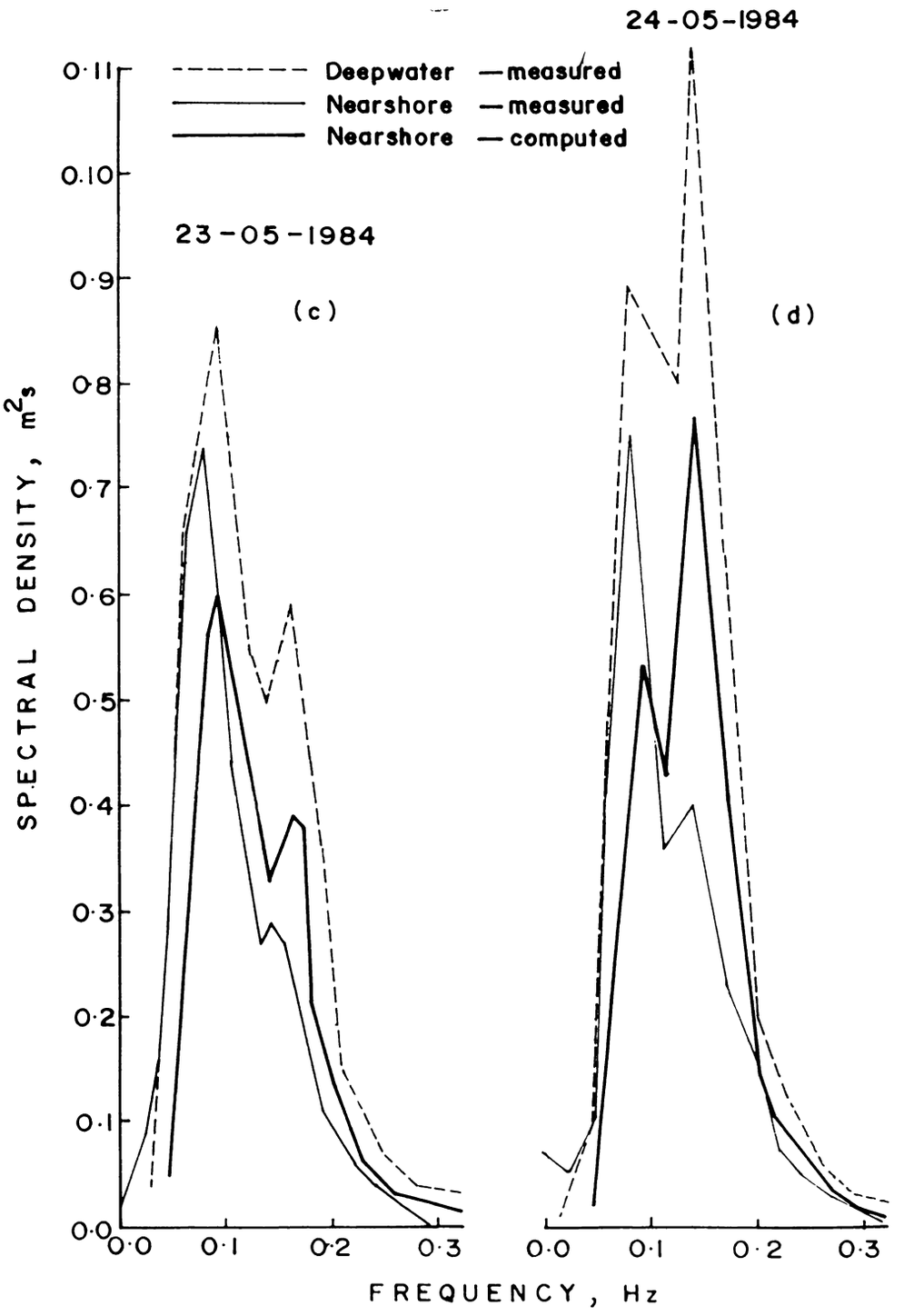

Fig.6.3 Comparison of Measured and Computed Spectra (C_f=0·010)
(contd.....)

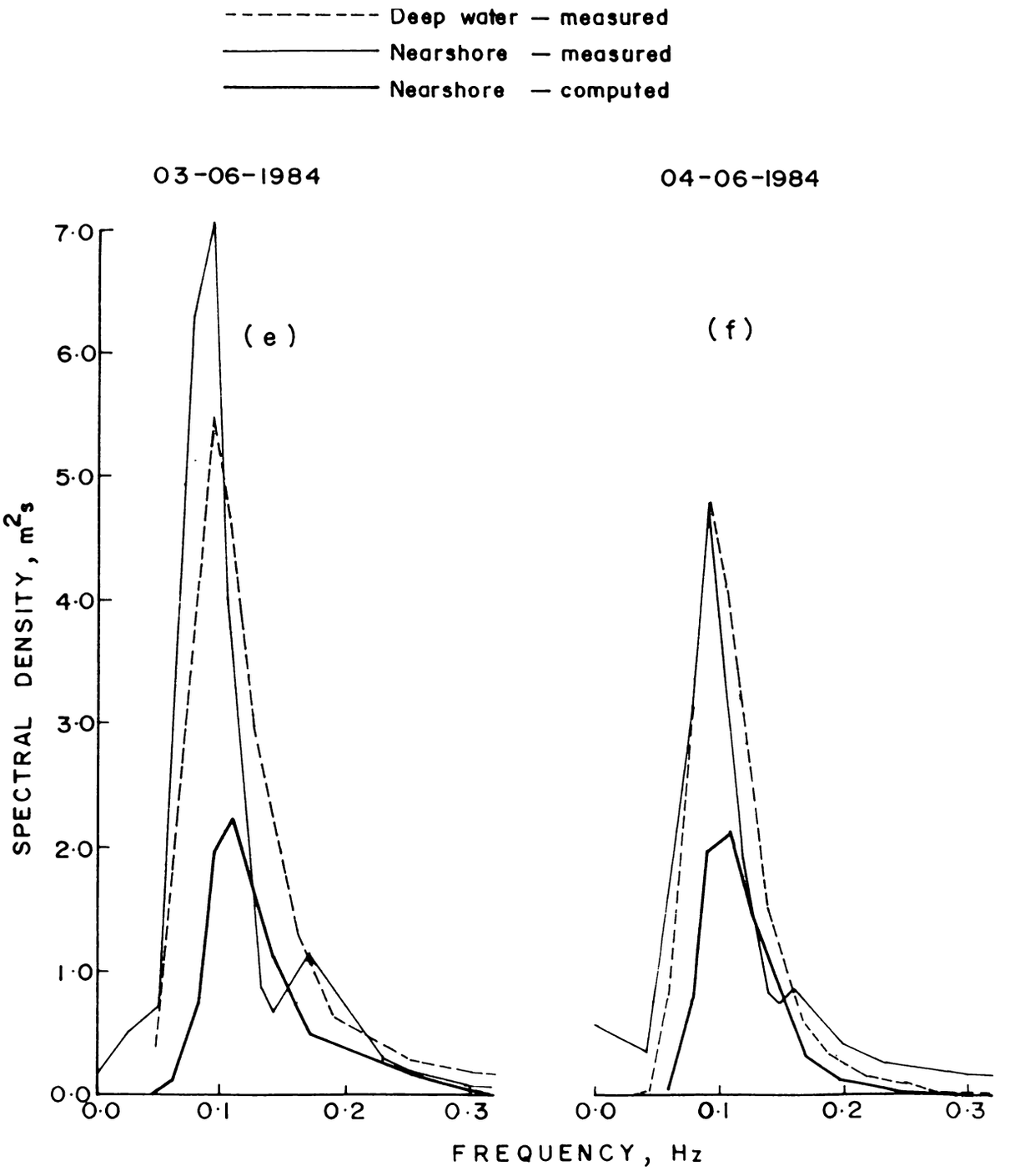

Fig.6.3 Comparison of Measured and Computed Spectra (C_f=0·010)

(contd.....)

given in Fig. 6.3(e-f). Since the cases presented here correspond to the most intense wave conditions with considerable shallow water energy input (as indicated by the high energy secondary peaks), the deviations of the computed spectra from the measured are maximum.

The present field evaluation along with the one by Wang and Yang (1981) for the Island of Sylt establishes the applicability of this model for different coasts with varying environmental conditions.

6.7. Summary

The wave spectral transformation model of Hubertz was modified to incorporate bottom frictional attenuation using the equations of Collins. Using offshore and inshore grids of depths, computations of nearshore spectra for different deep water conditions were carried out. The computed results show reasonably good comparison with the measured data and hence is recommended for use in the coastal waters of Kerala. A friction factor of 0.01 is suggested for use in the model. This model cannot be justifiably used in cases where there is significant atmospheric energy input in the shallow waters.

The results of this study together with that of Wang and Yang (1981) also suggests the universal applicability of this model.

CHAPTER 7

SUMMARY, CONCLUSIONS AND RECOMMENDATIONS

The study of transformation of waves as they propogate from deep water to shallow water is essential in understanding and predicting the shallow water waves. The present thesis is an outcome of the investigation carried out by the author to study the wave height and spectral transformation in the shallow waters of Kerala Coast and to suggest prediction models suitable for this Coast. The study is carried out by making synchronised deep water and nearshore wave measurements at two locations, viz. Alleppey and Trivandrum, which have strikingly dissimilar wave climate, shelf slope and sediment characteristics.

From a study of the wave height transformation, it is found that attenuation of wave height takes place during propagation in the shallow waters. A plot of the nearshore significant wave height against the deep water height showed that the rate of attenuation of wave height is different at the two locations indicated by two separate regression lines. While the attenuation is less off Trivandrum, it is as much as 50% for waves of 2 - 3 m height off Alleppey. The differences in attenuation between the two locations are found to be due to differences in the energy dissipation by bottom friction. As far as frictional dissipation is

concerned, bottom slope is found to have an over-riding effect over bottom roughness for the range of slope and sediment characteristics observed at these locations.

Since bottom slope plays the major role in the frictional dissipation, and consequently the attenuation of wave height and energy, it is used as the criterion for categorisation of the Kerala Coast into different zones of wave transformation. From the distribution of bottom slope (or width of shallow water zone) it is predicted that Trivandrum will have maximum intensity of waves followed by the northern most stretches (north of Cannanore). Cochin, Calicut and Tellicherry will have least energy levels, and Alleppey and Ponnani are zones of moderate energy levels. This prediction based on bottom slope is well supported by the available literature on wave climate for this coast.

Study of spectral transformation also confirmed the energy loss during propogation in the shallow waters. In general there is no shift in the peak of the transformed (nearshore) spectra. In many cases, during high energy conditions, the peak spectral density is found to increase, which may be due to the nonlinear wave-wave interaction. Multipeakedness is generally found both in deep and nearshore spectra. It is concluded that the secondary peaks in the observed nearshore spectra are due to sea waves only.

Of the various wave transformation processes, refraction, shoaling, bottom frictional attenuation and wave breaking were found to be the most important as far as this coast is concerned. Hence for the prediction of wave height and spectral transformation, numerical models incorporating these processes were employed.

For the prediction of wave height transformation, the model by Dobson with its subsequent modification by Coleman and Wright to incorporate bottom frictional attenuation was chosen. This model was further modified to facilitate the simultaneous usage of two grids, the coarse offshore and the fine inshore grid. The inclusion of this fine inshore grid enables the accurate computation of wave transformation in the inshore where the effects of transformation are very pronounced. Computed results using this modified programme were compared with measured data and a high correlation of 0.8 was obtained. It is concluded that the programme by Dobson with the suggested modifications is suitable for the Kerala coast when used with a friction factor of 0.02. Since this model has already been field tested in some steep shelf conditions by Bryant, it is concluded that this model may be universally applicable.

The extent of influence of bottom friction in the attenuation of wave height and energy was studied using the computed friction coefficient. In addition to Alleppey and

Trivandrum, the computations were carried out for Calicut for uniform deep water conditions. The percentage attenuations for deep water waves of height 2 m and period 12 s approaching normal to the coastline are 7, 52 and 74 % respectively at Trivandrum, Alleppey and Calicut. This reaffirm the energy level categorisation of the Kerala Coast made earlier based on the bottom slope, which controls the bottom frictional dissipation.

For prediction of nearshore wave spectrum, a spectral transformation model by Hubertz was chosen and modified to incorporate bottom frictional attenuation using the equations of Collins. The computations were carried out here also using offshore and inshore grids of depths. Computed nearshore spectra with a friction factor of 0.01 are found to compare well with the measured spectra. It is concluded that the model by Hubertz with the suggested modifications is suitable for the Kerala coast. The present results together with the results of field evaluation of a model with the same numerical procedure by Wang and Yang suggest the universal applicability of this model.

Both these models are designed for prediction of wave transformation and hence are not suitable in conditions of wave generation.

To sum up, the author feels that the present

investigation has greatly enhanced our knowledge concerning the transformation of waves in the shallow waters of our coast. The study conclusively proved that the differences in the observed wave climate along the Kerala coast is due to the bottom frictional attenuation and identified bottom slope as the major factor in it. A classification of the entire Kerala coast into different energy regimes based on this criterion is provided. The present investigation is a pioneering one as far as numerical prediction of wave height and spectral transformation is concerned. The models suggested here can be used for the other coastlines of the country since the universal applicability of these models are more or less confirmed with the present investigations.

Based on these studies the following related areas for future research are proposed:

(i) The present models are suitable only for the prediction of wave transformation. On many occasions, the shallow water will be under active wave growth. Hence these models may be coupled with wave hindcasting models to account for such situations.

(ii) The present models do not consider the effect of currents in wave transformation, since they are not important as far as this coastline is concerned. However, they may have to be considered while predicting waves near tidal inlets and other areas of

strong currents.

(iii) Diffraction and reflection may be important in some specific nearshore zones, which are fronted by rock outcrops with bay formations. These processes may also be incorporated in the models whenever predictions for such zones are required.

(iv) In the present investigation, friction factor was selected empirically since the values obtained from the available formulations without considering the bed ripple geometry were found to be underestimates. Further work may be done to correlate friction factor with bed geometry and evaluate the same in field conditions.

(v) Remote sensing appears to be a very useful tool for the study of wave transformation as it can provide synoptic information on waves (with direction) and other influencing factors like currents, inshore bathymetry, etc.

It is hoped that further research in the lines suggested above will unravel more information on wave transformation of this coast and will help in the development of models which can predict the shallow water wave height and spectra to a greater degree of accuracy.

REFERENCES

REFERENCES

Abraham, S., 1987. Analysis of waves off Cochin. M. Tech. Thesis, Mangalore University.

Antony, M.K., 1976. Wave refraction studies off Calangute beach, Goa with reference to sediment transport and rip currents, Indian Journal of Marine Sciences, 5(1): 8-13.

Arthur, R.S., Munk, W.H. and Issacs, J.D., 1952. The direct construction of wave rays, Transactions of the American Geophysical Union, 33(6): 855-865.

Baba, M., 1985. Long term wave monitoring along the Kerala Coast - some results, Proceedings of the National Conference on Dock and Harbour Engineering, Bombay, E-49-67.

Baba, M. and Harish, C.M., 1985. Wave height and period distribution along the southwest coast of India, Indian Journal of Marine Sciences, 14(1): 1-8.

Baba, M. and Harish, C.M., 1986. Wave energy spectra for the southwest coast of India, Indian Journal of Marine Sciences, 15(3): 144-152.

Baba, M., Harish, C.M., and Kurian, N.P., 1986. Influence of record length and sampling interval on ocean wave spectral estmates, Mahasagar - Bulletin of the National Institute of Oceanography, 19(2): 79-85.

Baba, M., Kurian, N.P., Hameed, T.S.S., Thomas, K.V. and

Harish, C,M., 1987. Temporal and spatial variations in wave climate off Kerala, southwest coast of India, Indian Journal of Marine Science, 16(1): 5-8.

Baba, M., Kurian, N.P., Thomas, K.V., Prasannakumar, M., Hameed, T.S.S., and Harish, C.M., 1983a. Study of the waves and their refraction in relation to beach erosion along the Kerala coast, Centre for Earth Science Studies, Technical Report No. 29-1983, 28 pp.

Baba, M., Joseph, P.S., Kuarian, N.P., Thomas, K.V., Hameed, T.S.S., Prasannakumar, M. and Harish, C.M., 1983b. Study of the waves and their refraction in relation to beach erosion along the Kerala coast, Centre for Earth Science Studies, Technical Report No. 31-1983, 12 pp.

Battjes, J.A., 1968. Refraction of Water waves, Journal of the Waterways Harbours Coastal Engineering Division, ASCE, 94, (WW4)

Battjes, J.A., 1982. A case study of wave height variations variations due to currents in a tidal entrance, Coastal Engineering, 6(1): 47-57.

Beach Erosion Board, 1953. Laboratory study of wave energy losses by bottom friction and percolation. Tech. Memo No.31, Beach Erosion Board, Corps of Engineers, 25 pp.

Bergan, P.O., Torum, A. and Tractteberg, A., 1968. Wave measurements by a pressure type wave gauge, Proceedings of the 11th Coastal Engineering Conference, ASCE I: 19-29.

Bhat, S.S., 1986. Short term analysis of wave parameters a case study. M. Tech. Thesis, Mangalore University.

Black, K.P., 1978. Wave measurements over shallow reef (Field measurement and data analysis), J.K.K. Look Laboratory of Oceanographic Engineering, University of Hawaii, Tech. Rep. No. 29-1983.

Bretschneider, C.L., 1963. A one-dimensional gravity wave spectrum, Proceedings of the Conference on Ocean Wave Spectra (Prentice-Hall, New Jersy).

Bretschneider, C.L., 1964. Discussion on Investigation of statistics of wave heights, Journal of Waterways, Harbours and Coastal Engineering Division, ASCE: 153-166.

Bretschneider, C.L. and Reid, R.O., 1954. Modification of wave height due to bottom friction, percolation and refraction, U.S. Army Corps of Engineers, Beach Erosion Board, Tech. Memo No.45, 36 pp.

Bryant, E., 1979. Comparison of computed and observed breaker wave heights, Coastal Engineering, 3(1): 39-50.

Chao, Y., 1974. Wave refraction phenomena over the continental shelf near the Chesapeake bay entrance, U.S. Army Coastal Engineering Research Centre, Technical memo No. 47

Chen, Y. and Wang, H., 1983. Numerical model for non stationary shallow water wave spectral transformations, Journal of Geophysical Research, 88(C14): 9851-9863.

Christoffersen, J.B. and Jonsson, I.G., 1985. Bed friction and dissipation in a combined current and wave motion, Ocean Engineering, 12(5): 387-423.

Chu, H.L., 1975. Numerical model for wave refraction by finite amplitude wave theories, Proceedings of the 2nd Symposium on Modelling Techniques, ASCE : 1082-1100.

Cicslak, A. and Kawalski, T., 1969. Wave pressure attenuation. Proceedings of the 22nd International Navigation Congress, Paris.

Coleman, J.M. and Wright, L.D., 1971. Analysis of major river systems and their deltas: procedures and rationale with two examples, Luisiana State University, Coastal Studies Institute, Technical Report 95: 125 pp.

Collins, J.I., 1972. Prediction of shallow water spectra, Journal of Geophysical Research, 77(15): 2693-2707.

Das, P.K., Hariharan, V. and Varadachari, V.V.R., 1966. Some studies on wave refraction in relation to beach erosion along the Kerala coast, Proceedings of the Indian Academy of Sciences, LXIV; 192-202.

Dattatri, J., 1973. Waves off Mangalore harbour - west coast of India, Journal of Waterways, Harbours and Coastal Engineering Division, ASCE 99(WW1): 39-58.

Dattatri, J. and Nayak, I.V., 1976. Ocean wave record analysis by Tucker's method - an evaluation,

Proceedings of the 15th Coastal Engineering Conference, ASCE, Canada, 289-300.

Dattatri, J., Jothisankar, N. and Raman, H., 1977. Comparison of Scott spectra with ocean wave spectra, Journal of Waterways, Port, Coastal and Ocean Engineering Division ASCE, 103(WW3): 375-378.

Deo, M.C. and Narasimhan, S., 1979. Probabilistic analysis of ocean waves - a study, Department of Civil Engineering, I.I.T., Bombay, 162 pp.

Dhanalakshmi, S., 1982. Wave refraction and nearshore circulation at Visakhapatnam, Indian Journal of Marine Sciences, 11(3): 153-158.

Dobson, R.S., 1967. Some applications of a digital computer to hydraulic engineering problems, No.80, Department of Civil Engineering, Stanford University, California, Technical Report No. 80, 115 pp

Earle, M.D. and Bishop, J.M., 1984. A practical guide to ocean wave measurement and analysis, Endeco,Inc. 78 pp.

Esteva, D. and Harris, D.L., 1970. Comparison of pressure and staff gauge records, Proceedings of the 12th Coastal Engineering Conference, ASCE, Washington, I: 101-116.

Forristall, V.Z., 1981. Measurements of a saturated range in ocean wave spectra, Journal of Geophysical Research, 86(C9): 8075-8084.

Forristall, G.Z., et al., 1980. Measurements of sea wave attenuation due to deformable bottoms, Manuscript of paper presented at ASCE Fall Convention.

Forristall, G.Z. and Reece, A.M., 1985. Measurements of wave attenuation due to a soft bottom, The SWAMP Experiment. Journal of Geophysical Research, 90(C2): 3367-3380.

Goda, Y., 1974. Estimation of wave statistics from spectral information, Proceedings of the International Conference on Ocean Wave Measurement and Analysis, ASCE, New Orleas, 320-337.

Goda, Y., 1975. Deformation of irregular waves due to depth controlled wave breaking, Report of the Port and Harbour Research Institute, Japan, 14(3): 60-106 (in Japanese).

Goda, Y., 1975. Irregular wave deformation in the surf zone, Coastal Engineering in Japan, 18: 13-26.

Goda, Y., 1983. Analysis of wave grouping and spectra of long travelled swell, Report of Port and Harbour Research Institute, 22(1): 3-41.

Goda, Y., Takayama, T. and Suzuki, Y., 1978. Diffraction diagrams for directional random waves, Proceedings of the 16th Conference on Coastal Engineering, 628-650.

Gouveia, A.D., Joseph, P.S. and Kurup, P.G., 1976. Wave refraction in relation to beach stability along the coast from Cape Ramas to Karwar, Mahasagar - Bulletin

National Institute of Oceanography, 9(1): 11-18.

Griswold, G.M., 1963. Numerical calculation of wave refraction, Journal of Geophysical Research,68(6): 1715-1723.

Grosskopf, W.G., 1980. Calculation of wave attenuation due to friction and shoaling - an evaluation, U.S. Army, Corps of Engineers, Coastal Engineering Research Centre Technical Paper No. 80 - 8,, 15 pp.

Grosskopf, W.G. and Vincent, C.L., 1982. Energy losses of waves in shallow water, U.S. Army, Corps of Engineers, Coastal Engineering Research Centre, Technical Aid No.82-2. 17 pp.

Hallermeier, R.J., 1983. Calculation of wave shoaling with dissipation over nearshore sands. U.S. Army, Corps of Engineers, Coastal Engineering Research Centre, Coastal Engineering Technical Aid No.83-1, 21 pp.

Harish, C.M., and Baba, M., 1986. On spectral and statistical characteristics of shallow water waves, Ocean Enginering, 13(3): 239-248.

Harris, D.L., 1972. Characteristics of wave records in the coastal zone, In: Waves on Beaches (Ed., Meyer, R.E.), Academic Press, New York, 1-52.

Harris, D.L., 1974. Finite spectrum analysis of wave records, Proceedings of the International Conference on Ocean wave measurement and analysis, ASCE, New Orleans, 107-124.

Harrison, W., and Wilson, W.S., 1964. Development of a method for numerical calculation of wave refraction. U.S. Army Corps of Engineers, CERC. Technical Memo No.6.

Hashimi, N.H., Kidwai, R.M., Nair, R.R., 1981. Comparative study of the topography and sediments of the western and eastern continental shelves around Cape Comerin, Indian Journal of Marine Sciences, 10(1): 45-50.

Hasselmann, K. and Collins, J.I., 1968. Spectral dissipation of finite-depth gravity waves due to turbulent bottom friction,Journal of Marine Research, 26(1):1-12.

Hasselmann, K., Barnett, T.P., Bouws, E., Carlson, H., Cartwright, D.E., Enke, K., Ewing, J.A., Gienapp, A., Hasselmann, D.E., Kruseman, P., Meerburg, A., Muller, P., Olbers, D.J., Richter, K., Sell, W., and Walden, H., 1973. Measurements of wind wave growth and swell decay during the Joint North Sea Wave Project (JONSWAP), Deutsches Hydrographisches Zeitsch rift,Reihe A, 8(12).

Henderson, G. and Webber, N.B. 1980. Verification of a wave refraction model utilising recorded and observed wave data, Proceedings of the 17th Coastal Enginering Conference, ASCE. 101-120.

Homma, M., Horikawa, K. and Komari, S., 1966. Response characteristics of underwater wave gauge, Proceedings of the 10th Coastal Engineering Conference,ASCE, I:99-114.

Houston, J.R., 1981. Combined refraction and diffraction of short waves using the finite element method, Applied Ocean Research, 3(4): 163-170.

Hsiao, S.V. and Shemdin, O.H., 1978. Bottom dissipation in finite-depth water waves, Proceedings of the 16th Coastal Engineering Conference, I: 434-448.

Hubertz, J.M., 1980. Electronic Computer Programme Abstract, Programme No.720-X6-R1CF0, U.S. Army, C.E.R.C.

Hubertz, J.M., 1981. Prediction of wave refraction and shoaling using two numerical models, U.S. Army, Corps of Engineers, Coastal Engineering Research Centre, Technical Aid No. 81-12, 15 pp.

Iversion, H.W., 1951. Studies of wave transformation in shoaling water, including breaking, In ; Gravity waves, National Bureau of standards, Circular No. 521, 9-32.

Iwagaki, M. and Kakimura, T., 1967. On the bottom friction factors off five Japanes Coasts, Coastal Engineering in Japan, 10 ; 13-22.

Janssen, P.A.E.M and de Voogt,W.J.P., 1985. On the effect of bottom friction on wind sea, In:Toba, Y. and Mitsayasu, H.,The Ocean Surface ; wave breaking , turbulent mixing and radio probing, D. Reidel Publishing Company; 586 pp

John, E.J. and Nayak , I.V., 1981. Use of wave refraction diagrams to identify areas vulnerable to erosion, Procedings of the first Indian Conference on Ocean Engineering , I.I.T, Madras ; I-14-22.

Johnson, J.W.,1947. The refraction ofsurface waves by currents, Transactions of the American Geophysical Union, 28(6):867-874.

Jonsson, I.G., 1980. A new approach to oscillatory, rough turbulent boundary layers, Ocean Engineering,7: 109-152

Jonsson, I.G., Skougaard, C. and Wang, J.D., 1970. Interaction between waves and currents, Proceedings of the 12th Conference on Coastal Engineering, I: 489-508.

Kahma, K.K., 1981. A study of the growth of the wave spectrum with fetch, Journal of Physical Oceanography, 11: 1503-1515.

Kamphuis, J.W., 1975. Friction factor under oscillatory waves, Journal of the Waterways, Harbours and Coastal Engineering Division, 101(WW2): 135-144.

Kamphuis, J.W., 1978. Attenuation of gravity waves by bottom friction, Coastal Engineering, 2: 111-118.

Karlesson, T.,1969. Refraction of continuous ocean wave spectra, Journal of Waterways, Harbours, and Coastal Engineering Division, ASCE, 95(WW4): 437-448.

Keulegan, G.H., 1948. Gradual damping of solitary waves, Jour. Res. Nat. Bur. Stand., 40: 487-498.

Kitaigorodskii, 1983. On the theory of the equilibrium range in the spectrum of wind-generated gravity waves, Journal of Physical Oceanography, 13: 816-827.

Kitaigorodskii, S.A., Krasitskii, V.P. and Zaslavskii, M.M., 1975. On Philips theory of equilibrium range in the

spectra of wind-generated waves, Journal of Physical Oceanography, 5: 410-420.

Komar, P.D., 1976. Beach processes and sedimentation, Prentice Hall, New Jersey, 429 pp.

Komar, P.D., 1983. Beach processes and erosion - an introduction, In: Handbook of Coastal Processes and Erosion, Komar, P.D.,(Ed.),CRC Press, Washington,301 pp

Kurup, P.G., 1977. Studies on the physical aspects of mud banks along the Kerala coast with special reference to the Purakkad mudbank, Bulletin of the Department of Marine Sciences, University of Cochin, VIII; 1-72.

Le Mehaute, B., 1982. Relationships between narrow band directional energy spectra and probability densities of deep and shallow water waves, Applied Ocean Research, 4(1):17-24.

Le Mehaute, B. and Wang, J.D., 1980. Transformation of monochromatic waves from deep to shallow water, U.S. Army Coastal Engineering Research Centre, Technical Report No.80-2: 43 pp.

Le Mehaute, B. and Wang, J.D. 1982. Wave spectrum changes on sloped beach, Journal of the Waterways, Port, Coastal and Ocean Division, ASCE, 108(WW1): 33-47.

Lee, T.T. and Black, K.P., 1978. The energy spectra of surf waves on a coral reef, Proceedings of the 16th Coastal Engineering Conference,ASCE, Hamburg,I:588-608.

Liu, P.L-F. and Dalrymple, R.A., 1984. The damping of gravity water waves due to percolation, Coastal Engineering, 8: 33-49.

Longuet-Higgins, M.S., 1956. The refraction of sea waves in shallow water, Journal of Fluid Mechanics,1(2):163-176.

Longuet-Higgins, M.S. and Stewart, R.W., 1960. Changes in the form of short gravity waves on long waves and tidal currents, Journal of Fluid Mechanics, 8: 565-583.

Longuet-Higgins, M.S. and Stewart, R.W., 1961. The changes in amplitude of short gravity waves on steady nonuniform currents, Journal of Fluid Mechanics, 10: 529-549.

Mac Pherson, H. and Kurup, P.G., 1981. Wave damping at the Kerala mud banks, Indian Journal of Marine Sciences, 10(3): 154-160.

Mahadevan, R. and Renukaradhya, P.S., 1983. Numerical calculation of wave refraction, Proceedings of the 2nd Indian Conference in Ocean Engineering, CWPRS, Pune, I: 71-82.

Mattie, M.G., 1982. Empirical guidelines for use of irregular wave model to estimate nearshore wave height. U.S. Army, Corps of Engineers, Coastal Engineering Research Centre, Technical Paper No.82-1, 18 pp

Mogel, T.R., Street, R.L., and Perry, B., 1970. Computation of alongshore energy and littoral transport,

Proceedings of the 12th Coastal Engineering Conference, Washington: 899-917.

Munk, W.H., 1949. The solitary wave theory and its applications to surf problems, Annals of the New York Academy of Sciences, 51: 376-462.

Namboothiri, S.M., 1985. Waves off Vizhinjam and their effects on the rubble mound breakwater, M. Tech. Thesis, Mangalore University.

Narasimhan, S. and Deo, M.C., 1979a. Spectral analysis of ocean waves - a study. Proceedings of the Conference on Civil Engineering in Oceans, ASCE, San Fransisco, 877-892.

Narasimhan, S. and Deo, M.C. 1979b. Spectral analysis of ocean waves -a study. Proceedings of the International Conference on Computer Applications in Civil Engineering Roorke, India, V: 7-12.

Nayak, B.U., 1980, Coastal Erosion in India - causes, Processes and remedial measures. Geotech - 80: 55-63.

Nayak, B.U. and Anand, N.M., 1981. Wave measurements off the Bombay coast, Proceedings of the 1st Indian Conference in Ocean Engineering, I.I.T., Madras, I: 75-80.

Neumann, G., 1953. On ocean wave spectra and a new method of forecasting wind generated sea, U.S. Army, Beach Erosion Board. Technical Memo No. 43.

Nielsen, P., 1983. Analytical determination of nearshore wave height variation due to refraction, shoaling and

friction, Coastal Engineering, 7: 233-251.

Nielsen, P., 1985. A short manual of coastal bottom boundary layers and sediment transport,Public Works Department, New South Wales, Technical Memorandum No 85/1, 56 pp.

Ou, S.H., 1977. Parametric determination of wave statistics and wave spectrum of gravity waves, Report of National Cing King University, Taiwan, 98 pp.

Philips, O.M., 1958. The equilibrium range in the spectrum of wind-generated waves. Journal of Fluid Mechanics, 4: 426-434.

Pierson, W.G., Neumann, G. and James, R.J.W., 1955. Observing and forecasting ocean waves, U.S. Navy Oceanographic Office, H.O. Publication 603.

Pierson, W.J., and Moskowitz, L. 1964. A proposed spectral form for fully developed wind sea based on similarity theory of S.A. Kitaigorodskii, Journal of Geophysical Research. 69: 5181-5190.

Ploeg, J., 1968. A general discussion on the selection of a design wave, Second Marine Engineering Seminar, Department of Public Works, Ottawa, Canada.

Prasad, A.L., Rao, K.H., Veenadevi, Y. and Rao, G.R.L., 1981. Wave refraction and sediment transport along Kunavaram, East coast of lndia, Indian Journal of Marine Sciences, 10(1): 10-15.

Prasannakumar, S., Shenoi, S.S.C. and Kurup, P.G., 1983. Littoral drift along shoreline between Munambam and Anthakaranazhi, Kerala coast, Indian Journal of Marine Sciences, 12(4): 209-212.

Premchand, K., 1987. Vertical current structure during northeast monsoon off Chellanam, southwest coast of India. Proceedings of the Symposium on Short-term variability of Physical Oceanographical features in the Indian waters, Cochin: 51-56.

Provis, D.G., and Steedman, R.K., 1986. Wave measurements in the Great Australian Bight, Paper presented at the Conference on Air-Sea Interaction and its consequences, Sydney.

Putnam, J.A., 1949. Loss of wave energy due to percolation in a permeable sea bottom, Transactions of the American Geophysical Union, 30(3): 349-356.

Putnam, J.A. and Johnson, J.W., 1949. The dissipation of wave energy by bottom friction, Transactions of the American Geophysical Union, 30(1): 67-74.

Reddy, B.S.R., Reddy, G.V., and Prasad, N.D., 1979. Wave conditions and wave induced longshore currents in the nearshore zone off Krishnapatnam, Indian Journal of Marine Sciences, 8(2): 61-67.

Reddy, M.P.M., 1970. A systematic study of wave conditions and sediment transport near Mormugoa Harbour,

Mahasagar - Bulletin of the National Institute of Oceanography, 3: 28-44.

Reddy, M.P.M., and Varadachari, V.V.R., 1972. Sediment movement in relation to wave refraction along the west coast of India, Journal of Indian Geophysical Union, 10: 169-191.

Reddy, M.P.M., Hariharan, V. and Kurian, N.P., 1979. Sediment movement and siltation in the navigational channel of the old Mangalore Port, Proceedings of the Indian Academy of Sciences, 88A, Part II: 121-130.

Reddy, M.P.M., Hariharan, V., and Kurian N.P., 1982. Beach stability along the coast from Ullal to Thanmirbhavi near Mangalore, Indian Journal of Marine Sciences, 11: 327-332.

Rye, H., 1977. The stability of some currently used wave parameters, Coastal Engineering 1(1): 3-30.

Scott, J.R., 1965. A sea spectrum for model tests and long term ship prediction, Journal of Ship Research, 9(3): 145-152.

Seelig, W.N. and Ahrens, J.P., 1980. Estimating nearshore wave conditions for irregular waves, U.S. Army, Corps of Engineers, Coastal Engineering Research Centre, Technical Paper No.80-3, 47 pp.

Shenoi, S.S.C. and Prasannakumar, S., 1982. Littoral processes along shoreline from Andhakaranazhi to

Azhikode on the Kerala coast, Indian Journal of Marine Sciences, 11(3): 201-207.

Shiau, J.C. and Wang, H., 1977. Wave energy transformation over irregular bottom, Journal of Waterways, Port, Coastal and Ocean Engineering Division, ASCE, 103(WW1): 57-68.

Silvester, R., 1974. Coastal Engineering, I - Generation, propogation and influence of waves (Elsevier Scientific Publishing Company), 457 pp.

Sivadas, T.K., 1981. A tide and wave telemetering system, Proceedings of the First Indian Conference in Ocean Engineering, I.I.T., Madras, I: VII: 57-60.

Skovgaard, O. and Bertelsen, J.A. 1974. Refraction computation for practical applications, Proceedings of the International Symposium on Ocean wave measurement and analysis, ASCE New Orleans: 761-772.

Skovgaard, O., Jonsson, I.G. and Bertelson, J.A., 1975. Computation of wave heights due to refraction and friction, Journal of the Waterways, Harbours and Coastal Engineering Division, ASCE, 101 (WW1): 15-32.

Snedecor, G.W. and Cochran, W.G., 1967. Statistical Methods (Oxford and IBH Publishing Co.),593 pp.

Steel, R.G.D. and Torrie, J.H., 1981. Principles and procedures of Statistics (McGraw - Hill, Inc.) 633 pp.

Thompson, E.F., 1974. Distribution of individual wave heights, Proceedings of the International Symposium on

Ocean Wave measurement and Analysis, ASCE, New Orleans.

Thompson, E.F., 1980. Energy spectra in shallow U.S. coastal waters, U.S. Army, Corps of Engineers, Coastal Engineering Research Centre, Technical Paper No.80-2, 149 pp

Thompson, E.F. and Harris, D.L., 1972. A wave climatology for U.S. coastal waters, U.S. Army, Coastal Engineering Research Centre, Reprint 1-72.

Toba, Y., 1973. Local balance in the air-sea boundary processes: 1. On the growth process of wind waves, Journal of Oceanographical Society of Japan,28: 109-121

Treloar, P.D., 1986. Spectral wave refraction under the influence of depth and current, Coastal Engineering, 9: 439-452.

Tsay, T-K. and Liu, P.L-F., 1982. Numerical solution of water-wave refraction and diffraction problems in the parabolic approximation, Journal of Geophysical Research, 87(C10): 7932-7940.

U.S. Army, Coastal Engineering Research Centre, 1977. Shore Protection Manual, Vol. I, II and III, U.S. Government Printing Office,Washingdon.

Van Ieperen, M.P., 1975. The bottom friction of the sea bed off Melkbosstrand, South Africa, a comparison of a quadratic with a linear friction model, Deutsches Hydrographisches Zeitschrift, 28, 72-88.

Varadarajulu, R., I972. Coastal Processes along the Visakhapatanam Coast, Ph.D Thesis, Andhra University.

Veerayya, M., Murthy, C.S. and Varadachari, V.V.R., 1981. Wave refraction and littoral currents off Colva Beach, Goa, Indian Journal of Marine Sciences, 10(1): 1-9.

Vijayakumar, P., 1971. Prediction of waves due to cyclonic storms in the Bay of Bengal - A case study. M. Tech. Thesis, University of Mysore.

Vincent, C.L., 1982. Shallow water wave modelling, Paper presented at the First International Conference on Meteorology and Air-Sea Interaction in the Coastal Zone, The Hague.

Vincent, C.L., Grosskopf, W.G., and Mc Tamany, J.M., 1982. Transformation of storm wave spectra in shallow water observed during the ARSLOE storm. Oceans '82. 1-6.

Wang, H. and Yang, W-C., 1976. Measurement and computation of wave spectral transformation at Island of Sylt, North sea, Mitt. Leichtwei Instituts fur Wasserbau, Technischen, Universitat Braunschweig, Heft, 52, 197-298.

Wang, H., and Yang, W-C., 1981. Wave spectral transformation measurements at Sylt, North Sea, Coastal Engineering, 5:1-34.

Wilson, W.S., 1966. A method for calculation and plotting of surface wave rays, U.S. Army, Coastal Engineering Research Centre, Technical Memo No.17.

Wright, L.D., 1976. Nearshore wave-power dissipation and the coastal energy regime of the Sydney - Jervis Bay

Region, New South Wales: A comparison,. Australian Journal of Marine and Freshwater Resarch, 27: 633-640.

Wright, L.D. and Coleman, J.M., 1972. River delta morphology: Wave climate and the role of the subaqueous profile, Science, 176: 282-284.

Wright, L.D. and Coleman, J.M., 1973. Variations in morphology of major river deltas as functions of ocean wave and river discharge regimes, Bulletin of American Association of Petroleum Geologists, 57: 370-398.

APPENDIX I

```
      PROGRAM WAVES.S
C
C     PROGRAM TO COMPUTE REFRACTED WAVES BY R.S DOBSON
C     CORRECTIONS FOR BOTTOM FRICTION ATTENUATION
C     INCORPORATED BY N.P KURIAN.
C     MODIFICATIONS TO FACILITATE
C     SIMULTANEOUS USE OF DEEP AND INSHORE GRID
C     AND SWITCH OVER FROM ONE GRID TO THE OTHER
C     PROVIDED BY N.P KURIAN ADDITIONAL CONTROLS
C     TO SELECT RAYS AND INCORPORATE CHANGES IN DEPTH
C     DUE TO SURGE OR TIDE ALSO PROVIDED BY N.P KURIAN
C     INPUT PARAMETERS
C     MI    =NO OF X-GRID UNITS OF OFFSHORE GRID
C     MJ    =NO OF Y-GRID UNITS OF OFFSHORE GRID
C     IGRCON=GRID UNIT IDENTIFIER,1=FEET,2=MILES,3=METERS
C     LIMNPT=MAX. NUMBER OF RAY COMPUTATION POINTS
C     NPRINT=FREQUENCY OF PRINTED OUTPUT FOR EACH RAY
C     INDGRD=INSHORE GRID IDENTIFIER
C     GRID  =WIDTH OF ONE OFFSHORE GRID UNIT
C     DCON  =MULTIPLIER TO CONVERT DEPTH UNITS TO FEET
C     DELTAS=MINIMUM STEP LENGTH ALONG RAY IN SHALLOW WATER
C     GRINC = STEP LENGTH ALONG RAY, IN DEEP WATER
C     XI=MINIMUM X-COORDINATE OF INSHORE GRID
C     W.R.T OFFSHORE GRID
C     YI=MINIMUM Y-COORDINATE OF INSHORE GRID
C     W.R.T. OFFSHORE GRID
C     SGRID =RATIO OF WIDTH OF INSHORE GRID UNIT TO
C     OFFSHORE GRID UNIT
C     MIS   = NUMBER OF X GRID UNITS IN INSHORE GRID
C     MJS = NUMBER OF Y GRID UNITS IN INSHORE GRID
C     DEP(I,J) = DEPTH AT GRID POINTS
C     NOSETS=NO. RAYS IN SET
C     TITL=IDENTIFYING TITLE FOR EACH SET
C     NORAYS= NO RAYS IN EACH SET
C     T=WAVE PERIODS,SECS
C     HO=DEEP WATER WAVE HEIGHT
C     H,Y=STARTING CO-ORDINATES
C     A=INITIAL DIRECTION OF RAY
C     [SXY] = SPECIAL UNIT MATRIX FOR USE WITH A SQ. GRID
C     FIT = S.D. OF THE LEAST SQUARE SURFACE
C     RESMAX = LIMITING DIFFERENCE BETWEEN SUCCESSIVE
C     APPROXIMATIONS
      COMMON IFR,FR,SURGE,SXY(12,6)
      COMMON DP(10),TITL(18)
      COMMON DEP(60,67),E(6)
      COMMON NN(7),D(12)
      COMMON B1,B2,CO,CXY
      COMMON DCDH,DCON,DELTAS,DRC,IRO,JRO,AMIS,AMJS
      COMMON DTGR,DXY,GRINC,HO,IGO,JGO,LIMNPT,NPRINT,NPT,PHX
      COMMON HNEW,PHY,RCCO,RHS,RK,IJF,IGF,IRF,JRF
```

```
      COMMON AX1,AX2,AY1,AY2,SIG,SK,TOP,V,WL,WLO,X1,X2,Y1,Y2
      COMMON SKP,INDGRD,RKP,GRID,T,FKF,SGRID,MIS,MJS,MI,MJ
 51   FORMAT(6I5,4F10.5)
 550  FORMAT(6F12.8)
 600  FORMAT(2F10.6,F12.10,2I4)
 400  FORMAT(I1)
 31   FORMAT(1H,'SURGE OR TIDAL HEIGHT =',F5.2,1X,'METERS',1X)
 30   FORMAT(F5.2)
 56   FORMAT(I5)
 57   FORMAT(18A4)
 58   FORMAT(I3,F8.2,F6.2)
 59   FORMAT(F7.3),2F7.2)
 71   FORMAT(1H,18A4/8H SET NO,I3,10H,PERIOD=,F7.2,7H
     1 SECS.,8H RAY NO .,I3)
 61   FORMAT(1H1,18A4/8H SET NO,13,10H,PERIOD=,F7.2,7H
     1 SECS. 8H RAY
     1 IND,13,13H,TIME STEP=,F8,4,6H SEC//1H,3X,'POINT'5X,1HX,8X
     1 8X, 'Y'6X,'ANGLE',5X,'DEPTH'4X,'MAX DIF',4X,'FIT',4X,
     1 'LENGTH',4X,'SP
     1 EED',4X,'HEIGHT',4X,'KR',7X,'KS,7X,'KF',8X,'HNEW',//
     1 IH,I7,3F9.2,29X,3F9.2)
 62   FORMAT(1HO,'ALL SETS COMPLETED, NO OF SETS=',I4)
 63   FORMAT(1HO,9X,'PROGRAM PARAMETERS'//1H,'GRID LIMITS',
     1 'ABSCICSA' =',I3,1H 'ORDINATES=',I3,/1H ,'PRINTED OUTPUT
     1 INTERVAL =',I2 ,'POINT'/''GRID SIZE UNIT=',F8.2,'METERS',
     1 1H 'DEEP WATER INCREMENTAL STEP =',F4.2,'GRID UNITS.')
 64   FORMAT(1HO,'PROGRAM STOPPED MI GRATER THAN 75 OR MJ
     1 GREATER THAN 75 NOT ALLOWED, MI='I4,7X,'MJ=',I4)
 1000 FORMAT(15F5.1)
C     READ BASIC DATA
      READ(7,550)((SXY(I,J),I=1,12),J=1,6)
C     INDGRD IS THE INSHORE GRID IDENTIFIER AND INDRAY THE
C     IDENTIFIER TO SELECT RAYS
      INDRAY=0
      READ(7,51)MI,MJ,IGRCVON,LIMNPT,NPRINT,INDGRD,GRID,DCON,
     1 DELTAS,GRINC
      IF(MI .GT. 75 .OR. MJ .GT. 75) GOTO 10
      RHS=MI
      RHS=RHS-1.99
      TOP=MJ
      TOP=TOP-1.99
      GOTO (16,17,18),IGRCON
 17   GRID=GRID*6080.2
 16   CALL METRIC(GRID,1)
 18   WRITE(1,63)MI,MJ,NPRINT,GRID,GRINC
      CALL METRIC(GRID,2)
C     CHECK FOR INSHORE GRID AND COMPUTE INSHORE GRID PARAMETERS
      IF(INDGRD .EQ. 0)GOTO 81
      READ(7,600)X1,Y1,SGRID,MIS,NJS
      X1=X1+SGRID
      X2=X1+(MIS-3)*SGRID
```

```
      Y1=Y1+SGRID
      Y2=Y1+(MJS-3)*SGRID
      AMIS=FLOAT(MIS-2)
      AMJS=FLOAT(MJS-2)
C     READ TIDE OR SURGE HEIGHT
 81   READ(7,30)SURGE
      WRITE(1,31)SURGE
C     READ WAVE DATA
      READ(7,56)NOSETS
      DO 110 NOSETS=1,NOSETS
 80   READ(7,57)TITL
      READ(7,58)NORAYS,T,HO
      CALL METRIC(HO,2)
      SIG=6.28318531/T
      COC=5.1204062*T
      DTGR=GRINC/CO
      WLO=CO*T
      DRC=WLO*0.6
      DO 110 NORAY=1,NORAYS
      READ(7,59)X,Y,A
C     SELECT WAVE RAY
      IF(INDRAY .EQ.3)GOTO 60
      READ(1,400)INDRAY
      GOTO(60,110,60,12),INDRAY
      IF(IFR .EQ. 1)GOTO 501
      IF(INDGRD .EQ. 0 .AND. NORAY .GT. 1)GOTO 501
 60   READ(6,1000)((DEP(I,J)),I=1,MI),J=1,MJ)
      IFR=1
      DO 500 I=1,MI
      DO 500 J=1,MJ
      DEP(I,J)=DEP(I,J)+SURGE
 500  CONTINUE
 501  CALL METRIC(HO,1)
      NPT=1
      UNIT=DTGR*GRID
      CXY=CO
      WL=WLO
      B1=1.
      B2=1.
      RK=1.
      RKP=1.
      SK=1.
      SKP=1.
      CALL METRIC(WLO,1)
      CALL METRIC(CO,1)
      WRITE(1,61)TITL,NOSET,T,NORAY,UNIT,NPT,X,Y,A,WLO,CO,HO
      CALL METRIC(HO,2)
      HNEW=HO
      CALL METRIC(WLO,2)
      CALL METRIC(CO,2)
      CALL RAYCON(X,Y,A)
```

```
      IF(IFR .EQ. 1)ENDFILE 6
110   CONTINUE
      WRITE(1,62)NOSETS
      GOTO 12
10    WRITE(1,64)MI,MJ
12    STOP
      END
      SUBROUTINE  RAYCON(X,Y,A)
      COMMON IFR,FR,SURGE,SXY(12,6)
      COMMON DP(10),TITL(18)
      COMMON DEP(60,67),E(6)
      COMMON NN(7),D(12)
      COMMON B1,B2,CO,CXY
      COMMON DCDH,DCON,DELTAS,DRC,IRO,JRO,AMIS,AMJS
      COMMON DTGR,DXY,GRINC,HO,IGO,JGO,LIMNPT,NPRINT,NPT,PHX
      COMMON HNEW,PHY,RCCO,RHS,RK,IJF,IGF,IRF,JRF
      COMMON AX1,AX2,AY1,AY2,SIG,SK,TOP,V,WL,WLO,X1,X2,Y1,Y2
      COMMON SKP,INDGRD,RKP,GRID,T,FKF,SGRID,MIS,MJS,MI,MJ
      ANG=A
      A=A*0.0174532925
      COSA=COS(A)
      SINA=SIN(A)
      H=HO
      IGO=1
      IRF=1
      IGF=1
      JRF=1
      IRO=1
      JRO=1
C     TAKE WAVE INTO SHALLOW WATER
 10   PX=X
      PY=Y
      X=COSA*GRINC+X
      Y=SINA*GRINC+Y
      IF(X .GE. RHS .OR. X .LT. 1.01)GOTO 25
      IF(Y .GE. TOP .OR. Y .LE. 1.01)GOTO 25
      CALL DEPTH(X,Y,XP,YP)
      NWRITE=1
      IF(DXY .LE. 0)GOTO 24
      IF(DXY .LT. DRC)GOTO 11
      NPT=NPT+1
      IF(NPT .GT. LIMNPT)GOTO 26
      IF(NPT /NPRIINT*NPRINT-NPT .NE. 0)GOTO 10
      ABB=((PX-X)**2+(PY-Y)**2)**0.5
      CALL FRICTN(ABB)
      GOTO21
C     SHALLOW WATER REFRACTION BEGINS
 11   X=PX
      Y=PY
      CALL CURVE(X,Y,A,FK,XP,YP)
 12   NPT=NPT+1
```

```
      IF(NPT .GT. LIMNPT)GOTO 26
      NWRITE=1
      CALL REFRAC(X,Y,A,FK,ABB)
      DO 205 I=1,7
      IF(NN(I) .EQ. 18)GOTO 18
      IF(NN(I) .EQ. 22)GOTO 22
      IF(NN(I) .EQ. 23)GOTO 23
      IF(NN(I) .EQ. 24)GOTO 24
      IF(NN(I) .EQ. 25)GOTO 25
      IF(NN(I) .EQ. 27)GOTO 27
      IF(NN(I) .EQ. 28)GOTO 28
205   CONTINUE
22    NWRITE=2
      GOTO 18
23    NWRITE=3
      GOTO 18
24    NWRITE=4
      GOTO 13
25    NWRITE=5
      GOTO 13
26    NWRITE=6
      GOTO 13
27    NWRITE=7
      GOTO 13
28    NWRITE=9
      GOTO 21
18    CALL HEIGHT(XP,YP,A,H,ABB)
      IF(DXY/HNEW .LE. 1.28)NWRITE=8
      IF(NWRITE .GT. 1)GOTO 13
      IF(DXY .LE. 25)GOTO 13
      IF(NPT/NPRINT*NPRINT-NPT .NE. 0)GOTO 12
13    ANG=A*57.29577931
21    CALL WRITER(X,Y,ANG,H,NWRITE,FIT,DIFMAX)
1000  FORMAT(15F5.1)
14    GOTO (10,12,19),IGO
19    RETURN
      END
      SUBROUTINE REFRAC(X,Y,A,FK,ABB)
      COMMON IFR,FR,SURGE,SXY(12,6)
      COMMON DP(10),TITL(18)
      COMMON DEP(60,67),E(6)
      COMMON NN(7),D(12)
      COMMON B1,B2,CO,CXY
      COMMON DCDH,DCON,DELTAS,DRC,IRO,JRD,AMIS,AMJS
      COMMON DTGR,DXY,GRINC,HO,IGO,JGO,LIMNPT,NPRINT,NPT,PHX
      COMMON HNEW,PHY,RCCO,RHS,RK,IJF,IGF,IRF,JRF
      COMMON AX1,AX2,AY1,AY2,SIG,SK,TOP,V,WL,WLO,X1,X2,Y1,Y2
      COMMON SKP,INDGRD,RKP,GRID,T,FKF,SGRID,MIS,MJS,MI,MJ
      DO 200 I=1,7
200   NN(I)=0
      NCUR=1
```

```
C       POSITION WAVE FOR REFRACTION
        GOTO(11,12,10)IGO
 11     FKM=FK
        IGO=2
 12     DS=CXY*DTGR
        IF(DS .LT. DELTAS)NN(6)=27
        IF(NN(6) .EQ. 27)RETURN
        RESMAX=0.00005/DS
 13     DO 110 I=1,40
        DELA=FKM*DS
        IF(ABS(DELA) .GE.1.)NN(7) =28
        IF(NN(7) .EQ. 28)RETURN
        AA=A+DELA
        AM=DELA*0.5+A,
        XX=COS(AM)*DS+X
        YY=SIN(AM)*DS+Y
C       CHECK FOR ENTRY INTO THE INSHORE GRID ,IF SO USE THE
C       INSHORE GRID OF DEPTHS
        IF(INDGRD .EQ. 0)GOTO 50
        GOTO (20,60),IRF
 60     IF(XX .GE. AMIS .OR. XX .LE. 1. .OR. YY .GE. AMJS .OR.YY
     1  .LE. 1.)JRO=2
        GOTO (50,90),JRO
 90     XX=X1-SGRID+(XX*SGRID)
        YY=Y1-SGRID+(YY*SGRID)
        IF(IGF .EQ. 1)GOTO 70
        READ(6,1000)((DEP(IJ,J),IJ=1,MI),J=1,MJ)
        IFR=1
        DO 500 K=1,MI
        DO 500 JJ=1,MJ
        DEP(K,JJ)=DEP(K,JJ)+SURGE
 500    CONTINUE
        IGF=1
 1000   FORMAT(15F5.1)
 70     GOTO(20,50),IRF
 20     IF(X .GE. RHS .OR. X .LE. 1.0)NN(5)=25
        IF(NN(5) .EQ. 25)RETURN
        IF(Y .GE. TOP .OR. Y .LE. 1.0)NN(5)=25
        IF(NN(5) .EQ. 25)RETURN
        IF(XX .GT. X1 .AND. XX .LT. X2 .AND.YY .GT. Y1 .AND.
     1  YY .LT. Y2)JRF=2
        GOTO(50,30),JRF
 30     IF(IGF .EQ. 2)GOTO 40
        READ(6,300)((DEP(II,J),II=1,MIS),J=1,MJS)
        DO 600 IA=1,MI
        DO 600 JA=1,NJ
        DEP(IA,JA)=DEP(IA,JA)+SURGE
 600    CONTINUE
        IGF=2
        ENDFILE 6
        IFR=2
```

```
300     FORMAT(19F4.1)
40      XX=(XX-X1+XGRID)/SGRID
        YY=(YY-Y1+SGRID)/SGRID
50      CALL CURVE(XX,YY,AA,FKK,XP,YP)
        IF(DXY .LE. 0)NN(4)=24
        IF(NN(4) .EQ. 24)RETURN
        GOTO (111,16),NCUR
111     FKM=(FK+FKK)*0.5
        IF(I .EQ. 1)GOTO 110
        IF(RESMAX .GT. ABS(FKP - FKM))GOTO 16
        IF(I .EQ. 38)FK38=FKM
110     FKP=FKN
        IF(RESMAX .GT. ABS(FK38 - FKM))GOTO 15
        NN(3)=23
        RETURN
15      FKM=(FKM +FK38)*0.5
        NCUR=2
        GOTO 13
16      IF(INDGRD .EQ. 0)GOTO 18
        GOTO(14,120),JRO
120     X=X1-SGRID+(X*SGRID)
        Y=Y1-SGRID+(Y*SGRID)
        WRITE(1,700)XX,YY
700     FORMAT(1H , 'RAY REENTERED ORIGINAL GRID AT X=',F5.2,
    1   2X,'Y=',F5.2)
        IRF=1
        JRO=1
14      GOTO(17,130),JRF
130     X=(X-X1+SGRID)/SGRID
        Y=(Y-Y1+SGRID)/SGRID
        WRITE(1,400)XX,YY
400     FORMAT(1H,'RAY ENTERED INSHORE GRID AT X=',F5.2,
    1   'Y=',F5.2)
        IRF=2
        JRF=1
17      ABB=SQRT((X-XX)**2+(Y-YY)**2)
18      X=XX
        Y=YY
        A=AA
        FK=FKK
        IF(NCUR .EQ. 2)NN(2)=22
        IF(NN(2) .EQ. 22)RETURN
        IF(X .GE. RHS .OR. X .LE. 1.0)NN(5)=25
        IF(NN(5) .EQ. 25)RETURN
        IF(Y .GE. TOP .OR. Y .LE. 1.0)NN(5)=25
        IF(NN(5) .EQ. 25)RETURN
        NN(1)=18
10      RETURN
        END
        SUBROUTINE CURVE(X,Y,A,FK,XP,YP)
        COMMON IFR,FR,SURGE,SXY(12,6)
```

```
      COMMON DP(10),TITL(18)
      COMMON DEP(60,67),E(6)
      COMMON NN(7),D(12)
      COMMON B1,B2,CO,CXY
      COMMON DCDH,DCON,DELTAS,DRC,IRO,JRO,AMIS,AMJS
      COMMON DTGR,DXY,GRINC,HO,IGO,JGO,LIMNPT,NPRINT,NPT,PHX
      COMMON HNEW,PHY,RCCO,RHS,RK,IJF,IGF,IRF,JRF
      COMMON AX1,AX2,AY1,AY2,SIG,SK,TOP,V,WL,WLO,X1,X2,Y1,Y2
      COMMON SKP,INDGRD,RKP,GRID,T,FKF,SGRID,MIS,MJS,MI,MJ
      GOTO (10,11),IGO
11    CALL DEPTH(X,Y,XP,YP)
      IF(DXY*200. .GT. WL)GOTO 10
      IF(DXY .LE. 0)RETURN
      JGO=2
      ARG=32.1725*DXY
      CXY=SQRT(ARG)
      DCDH=16.08625/CXY
      GOTO 14
10    CI=CXY
      JGO=1
      DO 120 I=1,50
      ARG=(DXY*SIG)/CI
      CXY=CO*PANH(ARG)
      RESID=CXY-CI
      IF(ABS(RESID) .LT. 0.0001)GOTO 13
120   CI=(CXY+CI)*0.5
13    RCCO=CXY/CO
      SCMC=(1. - RCCO**2)*SIG
      V=SCNC*DXY+RCCO*CXY
      DCDH=CXY*SCNC/V
14    PHX=E(4)*2. *XP+E(5)*YP+E(2)
      PHY=E(6)*2. *YP+E(5)*XP+E(3)
      FK=(SIN(A)*PHX-COS(A)*PHY)*DCDH*DCON/CXY
      RETURN
      END
      SUBROUTINE DEPTH(X,Y,XP,YP)
      COMMON IFR,FR,SURGE,SXY(12,6)
      COMMON DP(10),TITL(18)
      COMMON DEP(60,67),E(6)
      COMMON NN(7),D(12)
      COMMON B1,B2,CO,CXY
      COMMON DCDH,DCON,DELTAS,DRC,IRO,JRO,AMIS,AMJS
      COMMON DTGR,DXY,GRINC,HO,IGO,JGO,LIMNPT,NPRINT,NPT,PHX
      COMMON HNEW,PHY,RCCO,RHS,RK,IJF,IGF,IRF,JRF
      COMMON AX1,AX2,AY1,AY2,SIG,SK,TOP,V,WL,WLO,X1,X2,Y1,Y2
      COMMON SKP,INDGRD,RKP,GRID,T,FKF,SGRID,MIS,MJS,MI,MJ
      I=X+1
      J=Y+1
      XP=AMOD(X,1.)
      YP=AMOD(Y,1.)
      IF(NPT .EQ. 1)GOTO 11
```

```
      IF(IP .NE. I)GOTO 11
      IF(JP .EQ. J)GOTO 14
11    IP=I
      JP=J
      I0=I-1
      J0=J-1
      I1=I+1
      J1=J+1
      I2=I+2
      J2=J+2
      D(1)=DEP(I,J)
      D(2)=DEP(I1,J)
      D(3)=DEP(I1,J1)
      D(4)=DEP(I,J1)
      D(5)=DEP(I2,J)
      D(6)=DEP(I2,J1)
      D(7)=DEP(I1,J2)
      D(8)=DEP(I,J2)
      D(9)=DEP(I0,J1)
      D(10)=DEP(I0,J)
      D(11)=DEP(I,J0)
      D(12)=DEP(I1,J0)
      DO 110 K=1,6
      E(K)=0
      DO 110 L=1,12
      E(K)=E(K)+D(L)*SXY(L,K)
110   CONTINUE
14    DXY=(E(1)+E(2)*XP+E(3)*YP+E(4)*XP*XP+E(5)*XP*YP+E(6)
     1*YP*YP)*DECON
      RETURN
      END
      SUBROUTINE HEIGHT(X,Y,A,H,ABB)
      COMMON IFR,FR,SURGE,SXY(12,6)
      COMMON DP(10),TITL(18)
      COMMON DEP(60,67),E(6)
      COMMON NN(7),D(12)
      COMMON B1,B2,C0,CXY
      COMMON DCDH,DCON,DELTAS,DRC,IRO,JRO,AMIS,AMJS
      COMMON DTGR,DXY,GRINC,H0,IGO,JGO,LIMNPT,NPRINT,NPT,PHX
      COMMON HNEW,PHY,RCCO,RHS,RK,IJF,IGF,IRF,JRF
      COMMON AX1,AX2,AY1,AY2,SIG,SK,TOP,V,WL,WL0,X1,X2,Y1,Y2
      COMMON SKP,INDGRD,RKP,GRID,T,FKF,SGRID,MIS,MJS,MI,MJ
      WL=WL0*RCCO
      GN=12.5663706144*DXY/WL
      SH=(EXP(GN)-EXP(-GN))/2
      CG=(1. + GN/SH)*CXY
      SKP=SK
      RKP=RK
      IF(CG .LT. 0)RETURN
      SK=SQRT(C0/CG)
      RK=ABS(1. /B2)
```

```
      RK=SQRT(RK)
      H=HO*RK*SK
      GOTO(11,12),JGO
11    U=-2. *SIG*RCCO*CXY/(V*V)
      GOTO 10
12    U=-0.5/DXY
10    U=U*DCON
      DCDX=DCDH*DCON
      COSA=COS(A)
      SINA=SIN(A)
      P=-(COSA*PHX+SINA*PHY)*DCDH*DTGR*2.
      Q=((E(4)*2.+U*PHX*PHX)*SINA*SINA-(E(5)+U*PHX*PHY)*
     1 2.*SINA*COSA+(E(6)*2.+U*PHY*PHY)*COSA*COSA)*DCDH*CXY
     2 *DTGR*DTGR*2.
      B3=((P-2.)*B1+(4.-Q)*B2)/(P+2.)
      B1=B2
      B2=B3
      CALL FRICTN(ABB)
      RETURN
      END
      SUBROUTINE ERROR(FIT,DIFMAX)
      COMMON IFR,FR,SURGE,SXY(12,6)
      COMMON DP(10),TITL(18)
      COMMON DEP(60,67),E(6)
      COMMON NN(7),D(12)
      COMMON B1,B2,CO,CXY
      COMMON DCDH,DCON,DELTAS,DRC,IRO,JRO,AMIS,AMJS
      COMMON DTGR,DXY,GRINC,HO,IGO,JGO,LIMNPT,NPRINT,NPT,PHX
      COMMON HNEW,PHY,RCCO,RHS,RK,IJF,IGF,IRF,JRF
      COMMON AX1,AX2,AY1,AY2,SIG,SK,TOP,V,WL,WLO,X1,X2,Y1,Y2
      COMMON SKP,INDGRD,RKP,GRID,T,FKF,SGRID,MIS,MJS,MI,MJ
      IF(NPT .LT. 3)GOTO 11
      IF(EP .EQ. E(5)GOTO 12
11    DP(1)=E(1)
      DP(2)=E(1)+E(2)+E(4)
      DP(3)=E(1)+E(2)+E(3)+E(4)+E(5)+E(6)
      DP(4)=E(1)+E(3)+E(6)
      DIFMAY=0.
      SUM=0.
      DO 110 I=1,4
      DIF=ABS(D(I)-DP(I))
      IF(DIFMAY .LT. DIF)DIFMAY=DIF
110   SUM=DIF*DIF+SUM
      DIFMAY=DIFMAY*DCON
      SUM=SUM*0.25
      FIT=SQRT(SUM)
      EP=E(5)
12    DIFMAX=DIFMAY/DXY*100.
      RETURN
      END
      SUBROUTINE WRITER(X,Y,ANG,H,NWRITE,FIT,DIFMAX)
```

```
      COMMON IFR,FR,SURGE,SXY(12,6)
      COMMON DP(10),TITL(18)
      COMMON DEP(60,67),E(6)
      COMMON NN(7),D(12)
      COMMON B1,B2,CO,CXY
      COMMON DCDH,DCON,DELTAS,DRC,IRO,JRO,AMIS,AMJS
      COMMON DTGR,DXY,GRINC,HO,IGO,JGO,LIMNPT,NPRINT,NPT,PHX
      COMMON HNEW,PHY,RCCO,RHS,RK,IJF,IGF,IRF,JRF
      COMMON AX1,AX2,AY1,AY2,SIG,SK,TOP,V,WL,WLO,X1,X2,Y1,Y2
      COMMON SKP,INDGRD,RKP,GRID,T,FKF,SGRID,MIS,MJS,MI,MJ
62    FORMAT(' CURVATURE AVERAGED AT POINT',I4)
63    FORMAT(1H ,' RAY STOPPED.NO CONVERGENCE FOR CURVATURE')
64    FORMAT(1H ,'RAY STOPPED,SKIPPED BREAKING CONDITION DUE
     1 TO COARSE GRID AND REACHED SHORE')
65    FORMAT(1H ,' RAY STOPPED REACH BOUNDARY. X= ',F7.2,
     1 'Y= ',F7.2)
66    FORMAT(1H ,'RAY STOPPED NO. OF POINTS EXEED MAX. LIMIT=
     1 ',I4,' POINTS X= ',F7.2, 'Y= ',F7.2)
67    FORMAT(1H ,'RAY STOPPED.INCREMENT DISTANCE ALONG RAY
     1 LESS THAN ',F6.3, 'GRID UNITS X=',F7.2, 'Y= ',F7.2)
68    FORMAT(1H , 'RAY STOPPED , WAVE BREAKES , X= ',F7.2,
     1 'Y= 'F7.2)
69    FORMAT(1H,'RAY STOPPED ,CURVATURE ANNORMAL')
      CALL ERROR(FIT,DIFMAX)
      CALL METRIC(H,1)
      CALL METRIC(HNEW,1)
      CALL METRIC(DXY,1)
      CALL METRIC(WL,1)
      CALL METRIC(CXY,1)
      WRITE(1,61)NPT,X,Y,ANG,DXY,DIFMAX,FIT,WL,CXY,H,RK,SK
     1 ,FKF,HNEW)
      CALL METRIC(HNEW,2)
      CALL METRIC(DXY,2)
      CALL METRIC(WL,2)
      CALL METRICPCXY,2)
      CALL METRIC(H,2)
61    FORMAT(1H+,I7,3F9.2,F11.2,F10.2,F8.2,3F9.2,3F9.4,F10.2)
      GOTO(11,20,21,22,23,24,25,26,27),NWRITE
20    WRITE(1,62)NPT
      GOTO 11
21    WRITE(1,63)
      GOTO 12
22    WRITE(1,64)
      GOTO 12
23    WRITE(1,65)X,Y
      GOTO 12
24    WRITE(1,66)LIMNPT,X,Y
      GOTO 12
25    WRITE(1,67)DELTAS,X,Y
      GOTO 12
26    WRITE(1,68)X,Y
```

```
      GOTO 12
27    WRITE(1,69)
12    IGO=3
11    RETURN
      END
      SBROUTINE FRICTN(ABB)
      COMMON IFR,FR,SURGE,SXY(12,6)
      COMMON DP(10),TITL(18)
      COMMON DEP(60,67),E(6)
      COMMON NN(7),D(12)
      COMMON B1,B2,CO,CXY
      COMMON DCDH,DCON,DELTAS,DRC,IRO,JRO,AMIS,AMJS
      COMMON DTGR,DXY,GRINC,HO,IGO,JGO,LIMNPT,NPRINT,NPT,PHX
      COMMON HNEW,PHY,RCCO,RHS,RK,IJF,IGF,IRF,JRF
      COMMON AX1,AX2,AY1,AY2,SIG,SK,TOP,V,WL,WLO,X1,X2,Y1,Y2
      COMMON SKP,INDGRD,RKP,GRID,T,FKF,SGRID,MIS,MJS,MI,MJ
      RO=63.988659
      FR=00.02
      GRAV=32.1725
      PHIC=3.1415927
      DX=ABB*GRID
      IF(INDGRD .EQ. 0)GOTO 51
      IF(IRF .EQ. 2)GRD=GRD*SGRID
      DX=ABB*GRID
      IF(IRF .EQ. 2)GRID=GRID/SGRID
51    OH=HNEW*(SK/SKP)*(RK/RKP)
      AG=6.2831853*DXY/WL
      SINAG=(EXP(AG)-EXP(-AG))/2.
      PHI=(RO*PHIC**3)/(3. *GRAV**2)*((SK/SINAG)**3)
      HNEW=DH/((FR*OH*PHI*DX)/(SK*T**4)+1.0)
      FKF=HNEW/(SK *RK*HO)
      RETURN
      END
      SUBROUTINE METRIC(X,I)
      COMMON IFR,FR,SURGE,SXY(12,6)
      COMMON DP(10),TITL(18)
      COMMON DEP(60,67),E(6)
      COMMON NN(7),D(12)
      COMMON B1,B2,CO,CXY
      COMMON DCDH,DCON,DELTAS,DRC,IRO,JRO,AMIS,AMJS
      COMMON DTGR,DXY,GRINC,HO,IGO,JGO,LIMNPT,NPRINT,NPT,PHX
      COMMON HNEW,PHY,RCCO,RHS,RK,IJF,IGF,IRF,JRF
      COMMON AX1,AX2,AY1,AY2,SIG,SK,TOP,V,WL,WLO,X1,X2,Y1,Y2
      COMMON SKP,INDGRD,RKP,GRID,T,FKF,SGRID,MIS,MJS,MI,MJ
      GOTO(10,11),I
10    X=X*0.3048
      RETURN
11    X=X/0.3048
      RETURN
      END
```

EXAMPLE OF INPUT DATA FOR TRIVANDRUM

```
   .30861241   .23684207   .21770331   .23684207  -.08492823  -.05143541
  -.05143541  -.08492823   .00598086   .13038278   .13038278   .00598086
   .05322964   .19677030   .14413872   .10586122   .09031100  -.06758374
  -.03349283   .03349282  -.18241626  -.34031099  -.12440190   .12440190
   .05322964   .10586122   .14413872   .19677030   .03349282  -.03349283
  -.06758374   .09031099   .12440190  -.12440191  -.34031099  -.18241625
  -.12499998  -.12499998  -.12499998   .12499998   .12500000   .12500000
  0.00000000  0.00000000   .12499999   .12499999  0.00000000  0.00000000
   .05263157  -.05263157   .05263158  -.05263157  -.15789473   .15789473
   .15789475  -.15789473  -.15789473   .15789473   .15789473  -.15789473
  -.12499998  -.12499998  -.12499998  -.12499998  0.00000000  0.00000000
   .12500000   .12500000  0.00000000  0.00000000   .12499999   .12499999
    45   70    3  300    5000011775.00000   3.28100    .00500    .50000
030.000000007.0000000.056179775200380037
022.528439007.6064760.112676056300170023
00.60
00003
TRV PER 6 SEC  HT. 1M
00400006.00001.00
001.0000008.000180.00
013.00000Ø27.000225.00
031.5000038.500270.00
058.0000038.000315.00

FORT  06.DAT
 66.5 59.5 59.5 59.5 60.5 60.0 58.0 60.0 60.0 60.0 58.0 55.0 59.0 59.0 59.0
 49.0 49.0 42.0 42.0 38.0 34.0 31.0 31.0 29.0-10.0-10.0-10.0-10.0-10.0-10.0
-10.0-10.0-10.0-10.0-10.0-10.0-10.0-10.0-10.0-10.0-10.0-10.0-10.0-10.0-10.0
-10.0-10.0-10.0-10.0-10.0-10.0-10.0-10.0-10.0-10.0-10.0-10.0-10.0-10.0-10.0
 67.0 61.0 61.0 61.0 59.0 59.0 57.0 60.0 59.5 59.0 57.5 55.0 54.0 53.5 54.0
 48.0 47.0 43.0 41.5 38.5 35.5 33.5 32.0 28.0 17.8-10.0-10.0-10.0-10.0-10.0
-10.0-10.0-10.0-10.0-10.0-10.0-10.0-10.0-10.0-10.0-10.0-10.0-10.0-10.0-10.0
-10.0-10.0-10.0-10.0-10.0-10.0-10.0-10.0-10.0-10.0-10.0-10.0-10.0-10.0-10.0
 71.5 66.0 65.5 65.0 60.0 59.5 58.0 61.0 60.5 60.5 59.5 57.5 55.5 55.5 55.5
 50.5 50.0 46.0 43.5 39.0 34.5 31.5 28.0 24.5 18.0  8.5-10.0-10.0-10.0-10.0
-10.0-10.0-10.0-10.0-10.0-10.0-10.0-10.0-10.0-10.0-10.0-10.0-10.0-10.0-10.0
-10.0-10.0-10.0-10.0-10.0-10.0-10.0-10.0-10.0-10.0-10.0-10.0-10.0-10.0-10.0
```

EXAMPLE OF OUTPUT DATA FOR TRIVANDRUM

TRV PER 8 SEC HT. 3.5M

SET NO. 4. PERIOD = 8.00 SECS. RAYNO., 1, TIME STEP = 71.2821 SECS

POINT	X	Y	ANGLE	KR	KS	KF	HNE
1	20.47	27.00	300.00				
5	21.47	25.27	300.00	1.0000	1.0000	1.0000	3.5(
10	22.72	23.10	300.00	1.0000	1.0000	1.0000	3.5(
15	23.97	20.94	300.00	1.0000	1.0000	1.0000	3.5(
20	25.22	18.77	300.00	1.0000	1.0000	1.0000	3.5(
25	26.47	16.61	300.00	1.0000	1.0000	1.0000	3.5(
30	27.72	14.45	300.04	.9999	.9930	.9999	3.47
35	28.97	12.29	300.15	.9988	.9867	.9995	3.45
40	30,21	10.15	300.19	.9985	.9739	.9981	3.40
RAY ENTERED INSHORE GRID AT X = 16.91 Y=33.49							
45	17.38	32.67	300.05	.9918	.9396	.9920	3.24
50	18.57	31.62	299.99	.9834	.9385	.9911	3.20
55	19.75	28.57	299.98	.9752	.9372	.9901	3.17
60	20.92	26.54	300.00	.9667	.9353	.9891	3.13
65	22.10	24.50	300.00	.9583	.9344	.9881	3.10
70	23.27	22.47	299.98	.9501	.9339	.9870	3.07
75	24.44	20.45	299.91	.9420	.9327	.9859	3.03
80	25.60	18.42	299.99	.9333	.9322	.9847	3.00
85	26.77	16.41	300.47	.9218	.9296	.9835	2.95
90	27.95	14.43	301.23	.9073	.9261	.9821	2.89
95	29.15	12.50	302.12	.8888	.9185	.9801	2.80
100	30.33	10.69	304.90	.8648	.9154	.9757	2.70
104	31.20	9.51	308.26	.8410	.9958	.9582	2.81
105	31.38	9.29	309.08	.8336	1.0662	.9393	2.92
106	31.53	9.11	309.85	.8247	1.1888	.8885	3.05

RAY STOPPED, WAVE BREAKES, X = 31.53, Y = 9.11

APPENDIX II

```
      PROGRAM TRANF.S
C
C     A PROGRAM TO COMPUTE TRANSFORMATION OF WAVE SPECTRUM
C     OVER IRREGULAR  BOTTOM TOPOGRAPHY BY HUBERTZ (1980)-
C     MODIFIED TO INCORPORATE BOTTOM FRICTINAL ATTENUATION
C     BY N.P. KURIAN USING THE EQUATION OF COLLINS (1972).
C     AO IS THE TIDAL LEVEL ABOVE MSL IN METRES
C     AWS IS THE INPUT SPECTRAL DENSITY IN (M-SQUARED)-
C     SEC AT EACH BAND
C     D(I,J) IS THE ARRAY OF WATER DEPTHS IN METRES
C     DF IS TWICE THE CENTRAL FREQ. OF A BAND DIVIDED BY
C     THE BAND NUMBER K
C     DS IS THE INPUT WATER DEPTH AT OFFSHORE IN METRES
C     DX IS THE GRID SIZE IN X-DIRECTION IN METRES
C     DY IS THE GRID SIZE IN Y-DIRECTION IN METRES
C     ED IS THE TOTAL INPUT ENERGY IN METRE SQUARED
C     FR IS THE FRICTION FACTOR USED
C     IS IS THE NUMBER OF STATIONS WHERE OUTPUT IS DESIRED
C     IGRID IS THE NUMBER OF GRID LINES IN X-DIRECTION
C     ITMAX IS THE MAXIMUM NUMBER OF ITERATIONS TO FIND
C     NEW WAVE ANGLE AND HEIGHT
C     JGRID IS THE NUMBER OF GRID LINES IN Y-DIRECTION
C     K1 IS THE NUMBER OF FREQ. BANDS IN THE INPUT SPECTRUM
C     M IS THE NUBER OF GRID POINTS PERPENDICULAR TO
C     THE SHORE
C     MK IS THE ARRAY OF I-VALUES FOR STATION
C     LOCATION ON OFFSHORE
C     N IS THE NUBER OF GRID POINTS PARALLEL TO SHORE
C     NFIELD IS AN OPTION FOR SMOOTHING DEPTH AND
C     DEPTH DERIVATIVES
C     NK IS THE FIXED J-COLUMN WHERE STATIONS ARE LOCATED
C     THETAI IS THE WAVE APPROACH ANGLE IN DEGREES MEASURED
C     FACING COST FROM A POINT AT SEA
C     ZERO DEGREES IS STRAIGHT TOWARD COAST, POSITIVE
C     IN CLOCKWISE DIRECTION
C     THETA IS EQUAL TO THETAI IN RADIANS MINUS PI
C     U(I,J) IS THE CURRENT SPEED IN X-DIRECTION IN M/S
C     V(I,J) IS THE CURRENT SPEED IN Y-DIRECTION IN M/S
C
      PROGRAM CESS(INPUT,OUTPUT,TAPE6,TAPE9)
      DIMENSION AWS(50),AAW(50,25),IB(50,25),MK(6)
     1 ,HERZ(50),SPDE(30,6,6)
      DIMENSION HBREAK(50,25),CG(50,25)
      COMMON /CONI/D(50,25),U(50,25),V(50,25),Z(50,25)
      COMMON RRK(50,25),PHI(50,25),UBB(50,25)
      COMMON H(50,25),SI(50,25),S(50,25),DVDY(50,25)
      COMMON CC(50,25),DDDX(50,25),DDDY(50,25),T,SIGMA,M,N
      COMMON /CON/G,PI,PI2,RAD,EPS.DX,DY,DX2,DY2,FR,HZ
      COMMON /UV/DUDX(50,25),DUDY(50,25),DVDX(50,25)
```

```
      OPEN (9)
      REWIND (9)
      READ(9,5010)M,N,K1,ITMAX,IS,NK,NSUFCE,NFIELD
      READ(9,5010)(MK(I),I=1,IS)
      DO 70 I=1,50
      DO 70 J=1,25
      AAW(I,J)=0.0
      IB(I,J)=0.0
      HERZ(I)=0.0
      D(I,J)=0.0
      Z(I,J)=0.0
      PHI(I,J)=0.0
      DUDX(I,J)=0.0
      DVDX(I,J)=0.0
      DUDY(I,J)=0.0
      DVDY(I,J)=0.0
      RRK(I,J)=0.0
      H(I,J)=0.0
      SI(I,J)=0.0
      S(I,J)=0.0
      CO(I,J)=0.0
      DDDX(I,J)=0.0
      DDDY(I,J)=0.0
      UBB(I,J)=0.0
      U(I,J)=0.0
70    V(I,J)=0.0
5010  FORMAT(8I3)
      READ(9,5020)DX,DY,A0,DS,DF,FR
5020  FORMAT(4F7.2,2F7.5)
      READ(9,5030)((D(I,J),J=1,N),I=1,M)
      DO 71 II=1,M
      DO 71 JJ=1,N
71    D(II,JJ)=D(II,JJ)+AC
      DS=DS+AC
5030  FORMAT(20F4.1)
5031  FORMAT(15F5.2)
5040  FORMAT(9F6.4/10F6.4)
5041  FORMAT(2F8.5)
      WRITE(6,6010)M,N,K1,ITMAX,NSUFCE,NFIELD,DX,DY)
6010  FORMAT(1H1 ,1X,'M= ',I5,1X,'N= ',I5,3X, 'K1= ',I5,
     1  1X,' ITMAX= '
     1  ,I5,3X,' INSUFCE= ',I5,1X,' NFIELD',I5,33X,'DX= ',
     1  F7.2,,3X, 'DY=
     1  ',F7.2)
      WRITE(6,6020)DS
6020  FORMAT(1X,'THE DEEP WATER DEPTH='F8.3)
      WRITE(6,6040)AC,FR
6040  FORMAT(1X,'TIDAL LEVEL= ',F6.2,5X,
     1  'FRICTION FACTOR=',F6.4)
      DO 11 K=3,K1
      HERZ(K)=0.5*DF*FLOAT(K)
```

```
11      CONTINUE
        WRITE(6,6080)
6080    FORMAT(1X,'ENERGY DENCITY(M**2-SEC) AT OFFSHORE
     1  STATION FOR EACH FREQ. BAND')
        WRITE(6,6081)(HERZ(K),K=3,K1)
789     READ(9,5040,END=505)(AWS(I),I=3,K1)
        WRITE(6,6081)(AWS(I),I=3,K1)
        READ(9,5041)ED,THETA
6081    FORMAT(1X,10F7.4)
        WRITE(6,6090)ED
6090    FORMAT(1X,'TOTAL WAVE ENRGY AT OFFSHORE STATION =
     1  ',F7.4)
        G=9.80621
        PI=3.1415927
        PI2=PI*2.
        RAD=180./PI
        DO 10 I=1,M
        DO 10 J=1,N
        SUM=0.
        DO 60 L=3,K1
        DRK=((2.*PI*HERZ(L))**2)/G
        AG1=DRK*D(I,J)
        UB=(DF/2.)*AWS(L)*((G*DRK)/PI2*HERZ(L)*COSH(AG1)))**2
        SUM=SUM+UB
60      CONTINUE
10      UBB(I,J)=SQRT(SUM)
        M1=M-1
        N1=N-1
        DX2=DX*2.0
        DY2=DY*2.0
        EPS=0.01
        HO=2.828*SQRT(ED)
        THETA1=((THETA*RAD)-180.)*(-1.0)
        WRITE(6,6050)THETA1
6050    FORMAT(1X,'THE INITIAL WAVE DIRECTION OFFSHORE IS '
     1  ,F7.1,'DEGREES')
        CALL DEPTH
        CALL SMOOTH(NSUFCE,NFIELD)
        WRITE(6,6060)
6060    FORMAT(2X,'THE MATRIX OF WATER DEPTH IN METRES')
        WRITE(6,6070)((D(I,J),J=1,N),I=1,M)
6070    FORMAT(4X,25F5.1)
        DO 20 K=3,K1
        SIGMA=DF*PI*FLOAT(K)
        P=2.*PI/SIGMA
        HZ=1./T
        WRITE(6,6072)HZ
6072    FORMAT(1H1,1X,' START OF COMPUTED OUTPUT AT
     1  FREQUENCY ',F8.3,'HZ')
        CALL CURRENT
        CALL SNELL(THETA,HO,DS,IB)
```

```
      CALL ANGLE(ITMAX)
      CALL HEIGHT(ITMAX,HBREAK ,CG,IB)
      DDW=AWS(K)/ED
      DO 30 I=1,M
      DO 30 J=1,N
      E1=(H(I,J)**2)/8.
      AW(I,J)=E1*DDW
      Z(I,J)=(PI-Z(I,J))*180./PI
30    CONTINUE
      DO 40 I=1,IS
      LF=MK(I)
      SPDE(K,I,I)=AAW(LF,NK)
      HERZ(K)=HZ
40    CONTINUE
      WRITE(6,6110)
6110  FORMAT(1X,'WAVE APPROCHING ANGLE IN DEGREE ')
      WRITE(6,6071)((Z(I,J),1,N),I=1,M)
6071  FORMAT(4X,10F8.1)
      WRITE(6,6130)
6130  FORMAT(1H1,1X,' WAVE HEIGHT(METRS)')
      WRITE(6,6200)((H(I,J),J=1,N),I=1,M)
      WRITE(6,6140)
6140  FORMAT(1H1,1X'BREAKING POSITION (0 MEANS WAVE
     1 BREAKING))
      WRITE(6,6150)((IB(I,J),J=1,N),I=1,M)
6150  FORMAT(5X,25I4)
      WRITE(6,6100)HZ
6100  FORMAT(1X,' NEARSHORE SPECTRAL DENSITY AT HZ=',F8.3)
      WRITE(6,6210)((AAW(I,J),J=1,N),I=1,M)
      WRITE(6,6120)HZ
6200  FORMAT(4X,10F4.1)
6210  FORMAT(4X,10F6.2)
6120  FORMAT(//,1X,'END OF CALCULATION AT HZ=',F8.3)
20    CONTINUE
      DO 50 I=1,IS
      WRITE(6,6160)MK(I),NK
      WRITE(6,6173)(HERZ(K),SPDE(K,I,I),K=3,K1)
6160  FORMAT(1X1 'SPECTRAL DENSITY (M**2*SEC) AT STATION
     1 =',2I8)
6173  FORMAT(10X,F8.5,10X,F8.5)
50    CONTINUE
      GOTO 789
505   STOP
      END
      SUBROUTINE DEPTH
C     THIS SUBROUTINE CALCULATES THE X AND Y DERIVATIVES
C     OF THE DEPTHS AT EACH GRID POINT
      COMMON /CONI/D(50,25),U(50,25),V(50,25),Z(50,25)
      COMMON RRK(50,25),PHI(50,25),UBB(50,25)
      COMMON H(50,25),SI(50,25),S(50,25),DVDY(50,25)
      COMMON CC(50,25),DDDX(50,25),DDDY(50,25),T,SIGMA,M,N
```

```
      COMMON /CON/G,PI,PI2,RAD,EPS.DX,DY,DX2,DY2,FR,HZ
      COMMON /UV/DUDX(50,25),DUDY(50,25),DVDX(50,25)
      M1=M-1
      N1=N-1
      DO 157 I=2,M1
      DO 157 J=2,N1
      A=D(I+1,J)
      IF(A .LT. 0.0)A=0.0
      B=D(I-1,J)
      IF(B .LT. 0.0)B=0.0
      C=D(I,J+1)
      IF(C .LT. 0.0)C=0.0
      E=D(I,J -1)
      IF(E .LT. 0.0)E=0.0
      DDDX(I,J)=(A-B)/DX2
157   DDDY(I,J)=(C-E)/DY2
      DO 100 J=2,N1
      DDDX(M,J)=DDDX(M1,J)
      DDDX(1,J)=DDDX(2,J)
      DDDY(1,J)=(D(1,J+1)-D(1,J-1))/DY2
100   DDDY(M,J)=(D(M,J+1)-D(M,J-1))/DY2
      DO 101 I=2,M1
      DDDX(I,1)=(D(I+1,1)-D(I-1,1))/DX2
      DDDY(I,1)=DDDY(I,2)
      DDDY(I,N)=DDDY(I,N1)
101   DDDX(I,N)=(D(I+1,N)-D(I-1,N))/DX2
      DDDX(M,1)=DDDX(M1,1)
      DDDY(M,1)=DDDY(M,2)
      DDDX(M,N)=DDDX(M1,N)
      DDDY(M,N)=DDDY(M,N1)
      DDDX(1,1)=DDDX(2,1)
      DDDY(1,1)=DDDY(1,2)
      DDDX(1,N)=DDDX(2,N)
      DDDY(1,N)=DDDY(1,N1)
      RETURN
      END
      SUBROUTINE SMOOTH(NSUFCE,NFIELD)
C     THIS SUBROUTINE GIVES AN OPTION TO SMOOTH DEPTH
     1  VALUES AND OR THE  X,Y DERIVATIVES OF THE DEPTHS
      COMMON /CONI/D(50,25),U(50,25),V(50,25),Z(50,25)
      COMMON RRK(50,25),PHI(50,25),UBB(50,25)
      COMMON H(50,25),SI(50,25),S(50,25),DVDY(50,25)
      COMMON CC(50,25),DDDX(50,25),DDDY(50,25),T,SIGMA,M,N
      COMMON /CON/G,PI,PI2,RAD,EPS.DX,DY,DX2,DY2,FR,HZ
      COMMON /UV/DUDX(50,25),DUDY(50,25),DVDX(50,25)
      IF(NSUFCE .LT. 0)GOTO 30
      M1=M-1
      N1=N-1
      IF(NFIELD .LT. 0) GOTO 40
      DO 20 K=1,NSUFCE
      DO 10 I=2,M1
```

```
      DO 10 J=2,N1
      D(I,J)=(D(I,J)+D(I+1,J)+D(I-1,J)+D(I,J+1)+D(I,J-1))/5.
10    CONTINUE
20    CONTINUE
      IF(NFIELD .GT. 0)GOTO 30
40    CONTINUE
      DO 21 K=1,NSUFCE
      DO 11 I=2,M1
      DO 11 J=2,N1
      DDDX(I,J)=(DDDX(I,J)+DDDX(I+1,J)+DDDX(I-1,J)
     1  +DDDX(I,J+1)+DDDX(I,J-1))/5.0
      DDDY(I,J)=(DDDY(I,J)+DDDY(I+1,J)+DDDY(I-1,J)
     1  +DDDY(I,J+1)DDDY(I,J-1))/5.0
11    CONTINUE
21    CONTINUE
30    RETURN
      END
      SUBROUTINE CURRENT
C     THIS SUBROUTINE CALCULATES THE X AND Y
     1  DERIVATIVES OF THE CURRENT COMPONENTS AT EACH
     C  GRID POINT
      COMMON /CONI/D(50,25),U(50,25),V(50,25),Z(50,25)
      COMMON RRK(50,25),PHI(50,25),UBB(50,25)
      COMMON H(50,25),SI(50,25),S(50,25),DVDY(50,25)
      COMMON CC(50,25),DDDX(50,25),DDDY(50,25),T,SIGMA,M,N
      COMMON /CON/G,PI,PI2,RAD,EPS.DX,DY,DX2,DY2,FR,HZ
      COMMON /UV/DUDX(50,25),DUDY(50,25),DVDX(50,25)
      M1=M-1
      N1=N-1
      DO 202 I=2,M1
      DO 202 J=2,N1
      DUDX(I,J)=(U(I+1,J)-U(I-1,J)//DX2
      DUDY(I,J)=(U(I,J+1)-U(I,J-1)//DY2
      DVDX(I,J)=(V(I+1,J)-V(I-1,J))/DX2
202   DVDY(I,J)=(V(I,J+1)-V(I,J-1))/DY2
      DO 21 I=2,M1
      DUDX(I,1)=DUDX(I,2)
      DUDY(I,1)=DUDY(I,2)
      DVDX(I,1)=DVDX(I,2)
      DVDY(I,1)=DVDY(I,2)
      DUDX(I,N)=DUDX(I,N1)
      DUDY(I,N)=DUDY(I,N1)
      DVDX(I,N)=DVDX(I,N1)
      DVDY(I,N)=DVDY(I,N1)
21    CONTINUE
      DO 22 J=1,N
      DUDX(1,J)=DUDX(2,J)
      DUDY(1,J)=DUDY(2,J)
      DVDX(1,J)=DVDX(2,J)
      DVDY(1,J)=DVDY(2,J)
      DUDX(M,J)=DUDX(M1,J)
```

```
      DUDY(M,J)=DUDY(M1,J)
      DVDX(M,J)=DVDX(M1,J)
22    DVDY(M,J)=DVDY(M1,J)
      RETURN
      END
      SUBROUTINE SNELL(THETA,HH,DS,IB)
C     THIS SUBROUTINE CALCULATES THE INITIAL WAVE HEIGHT
C     AND ANGLE AT EACH GRID POINT USING THE INPUT BOUNDARY
C     WAVE HEIGHT AND DIRECTION
      DIMENSION IB(50,25)
      COMMON /CONI/D(50,25),U(50,25),V(50,25),Z(50,25)
      COMMON RRK(50,25),PHI(50,25),UBB(50,25)
      COMMON H(50,25),SI(50,25),S(50,25),DVDY(50,25)
      COMMON CC(50,25),DDDX(50,25),DDDY(50,25),T,SIGMA,M,N
      COMMON /CON/G,PI,PI2,RAD,EPS.DX,DY,DX2,DY2,FR,HZ
      COMMON /UV/DUDX(50,25),DUDY(50,25),DVDX(50,25)
      SH(ARG)=(EXP(ARG)-EXP(-ARG))/2.
      TAH(ARG)=(EXP(ARG)-EXP(-ARG)/(EXP(ARG)+EXP(-ARG))
      CALL WVNUM(DS,0.0,0.0,0.0,0.0,RK)
      AA=RK*DS
      TN=TAH(AA)
      DO 600 J=1,N
30    DO 600 I=1,M
      IF(D(I,J) .GT. 0.0)GOTO 33
      ANG=PI
      WVHT=0.0
      SS=0.0
      CC=-1.0
      GOTO 43
33    CONTINUE
      D1=D(I,J)
      CALL WVNUM(D1,0.0,0.0,0.0,0.0,RK)
      AA=RK*D(I,J)
      ANG=ASIN(SIN(THETA)*TAH(AA)/TN)
      ANG=PI-ANG
      ARG=2.00*AA
      SHOAL=SQRT(1.0/(TAH(AA)*(1.0+ARG)/SH(ARG))))
      REF=SQRT(COS(THETA)/COS(ANG))
      WVHT=HH*SHOAL*REF
      HB=0.12*TAH(AA)*PI2/RK
      IF(WVHT .GT. HB)WVHT=HB
      IN=1
      IF(WVHT .GT. HB)IN=0
      SS=SIN(ANG)
      CC=COS(ANG)
43    CONTINUE
      H(I,J)=WVHT
      IB(I,J)=IN
      Z(I,J)=ANG
      SI(I,J)=SS
      CO(I,J)=CC
```

```
      RRK(I,J)=RK
 600  CONTINUE
      IH=(N+1)/2.
      HR=HH/H(M,IH)
      DO 10 J=1,N
      DO 10 I=1,M
10    H(I,J)=HR*H(I,J)
700   RETURN
      END
      SUBROUTINE ANGLE(ITMAX)
C     THIS SUBROUTINE SETS VALUES OF WAVE ANGLE ON THE
C     BOUNDARY AND DEEP SWEEP DIRECTION BASED ON WAVE
C     APPROACH ANGLE , THEN
C     CALLS NEWANG
      DIMENSION SS(50,25),C(50,25)
      COMMON /CONI/D(50,25),U(50,25),V(50,25),Z(50,25)
      COMMON RRK(50,25),PHI(50,25),UBB(50,25)
      COMMON H(50,25),SI(50,25),S(50,25),DVDY(50,25)
      COMMON CC(50,25),DDDX(50,25),DDDY(50,25),T,SIGMA,M,N
      COMMON /CON/G,PI,PI2,RAD,EPS.DX,DY,DX2,DY2,FR,HZ
      COMMON /UV/DUDX(50,25),DUDY(50,25),DVDX(50,25)
      DO 777 I=1,50
      DO 777 J=1,25
      SS(I,J)=0.0
 777  C(I,J)=0.0
      M1=M-1
      N1=N-1
      DO 789 I=2,M1
      DO 789 J=2,N1
      SS(I,J)=0.25*(SI(I+1,J)+SI(I-1,J)+SI(I,J+1)
     1 +SI(I,J-1))+0.125((Z(I+1,J)-Z(I-1,J)*(CO(I-1,J)
     2 -CO(I+1,J)+(Z(I,J+1)-Z(I,J-1))(CO(I,J-1)-CO(I,J+1)))
      C(I,J)=0.25*(CO(I+1,J)+CO(I-1,J)+CO(I,J+1)+CO(I,J-1))
     1 +0.125*((Z(I+1,J)-Z(I-1,J)*(SI(I+1,J)-SI(I-1,J))+(Z(I,
     2 J+1)-Z(I,J-1))*(SI(I,J+1)-SI(I,J-1)))
 789  CONTINUE
      N2=N1/2
      THETA0=((Z(M1,N2)*RAD)-180.)*(-1.0)
      DO 302 J=1,N
      Z(1,J)=Z(2,J)
 302  CONTINUE
      IF(THETA0 .LT. 0.)GOTO 190
      DO 200 IT=1,ITMAX
      IFLAG=1
      IPT=0
      DO 210 J=2,N1
      DO 211 II=2,M1
      I=M-II+1
      IF(D(I,J) .LE. 0.0 .OR. D(I-1,J) .LE. 0.0)GOTO 211
      CO(I,J)=C(I,J)
      SI(I,J)=SS(I,J)
```

```
      CALL NEWANG(I,J,IFLAG,IT,IPT)
211   CONTINUE
210   CONTINUE
      IF(IFLAG .EQ. 1)GOTO 150
      IF(IPT .LE. 5)GOTO 150
200   CONTINUE
      GOTO 301
190   CONTINUE
      DO 400 IT=1,ITMAX
      IFLAG=1
      IPT=0
      DO 410 JJ=2,N1
      J=N-JJ+1
      DO 410 II=2,M1
      I=M-II+1
      IF(D(I,J) .LE. 0. .OR. D(I-1,J) .LE. 0.0)GOTO 410
      CO(I,J)=C(I,J)
      SI(I,J)=SS(I,J)
      CALL NEWANG(I,J,IFLAG,IT,IPT)
410    CONTINUE
      IF(IFLAG .EQ. 1)GOTO 412
      IF(IPT .LE. 5)GOTO 412
400   CONTINUE
      GOTO 180
150   WRITE(6,214)IT
      WRITE(6,216)IPT
214   FORMAT(10X,'WAVE ANGLES DETERMINED AFTER 'I5,
     1 'ITERATIONS')
216   FORMAT(10X,I5,5X,' NONCONVERGENT POINTS FOUND',
     1 CALCULATIONS PROCEED')
      RETURN
301   CONTINUE
212   WRITE(6,213)IT
213   FORMAT(10X,'ITERATION FOR WAVE ANGLE FAILED TO
     1 CONVERGE AFTER',I5,'ITERATIONS')
      RETURN
412   WRITE(6,214)IT
      WRITE(6,216)IPT
      RETURN
180   WRITE(6,213)IT
      RETURN
      END
      SUBROUTINE NEWANG(I,J,IFLAG,IT,IPT)
C     THIS SUBROUTINE USES THE WAVE NUBER DETERMINED
C     IN WVNUM AND THE IRROTATIONAL ASSUMPTION TO CALCULATE
C     A WAVE ANGLE AT EACH GRID POINT
      COMMON /CONI/D(50,25),U(50,25),V(50,25),Z(50,25)
      COMMON RRK(50,25),PHI(50,25),UBB(50,25)
      COMMON H(50,25),SI(50,25),S(50,25),DVDY(50,25)
      COMMON CC(50,25),DDDX(50,25),DDDY(50,25),T,SIGMA,M,N
      COMMON /CON/G,PI,PI2,RAD,EPS.DX,DY,DX2,DY2,FR,HZ
```

```
      COMMON /UV/DUDX(50,25),DUDY(50,25),DVDX(50,25)
      SH(ARG)=(EXP(ARG)-EXP(-ARG))/2.
      THETAO=((Z(I,J)*RAD)-180.)*(-1.0)
      ARG2=2.0*RRK(I,j)*D(I,J)
      SII=SH(ARG2)
      COSI=CO(I,J)
      SINI=SI(I,J)
      F=U(I,J)*COSI+V(I,J)*SINI
      FF=F+0.5*(1.0+ARG2/SII)*(SIGMA/RRK(I,J)-F)
      FI=(SIGMA-RRK(I,J)*F)/SII
      DKDY=(-COSI*DUDY(I,J)+SINI*DVDY(I,J))-
     1  (F1*DDDY(I,J)))/FF
      DKDX=(-(COSI*DUDX(I,J)+SINI*DVDX(I,J))-
     1  (F1*DDDX(I,J)))/FF
      FACI=U(I,J)*SINI-V(I,J)*COSI
      DEN1=(SINI-COSI*FACI/FF)/DY
      DEN2=(COSI+SINI*FACI/FF)/DX
      DEN=DEN1-DEN2
      IF(THETAO .LT. 0)GOTO 10
      ZNEW=(COSI*DKDY-SINI*DKDX+Z(I,J-1)*DEN1-Z(I+1,J)
     1  *DEN2)/DEN
      GOTO 11
10    ZNEW=(COSI*DKDY-SINI*DKDX+Z(I,J+1)*DEN1-Z(I+1,J)
     1  *DEN2)/DEN
11    IF(ABS(ZNEW-Z(I,J) .GT. (EPS*ABS(ZNEW)))GOTO 1
      GOTO 2
1     IFLAG=0
      IPT=IPT+1
      WRITE(6,3)I,J,IT,Z(I,J),ZNEW
3     FORMAT(10X,'I=',I5,5X,'J=',I5,5X,'ITERATION=',I5,5X,
     1  'OLD ANGLE (RADIANS)',F9.3,3X,'NEW ANGLE',F9.3)
20    CONTINUE
      IF(THETAO .LT. 0)GOTO 4
      Z(I,J)=Z(I,J)+0.7*(ZNEW-Z(I,J))
      GOTO 2
4     CONTINUE
      Z(I,J)=Z(I,J)+0.07*(Z(NEW-Z(I,J))
2     CONTINUE
      CO(I,J)=COS(Z(I,J))
      SI(I,J)=SIN(Z(I,J))
      DI=D(I,J)
      CO1=CO(I,J)
      SII=SI(I,J)
      U1=U(I,J)
      V1=V(I,J)
      CALL WVNUM(D1,CO1,SI1,U1,V1,RK)
      RRK(I,J)=RK
      RETURN
      END
      SUBROUTINE WVNUM(P,COSI,SINI,X,Y,RK)
C     THIS SUBROUTINE CALCULATES WAVE NUMBER AT A GRID POINT
```

```
C       THROUGH ITERATION OF THE DISPERSION RELATIONSHIP
        COMMON /CONI/D(50,25),U(50,25),V(50,25),Z(50,25)
        COMMON RRK(50,25),PHI(50,25),UBB(50,25)
        COMMON H(50,25),SI(50,25),S(50,25),DVDY(50,25)
        COMMON CC(50,25),DDDX(50,25),DDDY(50,25),T,SIGMA,M,N
        COMMON /CON/G,PI,PI2,RAD,EPS.DX,DY,DX2,DY2,FR,HZ
        COMMON /UV/DUDX(50,25),DUDY(50,25),DVDX(50,25)
        TAH(ARG)=(EXP(ARG)-EXP(-ARG))/(EXP(ARG)+EXP(-ARG)
        EPSK=0.001
        RK=PI2/(T*SQRT(G*P))
        DO 100 I=1,50
        A=SIGMA-X*RK*COSI-Y*RK*SINI
        A2=A**2
        ARG=RK*P
        F1=EXP(ARG)
        F2=1.0/F1
        SECH=2./(F1+F2)
        SECH2=SECH*SECH
        TT=TANH(ARG)
        FK=G*RK*TT-A2
        FFK=G*(ARG*SECH2+TT)+2.*(X*COSI+Y*SINI)*A
        RKNEW=RK-FK/FFK
        IF(ABS(RKNEW-RK) .LE. (ABS(EPSK*RKNEW)))GOTO 110
        RK=RKNEW
 100    CONTINUE
        WRITE(6,101)I,RK,T,P,X,Y,FK,FFK,A,F1,F2,ARG,TT
 101    FORMAT('ITERATION FOR K FAILED TO CONVERGE AFTER ',
     1  I6,/12F10.4)
        RETURN
 110    RK=RKNEW
        SIGMA=SIGMA-X*RK*COSI-Y*RK*SINI
        IF(RK .GT. 0)GOTO 120
        WRITE(6,130)P,COSI,SINI,X,Y,RK,SIGMA
 130    FORMAT(10X,'RK IS NEGATIVE-OUTPUT D,COSI,SINI,U,V,
     1  RK,A',7E12.4)
 120    RETURN
        END
        SUBROUTINE HEIGHT(ITMAX,HBREAK,CG,IB)
C       THIS SUBROUTINE USES THE WAVE NUMBER AND ANGLE
C       CALCULATED PREVIOUSLY AND THE WAVE ENERGY CONSEVATION
C       EQATION TO CALCULATE THROUGH ITERATION WAVE HEIGHT AT
C       EACH GRID POINT
        DIMENSION HBREAK(50,25),CG(50,25),IB(50,25)
        COMMON /CONI/D(50,25),U(50,25),V(50,25),Z(50,25)
        COMMON RRK(50,25),PHI(50,25),UBB(50,25)
        COMMON H(50,25),SI(50,25),S(50,25),DVDY(50,25)
        COMMON CC(50,25),DDDX(50,25),DDDY(50,25),T,SIGMA,M,N
        COMMON /CON/G,PI,PI2,RAD,EPS.DX,DY,DX2,DY2,FR,HZ
        COMMON /UV/DUDX(50,25),DUDY(50,25),DVDX(50,25)
        DO 123 I1=1,M
        DO 123 I2=1,N
```

```
      HBREAK(I1,I2)=0.0
123   CG(I1,I2)=0.0
      CALL GROUP(HBREAK,CG)
      M1=M-1
      N1=N-1
      N2=N/2
      THETAO=((Z(M1,N2)*RAD)-180.0)*(-1.0)
      IF(THETAO .LT. 0.)GOTO 100
      DO 10 II=1,M1
      I=M-II
      DO 20 IT=1,ITMAX
      H(I,N)=H(I,N1)
      IFLAG=1
      DO 30 J=2,N1
      IF(D(I,J) .LE. 0.)GOTO 30
      ZN=S(I,J)-PHI(I,J)
      CC1=(V(I,J)+CG(I,J)*SI(I,J))/DY
      CC2=(U(I,J)+CG(I,J)*CO(I,J))/DX
      HNEW=(CC1*H(I,J-1)-CC2*H(I+1,J))/CC1-CC2-ZN/2.0)
      IF(HNEW .LE. HBREAK(I,J))GOTO 850
      HNEW=HBREAK(I,J)
      GOTO 860
850   IF(HNEW .LT. 0.0)HNEW=0.0
860   IF(ABS(HNEW-H(I,J)) .GT. (EPS*ABS(HNEW)))GOTO 31
      H(I,J)=HNEW
      GOTO 30
31    IFLAG=0
      IF(IT .LT. ITMAX)GOTO 32
      WRITE(6,21)IT,I,J
32    H(I,J)=HNEW
30    CONTINUE
      IF(IFLAG .EQ. 1)GOTO 10
20    CONTINUE
21    FORMAT(10X,'ITERATION FOR HEIGHT FAILED TO CONVERGE
      AFTER ',I5,'ITERATIONS AT GRID POINT',I5,',',I5)
      WRITE(6,22)IT,I
10    CONTINUE
22    FORMAT(10X,'NEW HEIGHTS OBTAINED AFTER ',I5,
     1  'ITERATIONS ON ROW,I5')
      DO 40 I=1,M1
      DO 40 J=1,N1
      IF(H(I,J)-HBREAK(I,J))2,3,3
2     IB(I,J)=1
      GO TO 40
3     IB(I,J)=0
40    CONTINUE
      RETURN
100   CONTINUE
      DO 60 II=1,M1
      I=M-II
      DO 70 IT=1,ITMAX
```

```
      IFLAG=1
      DO 80 JJ=2,N1
      J=N-JJ+1
      IF(D(I,J) .LE. 0.)GOTO 80
      ZN=S(I,J)-PHI(I,J)
      CC1=(V(I,J)+CG(I,J)*SI(I,J))/DY
      CC2=(U(I,J)+CG(I,J)*CO(I,J))/DX
      HNEW=(CC1*H(I,J+1)+CC2*H(I+1,J))/(CC1+CC2+ZN/2.0)
      IF(HNEW .LE. HBREAK(I,J))GOTO 900
      HNEW=HBREAK(I,J)
      GOOTO 910
  900 IF(HNEW .LT. 0.0)HNEW=0.0
  910 IF(ABS(HNEW-H(I,J)) .GT. (EPS*ABS(HNEW)))GOTO 81
      H(I,J)=HNEW
      GOTO 80
   81 IFLAG=0
      IF(IT .LT. ITMAX)GOTO 82
      WRITE(6,21)IT,I,J
   82 H(I,J)=HNEW
   80 CONTINUE
      IF(IFLAG .EQ. 1)GOTO 60
   70 CONTINUE
      WRITE(6,22)IT,I
   60 CONTINUE
      DO 90 I=1,M
      DO 90 J=1,N
      IF(H(I,J)-HBREAK(I,J))52,53,53
   52 IB(I,J)=1
      GOTO 90
   53 IB(I,J)=0
   90 CONTINUE
      RETURN
      END
      SUBROUTINE GROUP(HBREAK,CG)
C     THIS SUBROUTINE CALCULATES VARIOUS TERMS USED IN
C     SOLUTIONS OF THE WAVE ENERGY CONSERVATION EQUATION
C     IN SUBROUTINE HEIGHT
      DIMENSION DTDX(50,25),DTDY(50,25)HBREAK(50,25),CG(50,25)
      COMMON /CONI/D(50,25),U(50,25),V(50,25),Z(50,25)
      COMMON RRK(50,25),PHI(50,25),UBB(50,25)
      COMMON H(50,25),SI(50,25),S(50,25),DVDY(50,25)
      COMMON CC(50,25),DDDX(50,25),DDDY(50,25),T,SIGMA,M,N
      COMMON /CON/G,PI,PI2,RAD,EPS.DX,DY,DX2,DY2,FR,HZ
      COMMON /UV/DUDX(50,25),DUDY(50,25),DVDX(50,25)
      SH(ARG)=(EXP(ARG)-EXP(-ARG))/2.
      COH(ARG)=(EXP(ARG)-EXP(-ARG))/2.
      TAH(ARG)=(EXP(ARG)-EXP(-ARG))/(EXP(ARG)+EXP(-ARG))
      M1=M-1
      N1=N-1
      DO 400 I=2,M1
      DO 400 J=2,N1
```

```
      DTDX(I,J)=(Z(I+1,J)-Z(I-1,J)/DX2
400   DTDY9I,J)=(Z(I,J+1)-Z(I,J-1))/DY2
      DO 401 J=2,N1
      DTDX(1,J)=DTDX(2,J)
      DTDY(1,J)=(Z(1,J+1)-Z(1,J-1))/DY2
      DTDX(M,J)=DTDX(M1,J)
401   DTDY(M,J)=(Z(M,I+1)-Z(M,J-1))/DY2
      DO 402 I=2,M1
      DTDX(I,1)=(Z(I+1,1)-Z(I-1,1))/DX2
      DTDY(I,1)=DTDY(I,2)
      DTDX(I,N)=(Z(I+1,N)-Z(I-1,N))/DX2
402   DTDY(I,N)=DTDY(I,N1)
      DTDX(1,1)=DTDX(2,1)
      DTDY(1,1)=DTDY(1,2)
      DTDX(1,N)=DTDX(2,N)
      DTDY(1,N)=DTDY(1,N1)
      DTDX(M,1)=DTDX(M1,1)
      DTDY(M,1)=DTDY(M,2)
      DTDX(M,N)=DTDX(M1,N)
      DTDY(M,N)=DTDY(M,N1)
      DO 500 I=1,M
      DO 500 J=1,N
      HBREAK(I,J)=0.0
      IF(D(I,J) .LE. 0.0)GOTO 500
      DEP=D(I,J)
      COSI=CO(I,J)
      SINI=SI(I,J)
      RK=RRK(I,J)
      TA=TAH(RK*DEP)
      HBREAK(I,J)=0.12*PI2*TA/RK
      CS=CCH(RK*DEP)
      SCHSQ=1.0/(CS**2)
      ARG2=2.0*RK*DEP
      SII=SH(ARG2)
      CSS=COH(ARG2)
      SECHSQ=SII**2
      CSS=COH(ARG2)
      SINHSQ=SII**2
      E=U(I,J)*COSI+V(I,J)*SINI+0.5*SIGMA*(1.0+ARG2/SII)/RK
      C=SQRT(G*TA/RK)
      FF=0.5*(1.0+ARG2/SII)
      CG(I,J)=FF*C
      PHI(I,J)=FR*G*RK*CG(I,J)*UBB(I,J)/(8.*((HZ*CS)
     1 **2)*(PI**3))
      DKDX=RK*((U(I,J)*SINI-V(I,J)*COSI)*DTDX(I,J)-(COSI
     1 *DUDX(I,J)+SINI*DVDX(I,J))-SIGMA*DDDX(I,J)/SIT)/E
      DKDY=RK*((U(I,J)*SINI-V(I,J)*COSI)*DTDY(I,J)-(COSI
     1 *DUDY(I,J)+SINI*DVDY(I,J))-SIGMA*DDDY(I,J)/SII)/E
      P=C*(SII-ARG2*CSS)/SINHSQ
      DKDDX=RK*DDDX(I,J)+DEP*DKDX
      DKDDY=RK*DDDY(I,J)+DEP*DKDY
```

```
      Q=0.5*G/(C*RK**2)
      DCDX=Q*(RK*SECHSQ*DKDDX-TA*DKDX)
      DCDY=Q*(RK*SECHSQ*DKDDY-TA*DKDY
      DCGDX=P*DKDDX+FF*DCDX
      DCGDY=P*DKDDY+FF*DCDY
      SS2=SINI**2
      CC2=COSI**2
      SIGXX=(2.*FF-0.5)*CC2+(FF-0.5)*SS2
      SIGYY=(2.*FF-0.5)*SS2+(FF-0.5)*CC2
      TAUXY=FF*SINI*COSI
      S(I,J)=CG(I,J)*(SINI*DTDX(I,J)-COSI*DTDY(I,J))
      S(I,J)=S(I,J)-(DUDX(I,J)+DVDY(I,J))-(COSI*DCGDX+
     1  SINI*DCGDY)-(SIGXX*DUDX(I,J)+TAUXY*DUDY(I,J)+TAUXY
     2  *DVDX(I,J)+TAUXY*DUDY(I,J)+SIGYY*DVDY(I,J))
500   CONTINUE
      RETURN
      END
```

EXAMPLE OF INPUT DATA FOR TRIVANDRUM

```
013010029010002006-01000
004005
1255.002510.000000.600048.000.031250.02000
-5.0-5.0-5.0-5.0-5.0-5.0-5.0-5.0-5.0-5.012.005.5-5.0-5.0-5.0-5.0-5.0-5.0-5.0-5.0
19.316.516.013.307.007.003.7-5.0-5.0-5.029.525.024.023.029.021.515.018.315.0-5.0
31.029.529.531.031.031.024.030.024.019.534.534.034.035.537.036.029.032.532.529.5
37.537.037.540.039.539.035.037.538.538.040.040.041.044.042.041.040.042.041.041.0
42.042.041.543.042.042.044.045.044.542.044.044.043.545.044.543.044.546.046.045.5
46.046.545.546.546.547.046.547.547.546.047.547.546.046.547.549.047.549.540.048.0
50.550.548.548.549.051.049.052.052.050.5
0.0060280.0415510.2904320.6632030.8555800.8561360.7080760.5410790.500030
0.5946690.5836600.3612610.2132490.1548110.1031470.0784650.0522810.0397890.040198
0.0385670.0356210.0266040.0166710.0111070.0085670.0096090.0101380.0080080.007176
00.1063402.44220
0.0108600.0215040.1064060.4859600.8917750.7969850.5858050.8020191.168311
1.0867120.6468930.3389620.2075280.1486740.1281320.0972430.0554420.0324000.027534
0.0252850.0225950.0251250.0295910.0278010.0247590.0254640.0290610.0317560.029708
00.1214202.44220
0.0072790.0290310.1108650.3594000.6280830.6030540.4211120.3352280.322908
0.3005980.3053630.3126540.2150120.1176300.0892570.0684170.0461260.0319980.027793
0.0278450.0250580.0181490.0121920.0082220.0058540.0051630.0052910.0065860.007311
00.0689302.44220
0.0475230.0657660.0755270.1915340.6089070.9521190.7544200.4095490.326952
0.3809820.3612570.3428970.3806090.3477650.2596560.1764890.1175290.0831790.071273
0.0764390.0799670.0715490.0556560.0385970.0305580.0300410.0254130.0196620.016334
00.0817002.52944
```

EXAMPLE OF OUTPUT DATA FOR TRIVANDRUM

SPECTRAL DENSITY (M**2*SEC) AT STATION := 3 6

.04688	.00059
.06250	.02942
.07813	.30323
.09375	1.02426
.10938	1.50598
.12500	1.28887
.14063	.95486
.15625	.71314
.17188	.47826
.18750	.35415
.20133	.31951
.21875	.30058
.23438	.23131
.25000	.16381
.26563	.15607
.28125	.17462
.29688	.15679
.31250	.11036
.32813	.07074

APPENDIX III

PUBLICATIONS OF THE AUTHOR IN THE RELATED FIELDS

1. M.P. M. Reddy, V. Hariharan and N.P. Kurian. Coastal erosion at Beengre,a fishing village near Mangalore- A preliminary study. Mahasagar - Bullettin of the National Institute of Oceanography,Vol.10(3 & 4),1976, pp. 97- 102.

2. M.P.M. Reddy, V.Hariharan and N.P. Kurian. Hydrographic features of nearshore waters along Mangalore coast. Indian Journal of Marine Science, Vol.7, 1978, pp. 141-145.

3. M.P.M Reddy, V. Hariharan and N.P.Kurian. Coastal currents near Mangalore. Journal of Institution of Engineers(India), Vol.58, 1978, pp.161-164.

4. M.P.M. Reddy, V. Hariharan and N.P. Kurian. Coastal currents of Mangalore and the possibility of the relationship with pelagic fish catches in the area. Indian Journal of Marine Sciences, Vol.6, 1979,pp.16-19.

5. M.P.M Reddy, V. Hariharan and N.P. Kurian Seasonal variations in hydrographic conditions of estuarine and oceanic waters adjoining the old Mangalore port. Indian Journal of Marine Sciences, Vol.8 1979, pp. 73-77

6. M.P.M Reddy, V Hariharan and N.P. Kurian. Sediment movement and siltation in the navigational channel of the Mangalore Port Proceedings of the Indian Accademy of Sciences. Vol.88 A(II-2),1979 pp. 121-150.

7. M.P.M Reddy, V Hariharan and N P. Kurian. Seasonal variations of hydrographic conditiona of estuarine and oceanic waters adjoining the old Mangalore port. Pageoph, Vol.117, 1979, pp.935-942.

8. V.Hariharan, M.P.M. Reddy and N.P.Kurian. Littoral and rip currents and beach profiles off Someswar. The Indian Geographical Journal, Vol 53, 1978, pp.14 20.

9. M P.M.Reddy, V Hariharan and N.P.Kurian. Beach stability along the coast from Ullal to Thannirbhavi near Mangalore Indian Journal of Marine Sciences, Vol.11, 1982, pp 327-332.

10. M. Baba N.P.Kurian, T.S.Shahul Hameed K.V.Thomas, M. Prasanna kumar and C.M. Harish. Studies on the waves and their refraction in relation to beach erosion along the Kerala Coast. CESS Technical Report No. 29, -1983.

11. M. Baba, P.S. Joseph, N.P. Kurian, T.S.Shahul Hameed, K.V.Thomas M. Prasannakumar and C.M. Harish. Studies on the waves and their refraction in relation to beach erosion along the Kerala Coast CESS Technical Report No. 31, -1983.

12. N P.Kurian, T.S. Shahul Hameed and M.Baba. Beach dynamics in relation to wave climate at Alleppey. CESS Technical Report No. 38 - 1984.

13. M. Prasannakumar, N.P.Kurian and M.Baba. A study of nearshore processes and beach profiles at Calicut. CESS Technical Report No. 40 - 1984.

14. N.P.Kurian, M.Baba and T.S.Shahul Hameed. A study of the monsoonal beach processes around Alleppey, Kerala. Proceedings of the Indian Academy of Sciences (Earth Planet. Sci.), Vol.94 (3) 1985, pp 323 - 332.

15. N.P.Kurian and M. Baba. Identification of zones of erosion. In Indias Enviroment. (Geological Society of India) 1986, pp 275 - 287.

16. T.S. Shahul Hameed, N. P. Kurian and M. Baba. Impact of permeable structure on shoreline development In: India s Environment. (Geological Society of India) 1986, pp. 275 287.

17. M. Baba, C M. Harish and N.P. Kurian. Influence of record length and sampling interval on ocean wave spectral estimates. Mahasagar Bulletin of the National Institute of Oceanography Vol 19(2) 1986. pp. 79 - 85.

18. M. Baba, N.P. Kurian, T.S.S. Hameed, K.V. Thomas, C.M. Harish . Temporal and spatial variation in wave climate off Kerala, South West Coast of India. Indian Journal of Marine Sciences, Vol.16, 1987, pp.5 - 8.

19. N.P. Kurian and M. Baba. Waves and littoral processes at Calicut. In Wave Climate and Beach Processes of the SW coast of India and their prediction. (Ed. M. Baba), Centre for Earth Science Studies Trivandrum (under publication).

20. M. Baba and N.P. Kurian Instrumentation, data collection and analysis In: Wave Climate and Beach Processes of the SW coast of India and their predictions. (Ed. M.Baba), Centre for Earth Science Studies, Trivandrum (under publication).

DISSERTATION

N. P Kurian Remote Sensing Applications for Estimation of Suspended Sediment Concentration in Coastal Waters of Cochin, Kerala Dissertation, P. G. Diploma in Remote Sensing Applications to Coastal Processes and Marine Resources. Indian Institute of Remote Sensing 1987, 37pp.